Åbo Akademi University

Meheretu Jaleta Dirbeba

# Thermochemical Conversion Characteristics of Vinasse

Front cover photo:

Modified from a picture of Finchaa Sugar Factory, an integrated sugar-ethanol mill in Ethiopia, with permission from the Ethiopian Sugar Corporation.


# Thermochemical Conversion Characteristics of Vinasse

Meheretu Jaleta Dirbeba

Academic Dissertation

Laboratory of Inorganic Chemistry
Johan Gadolin Process Chemistry Centre
Faculty of Science and Engineering
Åbo Akademi University
Åbo/Turku, Finland

***Supervisors***

Professor Anders Brink
Åbo Akademi University

Assistant Professor Nikolai DeMartini
University of Toronto

Professor Mikko Hupa
Åbo Akademi University

***Opponent and Reviewer***

Professor Klas Engvall
KTH Royal Institute of Technology
Department of Chemical Engineering
Stockholm, Sweden

***Reviewer***

Associate Professor Mika Järvinen
Aalto University
Department of Mechanical Engineering, Energy Conversion Research Group
Espoo, Finland

ISBN 978-952-12-3939-7 (printed)
ISBN 978-952-12-3940-3 (digital)
Painosalama Oy
Åbo/Turku, Finland, 2020

# PREFACE

The work presented in this thesis was conducted from 2014 to 2019 at the Laboratory of Inorganic Chemistry (now the Laboratory of Molecular Science and Engineering), Åbo Akademi University, as part of the activities at the Johan Gadolin Process Chemistry Centre (PCC). This work was also partly carried out within the projects CLIFF, Clustering Innovation Competence of Future Fuels in Power Production (2014–2017), and CLUE, Clean and Efficient Utilization of Demanding Fuels (2017–2019), as part of the activities of the PCC. Other research partners were VTT Technical Research Centre of Finland Ltd, Lappeenranta University of Technology, Aalto University, and Tampere University of Technology.

The lion's share of the funding for the work carried out in this thesis was received from the Graduate School in Chemical Engineering (GSCE) — a network of postgraduate studies in chemical engineering in four universities in Finland. Funding from the GSCE and Åbo Akademi University Foundation also enabled me to participate in conferences and courses that have enriched my doctoral study. The activities performed in Papers IV and V were in part financed by the Academy of Finland projects "Fate of Fuel Bound Nitrogen in Biomass Gasification" (Decision 289666) and "Behavior and Properties of Molten Ash in Biomass and Waste Combustion" (Decision 266384), respectively. Funding support, within the projects CLIFF and CLUE, was received from the National Technology Agency of Finland (Business Finland, formerly Tekes), ANDRITZ, Valmet Technologies Oy, Sumitomo SHI FW Energia Oy (formerly Amec Foster Wheeler Energia Oy), UPM-Kymmene Corporation, Clyde Bergemann GmbH, International Paper, Top Analytica Oy Ab, and Fortum. In addition, a three-month grant for the final period of my doctoral study was received from the Åbo Akademi Rector's Scholarship. Support was also received from Fundaçao para a Ciẽnciae a Tecnologia through IDMEC, under LAETA, project UID/EMS/50022/2013, for a part of the work performed in Paper IV. All funding supporters are gratefully acknowledged.

I am so thankful to the Ethiopian Sugar Corporation for supplying the sugar mill biomass samples used in this work. Without the kind assistance of the personnel at the Corporation, the objectives of this work would not have been fulfilled. In particular, Weyo Roba (CEO of the Corporation), Teshale Firdissa (Factory Operation Executive Officer), and the late Takele Desta (Factory Operation Sugar Technology Advisor) are thanked for facilitating for me the

acquisition of the samples. Moreover, all staff at Metahara Sugar Factory, especially Kasahun Mirkena (the then Sugar Production Team Leader) and Bekele Mirkena (the then Ethanol Production Team Leader), who were involved in the sample collection and preparation are greatly appreciated. The Technical University of Lisbon is acknowledged for providing the kiwi branches, olive branches, grape pomace, and torrefied grape pomace samples used in this work.

I owe my sincere gratitude to my supervisors, Prof. Mikko Hupa, Prof. Anders Brink, and Assistant Prof. Nikolai DeMartini (now at the University of Toronto) for their guidance, support, encouragement, and expertise. Especially, I am greatly indebted to Mikko for his continuous supervision despite his duties as the Rector of Åbo Akademi University and for his assistance in shaping this thesis work to its final form. My utmost thanks go to Prof. Anders Brink without whom this work would never have come to be. Anders has always been available for help, discussions, and to respond to my questions, including the silly ones! Moreover, his meticulous scrutiny of the manuscripts not only enhanced the quality of the work presented in this thesis but also enriched my scientific writing skills. Thank you also to Niko for his comments and suggestions despite his tight schedule there at the University of Toronto.

I would like to extend my deepest gratitude to the former and present leaders of the Laboratory of Inorganic Chemistry, Prof. Mikko Hupa and Prof. Leena Hupa, for giving me the opportunity to work in their research group. I always consider myself the luckiest person to be part of such a dynamic research team with versatile expertise and a conducive research environment. In addition, my heartfelt thanks to Mikko and Leena for their kind support in paving the way for my family to join me here in Finland — the peace of mind was vital for carrying out my research work properly.

I am so grateful to all my co-authors for their great contributions to and comments on the work presented in this thesis. Prof. Daniel Lindberg carried out all the FactSage thermodynamic calculations and analysis of the results. Dr. Maria Zevenhoven helped me with the analysis of the fuel fractionation data. Dr. Atte Aho guided me with the fast pyrolysis experiments and performed the analysis of the bio-oils with the GC-MS. Ida Mattsson (from the Laboratory of Organic Chemistry) conducted the NMR experiments and analyzed the NMR spectra. Dr. Oskar Karlström was the lead expert in the investigation of the influence of K/C ratio on the gasification reactivities of biomass chars presented in Paper IV. Prof. Leena's inputs for the work presented in Papers II

and V were invaluable. Prof. Mario Costa (from the Technical University of Lisbon) provided important inputs for the work presented in Paper IV.

It gives me great pleasure to thank all colleagues at the Laboratory of Inorganic Chemistry for making my Ph.D. life at the lab successful and cheerful. Luis Bezerra, Peter Backman, Tor Laurén, Jaana Paananen, Linus Silvander, Dr. Fiseha Tesfaye, Nina Bruun, and Dr. Rose-Marie Latonen (from the Laboratory of Analytical Chemistry) are all gratefully acknowledged for their help with the experimental work. Special thanks to my dear colleague and friend Jonne Niemi! Throughout the course of my Ph.D. studies, he has been a great company: an industrious person always ready to listen and help, both on and off the pitch! In addition, Jonne's saving the day by being a kind and a magic 'Joulupukki' is always warmly remembered!

Last but by no means the least, many thanks and lots of love to my wife Tigist (aka Titti) for her support, love, encouragement, patience, and understanding throughout all the ups and downs of my Ph.D. work. And, yes, I should acknowledge my cute kids, Sonan (aka Buchu) and Elellaan (aka Ellu) for always making me optimistic and motivated to go forward — your disruptions were — and are — always equally welcomed!

Åbo/Turku, January 2020

Meheretu Jaleta Dirbeba

# ABSTRACT

Vinasse, also known as stillage or spent wash, is an effluent from the distillery plant of the integrated sugar-ethanol process. It is characterized by an acidic pH, a black-reddish color, and being a dilute effluent with a dry solids content of 5–10 wt %. In addition, vinasse presents very high BOD (biological oxygen demand) and COD (chemical oxygen demand) due to its organic constituents, and it is generated at a rate of 10–15 liters per liter of ethanol produced.

Today, vinasse is mainly used in fertirrigation — providing the soil with water and at the same time fertilizing the soil for sugarcane plants. However, depending on the location and soil condition, the use of untreated or partially treated vinasse in fertirrigation creates the potential for environmental damage, including emission of greenhouse gases and pollution of soil and water. Moreover, utilization of vinasse in fertirrigation alone is not sufficient to address the total amount of vinasse produced. Thus, there is a need for alternative vinasse utilization options, such as thermochemical conversion.

Thermochemical conversion processes, such as pyrolysis, gasification, and combustion, in addition to alleviating the potential environmental problems posed by vinasse, offer the opportunity to convert the organics in the vinasse into fuels, chemicals, or electric power. Moreover, the ash from these processes can be returned back to the soil as fertilizer. The purpose of this study is to characterize properties important for thermochemical conversion of vinasse. Fast pyrolysis and gasification were the forms of thermochemical conversion investigated. Additionally, the release of inorganics during fast pyrolysis, gasification, and combustion of vinasse and vinasse ash-melting behavior were determined, as they are critical to the design and operation of vinasse thermochemical conversion technologies.

To properly establish the background for this study, it was important to determine the flows of ash-forming elements in a typical integrated sugar-ethanol mill. Mass and energy balances for an integrated sugar-ethanol mill were developed using mill data and by analyzing samples of biomass and biomass residues from the mill. The results revealed that although the vinasse, the final by-product from the mill, contains only about 2–3% of the mass and energy, it contains the highest concentration of ash-forming elements from the cane. The dominant cationic ash-forming elements in the vinasse are K and Ca, whereas Cl and S are the major anionic inorganic elements.

Product distribution and yield during fast pyrolysis of vinasse at 400 and 500 °C were determined using a drop-tube-type reactor, a reactor with a char

retention system inside. The results showed that the water-free pyrolysis-oil yield on a wt % dry vinasse basis was about 12, independent of the pyrolysis temperature. The low pyrolysis oil yield was probably due to the high potassium content of the vinasse. Alkali metals are known to catalyze the degradation of pyrolysis oils in the vapor phase, resulting in an increase in the gas and water yields and a decrease in oil yield. The char and gas yield trended with temperature in a fashion similar to that which occurs with other biomass fuels: the char yield decreased, and the gas yield increased at 500 °C when compared to 400 °C. About 45–55% of the carbon and more than 85% of the potassium in the vinasse were retained in the chars. The low bio-oil yield and high water content of the bio-oil indicate that fast pyrolysis is not an attractive option for the production of bio-oil from vinasse. However, fast pyrolysis may be an excellent means for the production of bio-char with a high K content for fertilizer and for sequestering approximately half of the carbon from the vinasse. Moreover, the recovery of most of the K with the chars suggests that the liquid and gaseous pyrolysis products can be burned in a boiler with lower levels of ash-related problems than the original fuel. This would allow for energy and inorganic chemicals to be recovered from vinasse while reducing some of the limitations of applying wet vinasse to agricultural lands.

Gasification of the vinasse chars by $CO_2$ at temperatures between 600 and 800 °C in a DSC-TGA was found to be dominated by volatilization of inorganics. Volatilization of the inorganics was significant at temperatures over 700 °C. Reduction of alkali carbonates and sulfates by carbon, evaporation of alkali chlorides, and autogasification are the main mechanisms by which the char sample weight loss occurred in the DSC-TGA. In addition to gasification of the char carbon by $CO_2$, the reduction of alkali carbonates and sulfates and autogasification were responsible for the consumption of the organic carbon from the chars. However, the vinasse char gasification rate was independent of $CO_2$ gas concentration in the gas concentration range considered, probably due to saturation of char surfaces with $CO_2$.

For other agro-industrial biomass fuels, i.e., kiwi branches, olive branches, grape pomace, torrefied grape pomace, and sugarcane bagasse, the char sample weight losses in the TGA at 800 °C in $CO_2$ were mainly due to gasification of char carbon by $CO_2$. These fuels had ash contents of about one order of magnitude lower than that of the vinasse. The char gasification reactivities of these fuels increased almost linearly with the K/C ratio in the range of 0% to 80% char conversion. After the gasification rates reached a maximum at a K/C mole ratio of around 0.1, the rates started to decrease, suggesting that the

catalytic char gasification rates might have been saturated with respect to K. Chars from one of the fuels, sugarcane bagasse, had a high Si content and a lower gasification reactivity. Formation of potassium silicates during gasification, which makes the K unavailable for catalytic reactions, may be the reason for the lower reactivity of chars from this fuel. For the vinasse chars, however, it was not possible to determine the influence of the K/C ratio on the gasification rate with the present experimental methods. This was because the char weight losses during gasification were dominated by release of inorganics hampering determination of the amount of char carbon gasified as a function of time, and consequently, determination of char conversion and gasification rates.

The release of inorganics during combustion and gasification of vinasse at 900 °C in a single-particle reactor (SPR) was determined by analyzing the ashes from the combustion/gasification experiments for their inorganic content. Similarly, to determine the levels of inorganics released from vinasse chars during the DSC-TGA experiments at 600–800 °C in $CO_2$ and $N_2$ gas atmospheres, the residues remained after the DSC-TGA experiments were also analyzed for their inorganic content. The DSC-TGA was also used to investigate the release of inorganics from the vinasse chars as a function of time and temperature. Results of analyses of the ashes/residues from the SPR/DSC-TGA showed that significant levels of the K, Na, Ca, Mg, S, and Cl in the vinasse and its chars were released under combustion, gasification, and inert gas conditions. However, none of the Si, Al, Fe, and P in the vinasse was released under the present experimental conditions although 50–70% of the Si, Al, and Fe and almost all of the P in the vinasse were $H_2O$- and $NH_4Ac$-soluble. Holding time, temperature, and gas atmosphere were found to have strong influences on the release of K and Cl from vinasse and its chars. It was observed that temperatures of 700 °C and above and longer holding times increased the release of K and Cl considerably, and the release levels were more pronounced in reducing gas conditions than in oxidizing conditions. However, Cl release was found to be higher in $CO_2$ than in $N_2$. This latter observation needs further investigation.

The initial or first melting temperature ($T_0$) for the vinasse ash was determined using a DSC. Thermodynamic calculations were made with FactSage to obtain the fraction of melt as a function of temperature. The DSC results revealed that the initial melting temperature of the vinasse ash is in the range of 640–645 °C. Moreover, results from the FactSage calculations showed that 15% and 70% of the ash is molten at about 650 °C and 670–690 °C,

respectively. However, it was observed that the ash melt fraction never reaches 100% below 1200 °C due to the presence of high-temperature melting oxides in the ash.

The release of significant levels of K and Cl from the vinasse and the low-temperature melting of the vinasse ash suggest that vinasse is a difficult fuel for conventional combustion and gasification processes. In particular, the use of a fluidized bed technology — a well-established technology for combustion or gasification of solid fuels — for heat and power production from vinasse seems unlikely due to the high risk of bed agglomeration. Nevertheless, some potential alternative options are worth investigating. One option is the high-temperature entrained flow gasification process. A pilot-plant scale of this process has been demonstrated to be feasible for the production of syngas and recovery of inorganic chemicals from black liquor, a by-product from pulp mills that shares some fuel properties with the vinasse. Another option is combustion of vinasse in a black liquor recovery boiler type in which the vinasse is spray-fed into the boiler in coarse droplets. This system minimizes the formation of ash fumes and hence, the ash-related problems in the boiler, and allows most of the inorganics from the vinasse to be recovered as bottom ash for use as fertilizer.

# SAMMANFATTNING

I den här avhandlingen studeras möjligheten till energi- och materialåtervinning ur bottensatsen från destillationssteget i ett sockerbruk med integrerad etanolproduktion. Bottensatsen, också kallad vinass, är en sur, rödsvart, vattenlösning med en torrhalt mellan 5 och 10 %. Lösningen innehåller både organiska och oorganiska föreningar och har högt BOD och COD värde. Vid produktion av en liter etanol uppstår 10 till 15 liter vinass.

Vinass används huvudsakligen vid näringsbevattning av sockerrörsfält. Beroende på jordmån kan det här vara problemfyllt, oberoende om behandlad eller obehandlad vinass används. Näringsbevattningen kan tillföra för höga halter av salter som kan förorena grundvattnet. Vid nedbrytningen av de ingående organiska föreningarna uppstår gasformiga emissioner, inkluderande växthusgaser såsom metan och koldioxid. Det är heller inte möjligt att utnyttja all den mängd vinass som uppstår för näringsbevattning, så det finns ett behov för alternativt utnyttjande av vinassen, t.ex. som råvara i termokemiska processer.

Termokemisk konversion, så som pyrolys (torrdestillation), förbränning och förgasning kan utgöra en möjlighet att omvandla de organiska föreningarna i vinass till biobränslen, kemikalier eller elektricitet. Askan som uppstår vid den termokemiska omvandlingen kan användas som en beståndsdel i gödsel och återföras till jorden. Syftet med den här avhandlingen är att karaktärisera de egenskaper hos vinass som är av betydelse för termokemiska omvandlingsprocesser. Pyrolys och förgasning var de processer som studerades med avseende på termisk bränsleomvandling. Dessutom undersöktes avgången av oorganiska ämnen vid förbränning, pyrolys och förgasning av vinass samt vinassaskans beteende som är av stor betydelse för hur termiska konversionsanläggningar ska dimensioneras och drivas.

Som en bakgrund för studien fastställdes mass- och energiflöden i en integrerad socker-etanolfabrik. Flödena bestämdes genom en kombination av driftsdata från en fabrik och laboratorieanalyser av sockerrör, sockerrörsblast och andra biprodukter som uppstår i processen. Studien fokuserade på strömmarna av oorganiska föreningar. Studien visade att endast 2-3 % av sockerrörets energiinnehåll och massa återfanns i vinassen, medan merparten av de askbildande elementen fanns upplösta i vinassen. De viktigaste katjoniska askbildande ämnena var kalium och kalcium medan de viktigaste anjoniska ämnena var klorid och svavel.

Produktsammansättning och utbyte vid snabb pyrolys av torkad vinass undersöktes vid 400 och 500 °C med hjälp av en fallrörsreaktor utrustad med ett koksuppsamlingssystem. Testerna visade att utbytet av vattenfri pyrolysolja var ca 12 % vid de här temperaturerna. En möjlig orsak till det låga utbytet är att vinass innehåller mycket höga halter av kalium, som kan katalysera sönderfallsprocesserna av pyrolysoljor till vatten och flyktiga gaser. Koksutbytet var lägre vid den högre temperaturen, medan gasutbytet var högre, vilket är vanligt för biomassor. Mellan 45 och 55 % av kolet i vinassen bildade koks medan hela 85 % av kaliumet återfanns i koksresten. Experimenten indikerar att produktion av pyrolysolja från vinass genom snabb pyrolys inte är ett konkurrenskraftigt alternativ, men att processen kan vara fördelaktig om man önskar producera ett biokoks med hög kaliumhalt. Den höga kaliumhalten i kokset indikerar samtidigt att de gaser och pyrolysoljor som uppstår i processen är betydligt enklare att elda i en panna än vinassen som sådan. Förgasningsexperiment med vinasskoks i en termovåg påvisade en kraftig avgång av oorganiska föreningar vid temperaturer över 700 °C. De oorganiska föreningarna avgick huvudsakligen genom förångning av alkaliklorider och genom reduktion av karbonater och sulfater av kol. Förgasningshastigheten var oberoende av halten $CO_2$ som användes vid experimenten, troligen på grund av att koksytan var mättad på koldioxid. För de andra restfraktionerna från jordbruk som undersöktes var det endast förgasning av kolet som bidrog till viktminskningen under vid koksförgasningen. De här experimenten gjordes gjorde även de i en termovåg. Temperaturen som användes var 800 °C och de biomassfraktioner som undersöktes var grenar från kiwiträd, grenar från olivträd, torkad druvspressmassa och sockerrörsblast. Jämför med vinass är askhalten i de här bränslena endast en tiondedel. Vid förgasning av koks producerat från de här biomassorna kunde ett linjärt samband mellan förgasningshastighet och K/C molförhållandet i konversionsintervallet 0 till 80 % konstateras. Det här gällde dock endast upp till ett molförhållande på 0,1, varefter förgasningshastigheten började avta. En möjligförklaring till det här är att reaktioner katalyserade av kalium mättades vid höga K/C molförhållanden. Koks från sockerrörsblast var inte lika reaktivt. Jämfört med de andra biobränslena hade det här kokset en hög kiselhalt. Bildning av kaliumsilikater kan vara en möjlig orsak till den lägre reaktiviteten, då det annars katalytiskt aktiva kaliumet då binds upp i silikaten. Det var inte möjligt att undersöka hur K/C molförhållandet påverkade förgasningen av vinasskoks. Orsaken till det här var svårigheter att uppskatta

kolhalten i kokset, då så stor del av viktminskningen berodde på avgång av oorganiska föreningar.

Elementanalys av askresten utgjorde grunden för att bestämma avgången av askbildande ämnen vid förbränning och förgasning av torkad vinass. Askan producerades genom att förbränna eller förgasa små prov av torkad vinass i en laboratoriereaktor. Askan som återstod efter termovågsexperimenten med $CO_2$- eller $N_2$-atmosfär analyserades också. I det här fallet upplöstes askresten i vatten som sedan analyserades. Termovågen användes även för att undersöka den avgången som en funktion av tid och temperatur. Experimenten visade att en betydande del av ämnena K, Na, Ca, Mg, S och Cl avgick vid förbränning och förgasning, medan det mesta av Si, Al och Fe, samt P återfanns askresten. Avgången påverkades av temperaturen samt av exponeringstiden. Framförallt K- och Cl-avgången påverkades av temperaturen. Vid långa exponeringstider och då temperaturen översteg 700 °C steg avgången av de här ämnena kraftigt. Avgången påverkades också av gasatmosfären. Mer K och Cl avgick då en reducerande atmosfär användes i stället för en oxiderande. Kloravgången var ännu större då en inert atmosfär användes.

Temperaturen då den första smälta fasen uppstod i askan, benämnd $T_0$, identifierades för vinassaska med hjälp av differentiell svepkalorimetri till 640-645 °C. Andelen smälta i askan som funktion av temperaturen undersöktes också med hjälp av jämviktsberäkningar. Beräkningarna visade att andelen smälta i askan uppgår till 15 % då temperaturen är ca 650 °C och 70 % då temperaturen är 670 – 690 °C. Beräkningarna visade vidare att vid temperaturer under 1200 °C så finns det fasta oxider närvarande i asksmältan.

Termisk konversion genom förbränning eller förgasning verkar inte vara lämplig för vinass på basen av experimenten. Både den höga avgången av K och Cl och den lättsmältande askan visar på det här. Askans smältbeteende tyder också på att fluidbäddteknik, som ofta kan användas vid förbränning och förgasning av biomassa, inte lämpar sig för termisk konversion av vinass pga. en hög risk för bäddagglomerering. Det finns ändå andra processer som det lönar sig att undersöka vidare. En sådan är högtemperatursuspensions-förgasning. Tekniken har använts i pilotskala för att förgasa svartlut för produktion av syntesgas och för återvinning av kokkemikalier. Svatlut är förmodligen det bränsle som mest påminner om vinass till sina egenskaper, vilket indikerar att även sodapannsteknologin kunde användas för vinassförbränning och på så sätt möjliggöra att den kaliumrika asksmältan kan tas tillvara.

# LIST OF PUBLICATIONS

This thesis work is based on the following original publications. They are referred to in the text of the thesis as **Paper I**, **Paper II**, **Paper III**, **Paper IV,** and **Paper V**.

**I.** **Dirbeba MJ**, Brink A, DeMartini N, Zevenhoven M, Hupa M. Potential for thermochemical conversion of biomass residues from the integrated sugar-ethanol process — Fate of ash and ash-forming elements. Bioresource Technology 234 (2017) 188–197. https://doi.org/10.1016/j.biortech.2017.03.021

**II.** **Dirbeba MJ**, Aho A, DeMartini N, Brink A, Mattsson I, Hupa L, Hupa M. Fast pyrolysis of dried sugar cane vinasse at 400 and 500 °C: Product distribution and yield. Energy Fuels 2019, 33, 1236–1247. https://pubs.acs.org/doi/10.1021/acs.energyfuels.8b03757

**III.** **Dirbeba MJ**, Brink A, DeMartini N, Lindberg D, Hupa M. Sugarcane vinasse $CO_2$ gasification and release of ash-forming matters in $CO_2$ and $N_2$ atmospheres. Bioresource Technology 218 (2016) 606–614. https://doi.org/10.1016/j.biortech.2016.07.004

**IV.** Karlström O, **Dirbeba MJ**, Costa M, Brink A, Hupa M. Influence of K/C ratio on gasification rate of biomass chars. Energy Fuels 2018, 32, 10695–10700. https://pubs.acs.org/doi/10.1021/acs.energyfuels.8b02288

**V.** **Dirbeba MJ**, Brink A, Zevenhoven M, DeMartini N, Lindberg D, Hupa L, Hupa M. Characterization of vinasse for thermochemical conversion — Fuel fractionation, release of inorganics, and ash-melting behavior. Energy Fuels 2019, 33, 5840–5848. https://pubs.acs.org/doi/10.1021/acs.energyfuels.8b04177

# AUTHOR'S CONTRIBUTIONS

In **Papers I**, **II**, **III**, and **V**, Dirbeba wrote the manuscripts. In **Paper IV**, Dirbeba is the second author. All analyses with ICP-OES, CHNS(O) analyzer, IC, SEM-EDX, and XRD were conducted by laboratory personnel. Dirbeba was responsible for most of the sample preparations and evaluation of the experimental results. All the FactSage calculations and evaluations of the results were carried out by Prof. Daniel Lindberg.

**Paper I**

Dirbeba planned the experiments and evaluated the experimental results with the co-authors. The fuel fractionation experiments were carried out at ALS Scandinavia AB, Sweden, and Dr. Maria Zevenhoven helped evaluating the data.

**Paper II**

Dirbeba planned and carried out the experiments with the co-authors. Ida Mattsson conducted the NMR experiments and evaluated the results.

**Paper III**

Dirbeba planned the experiments with the co-authors and conducted the DSC-TGA experiments. Dr. Rose-Marie Latonen conducted the FTIR experiments and helped the evaluation of the FTIR data.

**Paper IV**

Dirbeba planned the experiments with the co-authors and conducted the DSC-TGA experiments. Dr. Oskar Karlström is the first author and was responsible for the analysis of most of the experimental data.

**Paper V**

Dirbeba planned the experiments with the co-authors. Peter Backman did the DSC-TGA experiments.

# OTHER RELATED PUBLICATIONS BY THE AUTHOR

- **Dirbeba MJ**, Brink A, Hupa L, Hupa M. Vinasse as a potential for renewable energy and chemicals recovery. In: The Proceedings of the 1st International Conference on Smart Energy Carriers, January 21–23, 2019, Naples, Italy.
- **Dirbeba MJ**, Brink A, Zevenhoven M, DeMartini N, Lindberg D, Hupa L, Hupa M. Characterization of vinasse ash and ash-forming elements. In: The Proceedings of the 27th International Conference on Impacts of Fuel Quality on Power Production and the Environment, September 23–28, 2018, Lake Louise, AB, Canada.
- **Dirbeba MJ**, Aho A, DeMartini N, Brink A, Hupa M. Pyrolysis of dried sugarcane vinasse and black liquor at 400 and 500 °C. In: The Proceedings of the 13th International Conference on Energy for a Clean Environment, July 2–6, 2017, Ponta Delgada, São Miguel, Azores, Portugal.
- **Dirbeba MJ**, Karlström O, Brink A, DeMartini N, Costa M, Hupa M. Influence of heating rate on $CO_2$ gasification and release of inorganics for chars from biomass residues. In: The Proceedings of the Joint Meeting of the Portuguese and Scandinavian-Nordic Sections of the Combustion Institute, November 17–18, 2016, Instituto Superior Técnico, Lisboa, Portugal.
- **Dirbeba MJ**, Brink A, DeMartini N, Hupa M. Vinasse char $CO_2$ gasification kinetics. In: The Proceedings of the Nordic Flame Days, October 6–7, 2015, Copenhagen, Denmark.

# LIST OF ACRONYMS

| | |
|---|---|
| BOD | Biological oxygen demand |
| COD | Chemical oxygen demand |
| DSC-TGA | Differential scanning calorimetry-thermogravimetric analyzer |
| FTIR | Fourier-transform infrared spectrometer |
| GC-MS | Gas chromatograph–mass spectrometer |
| GHG | Greenhouse gas |
| GP | Grape pomace |
| HHV | Higher heating value |
| HTL | Hydrothermal liquefaction |
| IC | Ion chromatograph |
| ICP-OES | Inductively coupled plasma-optical emission spectrometer |
| KB | Kiwi branches |
| NMR | Nuclear magnetic resonance |
| OB | Olive branches |
| OECD/FAO | Organization for Economic Cooperation and Development/Food and Agriculture Organization of the United Nations |
| SCB | Sugarcane bagasse |
| SCWG | Supercritical water gasification |
| SEM-EDX | Scanning electron microscope-energy dispersive X-ray |
| SPR | Single-particle reactor |
| SST | Stainless steel |
| TAN | Total acid number |
| TGP | Torrefied grape pomace |
| XRD | X-ray diffractometer |

# TABLE OF CONTENTS

# 1. INTRODUCTION

## 1.1. Biomass-containing industrial by-products as resources for the production of energy and chemicals

Industrial processing of biomass for the production of biofuel, food, and other commercial products generates biomass-containing residues that are considered potential resources for the production of renewable energy and recovery of chemicals [1]. An example in which the process is already realized is the Kraft pulping process. Here, wood chips are cooked in a digester where lignin is dissolved from the cellulosic fibers of the wood with the aid of chemicals, an aqueous solution of NaOH and $Na_2S$. The resulting mass from the digester is separated into two product streams: pulp and black liquor. The pulp is the wood-fiber-containing part which is ultimately processed to paper, whereas the black liquor is a dilute solution containing the lignin and other dissolved organics from the wood as well as the cooking chemicals. The black liquor is further concentrated from a dry solids content of approximately 15 wt % to about 65–85 wt % in a series of evaporators. This concentrated black liquor is burned in a Kraft recovery boiler to generate heat and power for the mill and at the same time to recycle the pulping chemicals. Consequently, the recovery of the organic and inorganic fractions of black liquor as energy and cooking chemicals, respectively, is central to the economic viability of Kraft pulping mills. At the same time, the energy and chemicals recovery system precludes potential environmental damage(s) that would have been caused by the direct disposal of black liquor to the environment.

Another example in which the potential is not fully utilized is the sugarcane-based integrated sugar-ethanol process, whose primary products are sugar and bio-ethanol. Production of the bio-ethanol in the distillery plant of the integrated process generates an important by-product, vinasse, also known by various names as stillage, still bottoms, spent wash, mosto, slops, vinhaca, vinhoto, or dunder [2]. Vinasse is mainly used in fertirrigation — providing the soil with water and at the same time fertilizing the soil for sugarcane plants. In some cases, the vinasse is co-composted with filtercake [3] for use as fertilizer. Other potential biomass residues from the integrated process for renewable energy production and recovery of chemicals include straw, bagasse, and filtercake. While the straw is left unutilized in the sugarcane field or burned off prior to cane harvesting and transport, the bagasse is burned in a boiler to generate heat and power for the sugar mill. The filtercake is mostly

applied to the soil alone, as fertilizer, or after co-composting with the vinasse. Another potential biomass residue for the production of energy and chemicals is rapeseed oil cake from edible oil processing.

A common property of these fuels is that they contain large amounts of ash and ash-forming elements that pose challenges in thermochemical conversion processes.

## 1.2. Vinasse properties

The physicochemical characteristics of vinasse vary considerably due to several factors, including differences in raw material type (e.g., sugarcane, sugar beet, sugarcane juice, and sugarcane molasses), sugar and ethanol production processes [4,5], soil types, climatic conditions, and agricultural practices [6]. In general, in addition to its acidic nature (pH = 4–5 [2]) due to its organic acid components, vinasse is characterized by its black-reddish color and by being a dilute effluent containing 90–95 wt % [7] water, with the balance being solids. Usually, 60–70% of the vinasse solids are organics, while the remaining solids are inorganics. Besides, as a result of its organic composition, vinasse presents very high biological oxygen demand (BOD) and chemical oxygen demand (COD), ranging from about 50,000–60,000 mg BOD/L of vinasse and 90,000–100,000 mg COD/L of vinasse [8]. Furthermore, on average, 10–15 L of wet vinasse is generated per 1 L of ethanol production. In Brazil alone, nearly $370 \cdot 10^9$ L [9] of vinasse was generated during the 2012/2013 ethanol production season. This would be equivalent to approximately 125 TWh of thermal energy supply per annum.

Vinasse is one of the few fuels that shares fuel properties with black liquor. These properties include swelling during pyrolysis [6], having a heating value of 10–15 MJ/kg on a dry basis [2,10,11], and containing a substantial ash fraction. However, vinasse is acidic [2], and its ash is mainly composed of potassium salts, whereas black liquor is alkaline, with sodium salts being predominant.

## 1.3. Current-use challenges and potential-alternative-utilization options of vinasse

Optimum application of vinasse to soil increases cane and sugar yields [12] and enhances the quality of soil physicochemical and biological properties [13–15]. However, depending on the location and soil condition, the use of untreated or partially treated vinasse in fertirrigation creates the potential for environmental damage, including emission of greenhouse gases (GHG) [16]

and pollution of soil and water [5]. These potential environmental problems are mainly due to the unacceptable levels of BOD and COD in the vinasse and its acidic property. Moreover, utilization of vinasse in fertirrigation alone is not sufficient to address the total amount of vinasse produced, due to the cost of transporting the vinasse to agricultural lands farther away from the distillery for fertilizer. Therefore, there is a need to develop alternative vinasse utilization options.

One option that has raised some interest is anaerobic biodigestion through which microorganisms break down the biodegradable portion of vinasse, producing methane as the main gaseous product for fuel. However, the review by Christofoletti *et al.* [5] mentions that this process is slow and expensive and produces corrosive and obnoxious-odor gases.

Another potential option is thermochemical conversion, such as pyrolysis, gasification, or combustion of vinasse. These processes, in addition to alleviating the potential environmental problems posed by vinasse, can convert the organics in the vinasse into fuels, chemicals, or electric power. In addition, the ash from these processes can be recovered and recycled back to the soil for fertilizer. The term thermochemical conversion is defined in the literature in two slightly different ways. In one definition, used by Bergeron *et al.* [17] and Brown [18], thermochemical conversion refers to the use of elevated temperatures and pressures to break the chemical bonds in the biomass matrix. By breaking the chemical bonds, thermochemical conversion, in this case, either releases the energy content of biomass directly, as in combustion, or converts the biomass into liquid or gaseous fuels and chemicals, as in pyrolysis, gasification, and liquefaction. In another definition, e.g., in reference [19], thermochemical conversion refers only to the production of liquid or gaseous fuels and chemicals, and consequently, combustion is not included. In this thesis work, the first definition of thermochemical conversion is adapted.

Vinasse thermochemical conversion in conventional processes has not been successful so far, despite several efforts. This is in part due to the high concentration of ash-forming elements in the vinasse. It is well-established that ash-forming elements in biomass fuels are responsible for the ash-related problems in thermochemical conversion processes. These ash-related problems include ash deposition, fouling, slagging, agglomeration, and corrosion [20,21]. Moreover, ash-forming elements in biomass fuels, in particular alkali and alkaline earth metals, significantly affect product yield and distribution during pyrolysis [22,23], gasification [22,24], and liquefaction [25] of the fuels. Therefore, in addition to knowing vinasse thermochemical

conversion characteristics, understanding the behavior of vinasse ash and ash-forming elements during vinasse thermochemical conversion is essential for overcoming the problems associated with this fuel. For the vinasse, the properties of ash and ash-forming elements of interest include ash-melting behavior and the levels of ash-forming elements released during thermochemical conversion. Moreover, characteristics of vinasse fast pyrolysis and $CO_2$ gasification have not been sufficiently investigated.

Another challenge for thermochemical conversion of vinasse is the large amounts of energy required to concentrate the dilute effluent to a high solids content. However, this is beyond the scope of the present study. Nevertheless, there are some options that can potentially address this problem. These options include heat and materials integration in the sugar, ethanol, and energy production units [26–28] and improving the energy efficiency of the integrated process through technology upgrading [29].

## 1.4. Objectives of this thesis

The objective of this thesis work is to characterize properties important for thermochemical conversion of vinasse from the integrated sugar-ethanol process. The aim is to provide necessary information for modeling and designing thermochemical conversion processes with high thermal and conversion efficiencies and low emissions. The specific objectives include:

(a) Determining product distribution and yield during fast pyrolysis of sugarcane vinasse at 400 and 500 °C as well as characterizing the pyrolysis products for their elemental and chemical compositions. **Paper II** deals principally with this task.

(b) Assessing vinasse char $CO_2$ gasification characteristics and causes for char sample weight losses in $CO_2$ and $N_2$ gas atmospheres at temperatures between 600 and 800 °C. **Paper III** focuses on these activities. In addition, the influence of K/C ratio on $CO_2$ gasification reactivities of other agro-industrial-biomass chars at 800 °C was investigated. **Paper IV** deals with this activity.

(c) Determining ash-melting behavior of vinasse ash as a function of temperature. A part of **Paper V** addresses this objective.

(d) Determining the levels of ash-forming elements released from vinasse during fast pyrolysis, $CO_2$ gasification, and combustion. In addition to dealing with the objectives listed under (a) to (d) above, **Papers II**, **III**, and **V** discuss these release levels.

As background work to achieve the above-listed objectives, determining the concentration and flow of ash and ash-forming elements in the integrated sugar-ethanol process was necessary. Moreover, the distribution of ash-forming elements in the various biomass and biomass residues from the integrated process was studied. This was to determine the type of association of inorganics in the biomass fuels and whether there exists any correlation between the type of association and the levels of inorganics released during thermochemical conversion. For these reasons, solids and energy balances were performed for a typical sugar mill, and elemental analysis and fuel fractionation were carried out for the biomass and biomass residues from the mill. Results of the background work are given in **Paper I**. For the vinasse, the fuel fractionation results are given in **Paper V**. Table 1 shows the tasks performed in this thesis to achieve the envisaged specific objectives, (a) to (d) above.

***Table 1.*** *Tasks performed to meet the objectives of this thesis work.*

| Specific objectives | Tasks | Publications (Papers) |
|---|---|---|
| Background | Potential for thermochemical conversion of biomass residues from the integrated sugar-ethanol process — Fate of ash and ash-forming elements | I |
| (a) | Fast pyrolysis of dried sugarcane vinasse at 400 and 500 °C: Product distribution and yield | II |
| (b) | Sugarcane vinasse $CO_2$ gasification and release of ash-forming matters in $CO_2$ and $N_2$ atmospheres | III |
| (b) | Influence of K/C ratio on gasification rate of biomass chars | IV |
| (c) | Characterization of vinasse for thermochemical conversion — Fuel fractionation, release of inorganics, and ash-melting behavior | V |
| (d) | Release of inorganics during vinasse fast pyrolysis, $CO_2$ gasification, and combustion | II, III, and V |

## 1.5. Organization of this thesis

This thesis consists of six chapters: Introduction, Background, Literature Review, Materials and Methods, Results and Discussion, and Conclusions and Recommendations for Future Work. The Introduction, Chapter 1, outlines some important properties of vinasse and the problems associated with the current use of vinasse and the need for alternative utilization options. The objectives of the thesis, the tasks carried out to achieve the objectives, and the organization of the thesis are also provided in this chapter. Chapter 2 covers the background information needed for this work, including descriptions of

the integrated sugar-ethanol production process and the various by-products/biomass residues. Chapter 2 also discusses mass and energy balances in the integrated process and the concentration, amount, and distribution of ash-forming elements in the biomass and biomass residues from the integrated process. A literature review on thermochemical conversion of vinasse and catalytic gasification reactivities of biomass chars is described in Chapter 3, while Chapter 4 lays out the materials used and the methodologies followed in this thesis. In Chapter 5, the results of the study are presented and discussed with respect to data from the literature. Finally, the main conclusions drawn from the present study and their practical implications, as well as some recommendations for future work, are given in Chapter 6.

# 2. BACKGROUND

## 2.1. The integrated sugar-ethanol process

Figure 1 shows the production steps for the integrated sugar-ethanol process from **Paper I**. The production steps and the various product and by-product streams given in the figure are described below.

*The sugarcane plant*

Sugarcane is the main input raw material for the integrated sugar-ethanol process. It is a perennial grass that belongs to the genus *Saccharum* and grows in tropical and subtropical regions. The top-right corner figure in Figure 1 shows the different above-ground parts of a sugarcane plant, i.e., the parts of the cane excluding the roots. It consists of the stem, leaves (both dry and fresh), and tops. The stem, which is also known as the *stalk*, is the part that is transported to the mill as it contains most of the sucrose for sugar and/or ethanol production. The tops constitute the part of the plant, including fresh green leaves, between the growing top tip and the uppermost node of the stem [30]. According to OECD/FAO [31], the average annual world sugarcane production is approximately 2 billion metric tons, out of which about 15% is used to produce ethanol for biofuel.

*Harvesting and transport*

Once the sugarcane plant is ripened, which usually takes about 12–24 months, it is harvested either manually or mechanically. Tops and leaves of the plant are mostly left in the cane field as *straw* (also known as *trash*) after mechanical harvesting. For cases in which manual cane harvesting is used, the leaves are burned off and the tops are chopped off the cane stalks prior to manual harvesting. The sugarcane stalks are then transported to the mill to be processed. Typical composition of clean cane stalks is 70 wt % water, and the remaining wt % is solids [32], both soluble and insoluble solids. The soluble solids are mainly sucrose, while the insolubles are predominantly fibers consisting of celluloses, hemicelluloses, and lignin. In practice, some soils and trashes are delivered to a sugar mill together with the cane stalks as impurities. These impurities in the cane stalks often limit the mill capacity and cause poor product quality.

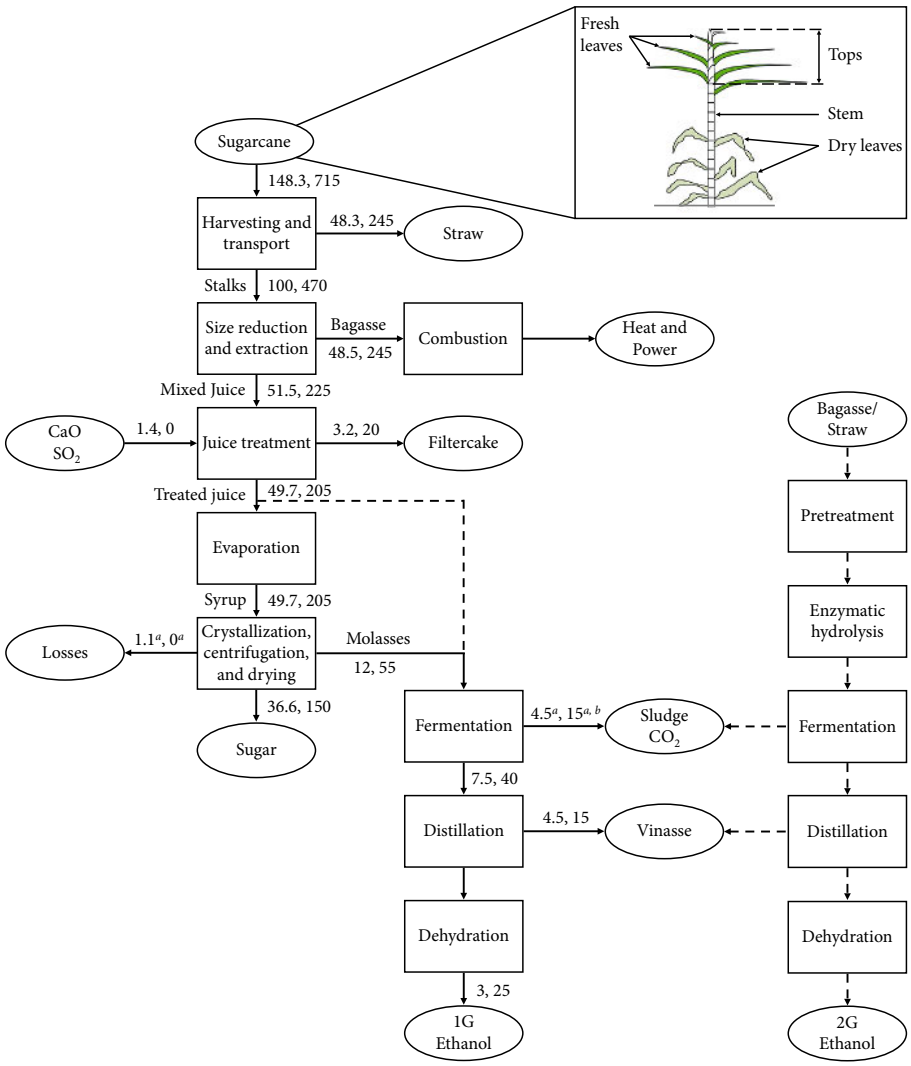


***Figure 1.*** *The integrated sugar-ethanol production process and solids and energy balances for 100 t/h of dry cane stalks, prepared cane, as input. The values given as 100, 470 are for solids (in t/h) and thermal energy (in MW), respectively.* [a]*The values were obtained by difference.* [b]*The value was assumed to be energy content of the sludge plus heat released and lost during fermentation. Adapted with permission from* ***Paper I****. Copyright 2017 © Elsevier. The upper-right-corner figure shows a sugarcane plant and its parts taken from Canilha et al.* [30].

*Size reduction and extraction*

The cane stalks that are supplied to the mill first undergo size reduction or cane preparation, during which they are chopped into pieces using a series of cane

knives and shredded into fibers with a shredder. The final fiberized cane stalks are usually called *prepared cane*. The purpose of the cane preparation unit is to expose or open up the sucrose-containing cells of the stalks for the next unit operation, extraction.

In the extraction unit, the prepared cane is washed with warm water, which is at a temperature of 60–65 °C, as it passes through a mill tandem or a diffuser system, or both used in parallel. In any of the arrangements, the purpose is to recover, as much as possible, sucrose from the cane in the form of a liquid solution called juice. The juices recovered from the different mill sets or diffuser systems are mixed; the *mixed juice*, also referred to as *raw juice*, is first screened and then pumped to the *juice treatment station*, also known as the *juice clarification process*. The sucrose-lean fibrous material leaving the juice extraction unit, *bagasse*, contains approximately 50 wt % moisture and 50 wt % fiber. It is mainly combusted in a boiler to generate heat and power for the mill. Usually, sugar mills produce surplus bagasse as well as electricity. The surplus electricity is mostly exported to a national grid, whereas the excess bagasse, as well as the straw, is being investigated as a means to produce second-generation (2G) bioethanol via the enzymatic hydrolysis route [33] shown in Figure 1. Moreover, bagasse and/or straw pyrolysis [34–40] and gasification [41–44] studies have been conducted for bio-oil and syngas production, respectively.

*Juice treatment or clarification*

The raw juice supplied to the juice clarification process is composed of about 80–85 wt % water; the balance is solids [45], mainly sucrose. It is acidic, pH = 5–6 [32], and contains suspended solids and proteinaceous materials as impurities. For the purposes of mainly neutralizing the pH and removing the impurities, the raw juice is treated with heat, lime, and $SO_2$ (in the case of direct white sugar production) and allowed to settle in a clarifier. The underflow or mud from the clarifier is strained through a filter to recover residual sucrose from the mud as filtrate. The filtrate is mostly recycled back to the extraction step or mixed juice. Fine bagasse, known as *bagacillo*, which is obtained by screening the bagasse, is added to the mud as a filtration aid. The filtration process generates a by-product called *filtercake*, also known as *pressmud*, which is the residue retained on the filter. The filtercake contains most of the phosphate from the raw juice. The phosphate in the raw juice precipitates out of the juice as calcium phosphate during the juice clarification process and is separated from the filtrate with the filtercake. For this reason,

the filtercake is mainly used as fertilizer or soil conditioner either alone or after co-composting it with vinasse.

*Evaporation, crystallization, centrifugation, and drying*

The supernatant from the clarifier known as *clarified* or *clear juice* is concentrated in multiple-effect evaporators to produce a syrup with 60–65 wt % dissolved solids. The syrup is then further concentrated by boiling under vacuum to crystallize the sucrose. The resulting mixture of sugar crystals and mother liquor, commonly referred to as *massecuite*, is separated using centrifuges. The sugar crystals are then dried, cooled, conditioned, weighed, bagged, and stored. The massecuite from the centrifuges is typically subjected to further rounds of crystallization and centrifugation to maximize sugar recovery, until finally, exhausted massecuite called *molasses* remains. The molasses is viscous with a typical solids content of 75–85 wt % [32], mainly sugars and inorganics, and its pH is usually in the range of 5–6 [32]. It is largely used as a raw material for first-generation (1G) bio-ethanol production.

*Fermentation, distillation, and dehydration*

The bio-ethanol production process involves pretreatment of the molasses; fermentation of the residual sugars in the treated molasses; and distillation, rectification, and dehydration of the fermented mass. The molasses pretreatment includes mainly pH adjustment and dilution with water. The dilution is to adjust the concentration of sugars in the molasses to a level suitable for yeast cells, the microorganism responsible for fermentation. The diluted molasses is often referred to as *mash*. At the yeast propagation stage of fermentation, nutrients such as urea and diammonium phosphate are added to the mash for yeast growth. During mash fermentation, in either batch or continuous reactors, the yeast cells convert the sugars into ethanol and $CO_2$ under anaerobic conditions. The $CO_2$ gas can be scrubbed to remove entrained impurities from the fermentation process and can then be sold to bottling companies as food-grade $CO_2$. In addition to the $CO_2$ as a gaseous fermentation by-product, some sediments are left in the fermentation reactors as *sludges*, which are usually disposed of to the cane field. The fermented mash, also called *beer*, is first centrifuged for the purpose of recycling the yeast mass, and then the de-yeasted beer is distilled, rectified, and dehydrated in a series of distillation units. The dehydration stage removes traces of water left in the ethanol after rectification so that the bio-ethanol can be utilized as a fuel for vehicles. The distillation step generates the dilute effluent, *vinasse*, described in sections 1.1–1.2. In some processes, as shown with the dashed lines in Figure 1

for the 1G bio-ethanol, the clear juice from the clarification process is partially or entirely directed to the distillery for bio-ethanol production.

## 2.2. Solids and energy balances in the integrated process

Solids balance in the integrated process, coupled with the concentration of ash-forming elements in the by-products from the integrated process, serve as a basis for determining the fraction of the ash-forming elements from the cane that end up in the by-products. Determination of the amounts of ash-forming elements in the various biomass residues, as well as knowledge of their energy share, is essential for assessing the potential of the biomass residues for thermochemical conversion. Here, the solids and energy shares of the products and by-products from the integrated process are presented. The concentration of ash-forming elements in the by-products and the percentages of K and Cl they share from the whole cane are given in sections 2.3 and 2.4, respectively. K and Cl are selected since they are the main ash-forming elements responsible for the ash and ash-related problems in thermochemical conversion processes. Details of the solids and energy balances, as well as the flow of ash and ash-forming elements in the integrated process, are available in **Paper I**.

Solids and energy balances, on a dry basis, for a typical integrated sugar-ethanol mill using 100 t/h of prepared cane as the starting (or input) material are given in Figure 1. The energy balance values are on an ash-free basis. The average 16 kg of straw (dry basis) to 100 kg of prepared cane stalks (wet basis) ratio suggested by Leal *et al.* [46] was used to calculate mass flows for the whole cane and cane straw. Energy balance closure on the fermentation unit is not expected due to energy lost with the sludge and heat released and lost during the exothermic fermentation reaction. Even the energy balance closures on the evaporation and crystallization processes were obtained partly by difference. In practice, however, it is unlikely to close energy balances on these units. This is because, in addition to energy loss with the solids lost, there is heat released and lost during evaporation and crystallization processes because of some sugar inversion and thermal degradation reactions.

As seen from Figure 1, the straw, which is mostly left in the cane field unutilized, and the bagasse each represent approximately one-third of the solids and energy from the whole cane. The remaining one-third of the solids and energy from the whole cane is found in the mixed juice, mainly as sugars. It is only this latter portion of the solids and energy from the cane which ultimately ends up in the products, sugar and ethanol, and by-products, filtercake and vinasse. The filtercake accounts for only about 2% and 3% of the

solids and energy in the whole cane, respectively. Yet, a significant amount of the filtercake, approximately 40%, comes from the lime and sulfur added during the juice treatment stage. The solids and energy shares of the product sugar are about 25% and 20%, respectively, of the amounts in the whole cane, while the corresponding values for the bio-ethanol are only about 2% and 3.5%. The final by-product from the integrated process, vinasse, contains approximately 3% and 2% of solids and energy, respectively, from the whole cane. Nevertheless, the amounts of the bio-ethanol and vinasse, and thus their energy shares, increase considerably in cases where the cane juice, in addition to the molasses, is partly or entirely used for ethanol production. This scenario is shown with the dashed lines in Figure 1 for the 1G bio-ethanol production route.

## 2.3. Concentration of ash-forming elements in the biomass and biomass residues from the integrated process

Figure 2 shows the concentration of ash-forming elements, on a wt % dry biomass basis, in the stalks, tops, leaves, prepared cane, bagasse, filtercake, molasses, and vinasse from an integrated sugar-ethanol mill. The data in the figure are taken from **Papers I** and **III**.

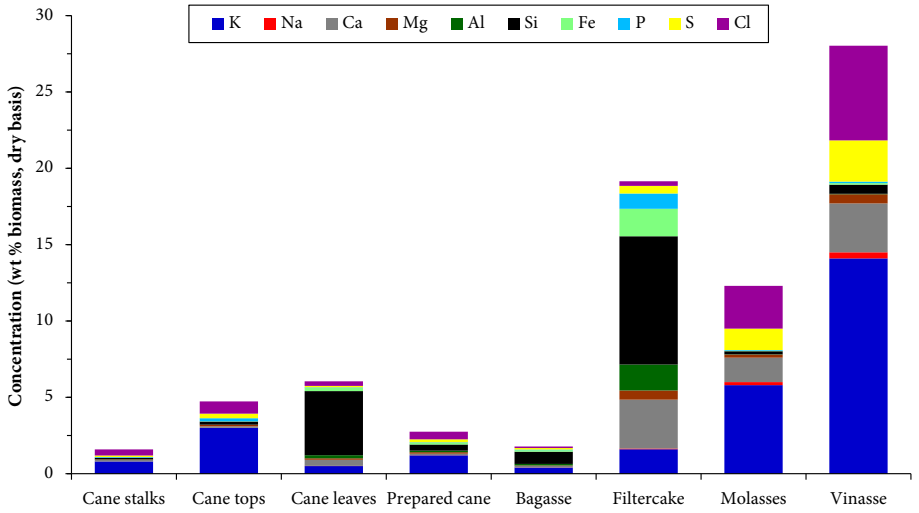


***Figure 2.*** *Concentration of ash-forming elements, on a wt % dry biomass basis, in the different parts of a sugarcane plant and the various biomass residues from the integrated sugar-ethanol process. Data for the stalks, tops, leaves, prepared cane, bagasse, filtercake, and molasses are from* ***Paper I****. Data for the vinasse are from* ***Paper III****.*

In general, among the three different parts of a sugarcane plant, the leaves contain the highest concentration of ash-forming elements followed by the tops, while the stalks have the least. This is mainly due to higher metabolic activities, demanding more inorganic elements as nutrients, in the leaves and tops than in the stalks. Moreover, it can be observed from the figure that the concentration of ash-forming elements generally increases in the integrated sugar-ethanol process from the input raw material, prepared cane, to the final by-product, vinasse. This trend is in part due to the removal of organics from the process as products (e.g., sugar and ethanol) and by-products (e.g., bagasse and filtercake) at a higher degree than for the inorganics. The high concentration of ash-forming elements in the filtercake, in this particular case, is partly due to contamination of the filtercake sample with soil during sample collection. Nevertheless, literature data show that there are large variations in the concentrations of ash-forming elements in sugarcane plants and the various biomass residues from the integrated sugar-ethanol process. The variations are due to several factors, including differences in cane varieties and maturity levels [47,48], environmental conditions (e.g., weather and soil types) [47], agricultural practices [6], and production processes [4,5].

Moreover, Figure 2 shows that the vinasse has the highest concentrations of K and Cl, whereas the bagasse contains the least. The molasses, the precursor for the vinasse, has the second-most abundant K and Cl. The tops and leaves, which make up the straw, contain considerable levels of K and Cl, whereas the filtercake is rich in Ca, Al, Si, Fe, and P. Aside from the sample contamination with soil, as noted earlier, the addition of $SO_2$ gas and lime as $Ca(OH)_2$ to the raw juice for treatment increases the concentration of Ca in the filtercake. The added lime also increases the P content of the filtercake by precipitating phosphates present in the juice. The Ca and P are removed from the juice with the filtercake, mainly as $Ca_3(PO_4)_2$ and $CaSO_3$. However, these latter ash-forming elements are less troublesome for thermochemical conversion processes than are the K and Cl. For example, according to Zevenhoven *et al.* [49], they mainly remain in the bottom ash or are carried over with the flue gas as fly ash during combustion.

## 2.4. Fate of K and Cl in the integrated process

Figure 3 shows the percentages of K and Cl in the four main by-products from the integrated sugar-ethanol process based on the amounts of the elements in the whole cane. The values were calculated based on the solids balance and concentrations of the elements given in sections 2.2 and 2.3. The K and Cl

amounts in the straw were calculated based on the straw mass flow, K and Cl concentrations in the tops and leaves, and an average ratio of 9 kg leaves (dry basis) to 1 kg tops (dry basis). The ratio of leaves to tops was calculated from the experimental data found in the report by Hassuani *et al.* [43]. The K and Cl levels in the whole cane were obtained from the sum of the amounts in the prepared cane and straw for the corresponding elements. The mass balance closures are 80% and 76% for K and Cl, respectively. The missing K and Cl are mainly due to material losses and formation of deposits in the evaporators, vacuum pans (crystallizers), and distillation columns. The collection of the molasses and vinasse samples and the rest of the biomass samples from the integrated process during two different production seasons might have also contributed to the discrepancy in the mass balance closures.

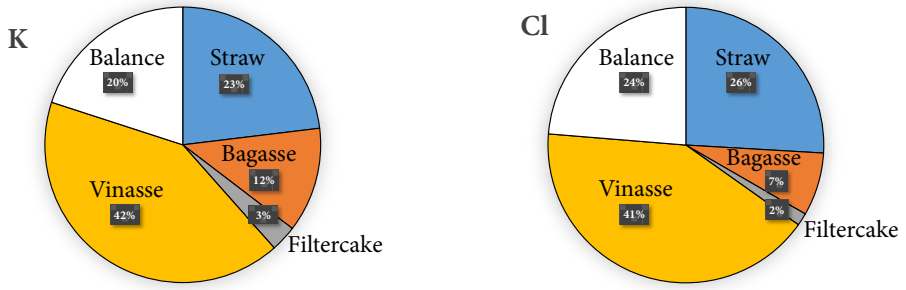


***Figure 3.*** *The percentages of K and Cl in the biomass residues from the integrated sugar-ethanol process based on the amounts in the whole cane. Data from* ***Paper I****.*

Figure 3 also shows that approximately 25% of the K and Cl in the whole cane is found in the straw. The remaining 75% of these elements from the whole cane is in the prepared cane (cane stalks). This amount of K and Cl in the prepared cane splits into two streams: roughly 10% remains in the bagasse, while the balance, 65%, is leached from the cane with the raw juice. As seen in Figure 3, about 40% of the K and Cl from the whole cane ends up in the final by-product, vinasse. However, the filtercake contains only about 2–3% of the K and Cl from the whole cane.

## 2.5. Distribution of ash-forming elements

In addition to the concentration of ash-forming elements in a biomass fuel, the distribution of ash-forming elements in the fuel is an important factor for the design, development, and operation of thermochemical conversion processes. Fuel or chemical fractionation is an advanced method developed to characterize the distribution of ash-forming elements in a solid fuel. The

method was first developed by Benson and Holm [50] for coal, and later Baxter *et al.* [20] applied a modified version of the method to seven biomass fuels. Zevenhoven [51] has made further refinements in the method for biomass characterization. The method can be used to determine the type of association of ash-forming elements in the fuel, i.e., whether the inorganics in the fuel are present as minerals or organically bound species. Knowledge of the association of ash-forming elements in biomass fuels may provide information on the volatility of the ash-forming elements during a thermochemical conversion process, and on their water leachability prior to thermochemical conversion. It involves sequentially leaching a solid fuel in increasingly aggressive solvents: $H_2O$, $NH_4Ac$, and HCl. The typical salts leached out by $H_2O$ are alkali sulfates, carbonates, and chlorides [52]. Elements leached out by $NH_4Ac$ are the ion exchangeable elements, such as Ca. The organically associated K and Na are believed to also be leached by $NH_4Ac$. HCl leaches the water-insoluble carbonates and calcium oxalate ($CaC_2O_4$). Silicates and other minerals remain mainly in the insoluble fraction. Organically bonded sulfur and chlorine may be found in the rest fraction as well.

The $H_2O$- and $NH_4Ac$-soluble ash-forming elements are sometimes referred to as the more "reactive"/"volatile" species [53]. These species are assumed to be released during thermochemical conversion of biomass and may deposit on superheater tubes and other heat exchangers of a boiler/gasifier, causing the ash-related problems. Moreover, the HCl-soluble ash-forming elements and those remaining in the fraction after leaching with HCl, i.e., those in the rest fraction, are denoted as the "less-reactive" species [53]. In contrast to the $H_2O$- and $NH_4Ac$-soluble ash-forming elements, the latter species might not cause the ash-related problems as they largely form coarse ash particles that can be removed from the boiler/gasifier as bottom ash.

Figure 4 shows the distribution of ash-forming elements in the sugarcane stalks, tops, leaves, bagasse, and vinasse. The data used in the figure for the stalks, tops, and leaves were taken from **Paper I**, whereas for the vinasse, the data were from **Paper V**. For the bagasse, the elemental analysis and chemical fractionation data were from Jordan *et al.* [54]. The inner-left-corner figure in Figure 4 shows a magnified version for the distribution of Si, Al, and Fe in the biomasses.

Figure 4 also shows that all the ash-forming elements, except Si, Al, and Fe, in all the biomass samples are mainly in the $H_2O$- and $NH_4Ac$-soluble fractions, with most of the ash-forming elements being almost completely water-soluble.

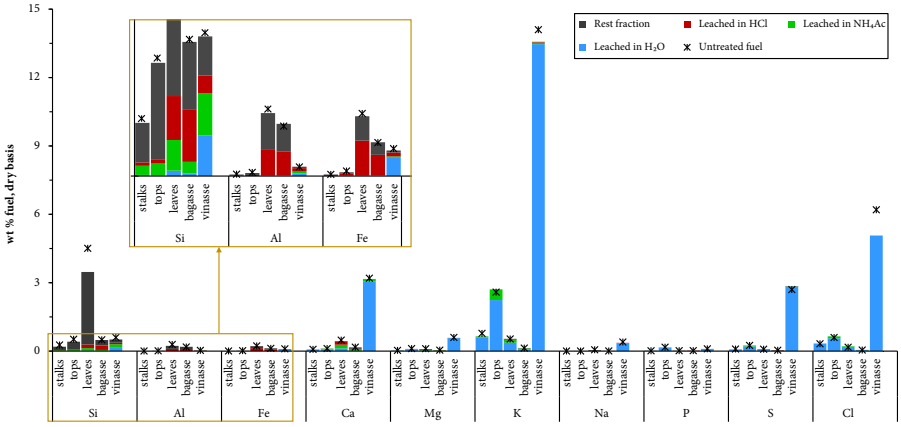


***Figure 4.*** *Distribution of ash-forming elements in the sugarcane stalks, tops, leaves, bagasse, and vinasse. Data for the stalks, tops, and leaves are from* ***Paper I****. Data for the vinasse are from* ***Paper V****. Data for the bagasse were taken from reference* [54].

It can be observed from the figure that Si, Al, and Fe in the stalks, tops, leaves, and bagasse are mainly in the HCl-soluble and rest fractions. Most of the Si, Al, and Fe in other solid biomass fuels [52,55] are also in the acid-soluble and rest fractions. However, significant levels of these ash-forming elements in the vinasse, about 50% of the Si and Al and 70% of the Fe, are $H_2O$- and $NH_4Ac$-soluble. This anomalous property of the Si, Al, and Fe in the vinasse is attributed to the fact that vinasse originates from cane juice, which is obtained by water-leaching of the prepared cane, and that it is acidic. The acidic nature of vinasse enhances the dissolution of Si, Al, and Fe in the vinasse that would otherwise have been present in the insoluble form.

## 2.6. Summary

The straw and bagasse each constitutes approximately one-third of the mass and energy from the whole cane, making them potential biomass residues for thermochemical conversion. The bagasse is a trouble-free fuel for thermochemical conversion since its K and Cl concentrations are low. However, the significant levels of these problematic ash-forming elements in the straw indicate that the straw is a difficult fuel for thermochemical conversion. Nevertheless, the leaching of most of the K and Cl by water from the straw, tops and leaves, suggests that water washing the straw prior to a thermochemical conversion process could upgrade the fuel. The filtercake represents about 2–3% of the mass, energy, and K and Cl from the whole cane.

The low level of K and Cl in the filtercake indicates that it can be burned or gasified trouble-free in conventional boilers or gasifiers.

The vinasse, the final by-product from the integrated sugar-ethanol process, contains only about 2–3% of the mass and energy, but about 40% of the K and Cl from the whole cane. Furthermore, almost all the K and Cl in the vinasse are $H_2O$- and $NH_4Ac$-soluble, indicating that these ash-forming elements may be effectively released from the vinasse during thermochemical conversion process. The high levels of K and Cl in the vinasse, together with its high water content, have been the main challenges for vinasse thermochemical conversion in conventional systems. Nonetheless, interests are emerging from boiler suppliers in the business of designing and developing special commercial-scale boilers for vinasse combustion. This interest, together with the efforts made so far in vinasse combustion, gasification, pyrolysis, and liquefaction, are reviewed in the next chapter.

# 3. LITERATURE REVIEW

## 3.1. Vinasse combustion

Combustion is the most highly developed and most commonly used thermochemical conversion technology for heat and power production from biomass [56]. In addition to generating useful energy, the technology is an effective means for waste disposal as well as for the recovery of chemicals of economic value. An example is the Kraft recovery boiler, described in section 1.1, for burning black liquor from pulp mills. For vinasse, however, combustion technology has not been successful despite several efforts over the last century.

According to Kujala *et al.* [57] (cited in Cortez and Pérez [7]), the concept of vinasse concentration followed by combustion dates back to the 1920s, when the Porion Furnace was developed by Whitaker and U.S. Industrial Chemicals Inc. Detailed descriptions of historical developments in vinasse combustion are available from Cortez and Pérez [7], Cortez *et al.* [58], and Akram *et al.* [59]. Here, the historical developments in vinasse combustion are summarized.

The early (from the 1920s to the 1960s) technologies for vinasse combustion, including the Porion Furnace, were mainly for the purposes of recovering ash from vinasse for fertilizer and destroying the organic fraction of the vinasse. The latter purpose was to mitigate the problems arising from vinasse disposal to the environment. For example, Reich [60] proposed first concentrating vinasse to 70–80% solids and then producing activated carbon and "potash liquor". The proposed process involves carbonizing (or pyrolyzing) the concentrated vinasse at around 340–350 °C, followed by treating the resulting char containing potassium salts at 870 °C, and finally leaching the salts from the char with water. The leachate or "potash liquor" is rich in KCl and $K_2SO_4$ for fertilizer use. The char from the leaching system is treated with HCl and then dried to be used as activated carbon. Chakrabarty [61] used the same principle as Reich to build a pilot plant for the recovery of potassium salts from vinasse, except that crystallized $K_2SO_4$ is produced. Moreover, several investigators, including Dymond [62], Cortez *et al.* [58], Cortez and Pérez [7], and Akram *et al.* [59], mentioned that two vinasse incineration plants were installed in Brazil in the 1940s for the recovery of ash from vinasse for use as fertilizer. However, the incinerators were closed shortly afterward for economic reasons [7,55]. Furthermore, Gupta *et al.* [63] combusted vinasse concentrated to 30–40% dry solids in a fluidized bed

column at 700 °C where the ash was collected from the bottom of the column for use as fertilizer. A similar system was described by Dubey [64] for co-combusting vinasse containing 60 wt % solids with bagasse. However, Monteiro [65] reported that vinasse incineration for fertilizer production was not economically feasible in the Brazilian case.

Attempts to combust vinasse for energy recovery, as well as for fertilizer production and waste disposal, started in the mid-1970s when Kujala *et al.* [57] suggested vinasse combustion in a fluidized bed reactor followed by heat recovery in an afterburner. Moreover, Yamauchi [66] (cited in Sheehan and Greenfield [67]), co-fired vinasse concentrated to 21% solids with heavy fuel oil. Here, the heat from the flue gases and ash was used to concentrate the vinasse, and the ash was subsequently separated from the flue gases to be used as fertilizer. According to Cortez *et al.* [58] and Spruytenburg [68], a Dutch company, Hollandse Constructie Groep BV (HCG), installed two vinasse incineration plants for a distillery in Thailand. In the same year, Nilsson [69] reported that the Swedish company Alfa Laval AB conducted technical and economic feasibility studies of vinasse combustion. Cortez *et al.* [58] also reported that another Dutch Company, NEM BV, installed two vinasse combustion boilers in Bangyikhan distillery in Bangkok, Thailand. They reported that the boilers operated satisfactorily for 12 years. In all the boilers from the three companies, a swirl combustion technology for burning vinasse concentrated to 60 wt % dry solids was used. Although Polack *et al.* [2] could not succeed in combusting Louisiana vinasse, Cortez and Pérez [7] were successful in co-combusting Shepherd Oil Distillery vinasse concentrated to 45 wt % dry solids with heavy fuel oil. The latter authors suggested that the co-combustion of vinasse with heavy fuel oil is feasible when the fuels are mixed in ranges from 5%/95% to 50%/50% vinasse to heavy fuel oil proportions. Patel [6], in his doctoral thesis work, reported self-sustained combustion of vinasse in an inclined lab-scale reactor when the vinasse is concentrated to a minimum of 60 wt % solids content. Patel also determined the ignition and combustion characteristics, including swelling, ignition delay, flaming, and char glowing properties, of dried vinasse and vinasse concentrated to 65 wt % solids. However, a recent study by Akram *et al.* [59] showed that co-firing of vinasse containing 58 wt % solids with coal in a laboratory-scale fluidized-bed combustion facility caused bed agglomeration problems.

Although most of the above reports indicate success in vinasse combustion, there are no industrial-scale vinasse combustion technologies currently in operation. Nevertheless, boiler suppliers have recently shown interest in

designing and developing special boilers for burning concentrated vinasse. For example, Valmet was the main funder for a project on vinasse concentration conducted by Larsson and Tengberg [70]. Additionally, Crealabs S.R.L. [71], a local consulting company in Buenos Aires, Argentina, has patented combustion of vinasse concentrated to 60 wt % dry solids in a recovery boiler followed by recovery of potassium as potassium sulfate from the bottom ash. Furthermore, Andritz AG has recently conducted a study on the design and development of a special type of boiler for combusting concentrated vinasse for a customer in Argentina [personal communication with Andritz AG].

## 3.2. Vinasse gasification

Biomass gasification is considered as one of the promising routes for syngas or combined heat and power production because of its potential for providing high energy efficiency cycles [72]. For this reason, wide ranges of biomasses and waste products have been studied as potential fuels for gasification. However, information in the literature on gasification of vinasse is very limited. Patel [6] studied gasification of vinasse concentrated to 70–75 wt % dry solids using a vertical spray-type laboratory-scale reactor at a temperature range of 680–730 °C and under sub-stoichiometric air conditions. His report shows that about 95% carbon conversion was achieved, and the gaseous product was composed of mainly $CO_2$, CO, $H_2$, $CH_4$, $H_2O$ vapor, and $H_2S$.

However, gasification of vinasse using $CO_2$ gas as a gasifying agent in lieu of oxygen from the air has not been studied. $CO_2$ gas for vinasse gasification can be obtained from boiler flue gases of the integrated sugar-ethanol process. According to Sadhwani *et al.* [73], utilization of $CO_2$ gas from flue gases for biomass gasification serves a dual purpose: reduction of GHG emissions and generation of syngas. Vinasse $CO_2$ gasification characteristics, which are important for the design and development of industrial-scale vinasse gasification processes, that require study include the release of inorganics from vinasse.

Another type of gasification process, called supercritical water gasification (SCWG), is a process through which wet biomasses are converted to gaseous fuels, mainly $CH_4$, $H_2$, and CO, at temperatures and pressures above the critical point of water. According to several reports, e.g., [74–77], the main advantage of SCWG is that biomasses with very high moisture content, i.e., ≥ 80 wt %, can be converted without prior drying. This would make vinasse a potential fuel for SCWG processes. Moreover, Loppinet-Serani *et al.* [78] have investigated SCWG of vinasse from a wine distillery at 400, 450, and 500 °C

and 25 MPa. The vinasse used in their study shares some properties with sugarcane vinasse: both vinasses have similar heating values, and potassium is their dominant cationic inorganic element. Their report shows that the SCWG gas-phase product consists of mainly $CO_2$, CO, $H_2$, and $CH_4$ and that the concentrations of the latter three gases in the gas phase improved with temperature, while $CO_2$ decreased. However, the authors reported that most of the potassium from the vinasse was found in the aqueous phase product, making SCWG a challenging process for the recovery of potassium for fertilizer. In addition, according to Richard *et al.* [79], potassium, mainly as KCl, is known to cause serious corrosion problems in SCWG reactors. Furthermore, recently, Costa [80], in her M.Sc. thesis work, has demonstrated using Aspen Plus software modeling that SCWG of vinasse is not economically feasible.

## 3.3. Catalytic $CO_2$ gasification reactivities of biomass chars

Most biomasses contain both K and Ca as their main cationic ash-forming elements. These elements, as well as their compounds, e.g., carbonates, are known to catalyze biomass char gasification reactions. Several reports in the literature, for instance, Li and Van Heiningen [81], suggest that the reaction mechanisms for catalytic gasification of biomass chars are similar to those for graphitized carbon [82], activated carbon [83], and ash-free coal chars doped with alkali carbonates [84]. Most of these works suggest that catalytic gasification reactions occur via a redox mechanism involving oxygen transfer to a free carbon site, resulting in carbon-oxygen surface complexes. For example, the redox reaction mechanisms given in Eqs. (1)–(4) are proposed by Sams and Shadman [82] for catalytic $CO_2$ gasification of graphitized carbon by alkali carbonates. In reactions (1)–(4), M is an alkali metal, and ($-CO_2M$) and ($-COM$) are the fully oxidized and partially reduced species, respectively. Sum of the reactions in Eqs. (2) and (3) gives the Boudouard reaction, Eq. (4).

$$M_2CO_3 + C \leftrightarrow (-CO_2M) + (-COM) \quad (1)$$

$$(-CO_2M) + C \leftrightarrow (-COM) + CO(g) \quad (2)$$

$$(-COM) + CO_2(g) \leftrightarrow (-CO_2M) + CO(g) \quad (3)$$

$$C + CO_2(g) \leftrightarrow 2CO(g) \quad (4)$$

However, it is difficult or even impossible to investigate, using raw biomass fuels, the influence of these metals or their compounds on the catalytic gasification reactivities of biomasses. This is because other inorganic elements, such as Na and Mg [22,85], which are mostly present in biomass in trace

amounts compared to K and Ca, may influence the catalytic gasification rates. Consequently, in order to study the influence of K or Ca on gasification rates, many investigators, e.g., [22,24,85], first demineralized the raw biomass and then doped it with controlled amounts of K or Ca. In general, biomasses doped with higher amounts of K or Ca showed higher reactivities, although there are some exceptions. Perander *et al.* [24], for example, demonstrated that, for the same amount of Ca, the gasification rates depended on the type of procedure used to dope the biomass with the catalyst.

Although several studies on factors affecting char gasification reactivities are available in the literature, the influence of catalyst accumulation on the char surface as the carbon is consumed by gasification has not been investigated. The accumulated catalyst can continue to participate in the char gasification reactions via complex migration [83,86–88]. As the carbon is consumed, the ratio of the catalyst to carbon increases as a function of the degree of char conversion. However, since other factors such as loss of K occur, it is difficult to predict how the catalyst/carbon ratio changes as a function of char conversion. For the vinasse, it would be interesting to see how the influence of catalyst/carbon ratio on char gasification rate compares with that of other agro-industrial biomass fuels.

## 3.4. Vinasse pyrolysis and liquefaction

Pyrolysis is a thermochemical conversion route in which biomass is thermally treated in the absence of oxygen for the production of solid (char), liquid (bio-oil), and gaseous products. It is also the first stage of biomass combustion and gasification [89]. Depending on how fast the biomass is heated to the pyrolysis temperature, there are two main variants of biomass pyrolysis: conventional (or slow) and fast [89–91]. Slow pyrolysis is characterized by low heating rates and long residence times of the pyrolysis vapors in the pyrolyzer, and it is used to obtain high char yields [89–95]. On the other hand, fast pyrolysis requires high heating rates and short residence times and rapid cooling of the pyrolysis vapors with the target of maximizing the bio-oil yield [89–95]. Reactor configuration, such as bubbling and circulating fluidized beds, and finely-ground biomass particles are among the key parameters to achieve high heat transfer and heating rates in fast pyrolysis processes.

According to Bridgwater [92], biomass slow pyrolysis for the production of charcoal has been used for thousands of years, whereas interest for bio-oil production from biomass via fast pyrolysis has grown considerably over the last 40 years. The increase in bio-oil interest is due to several advantages of the

bio-oil over its parent fuel, solid biomass. These advantages include reduced storage and transportation costs and higher energy density. In addition, the bio-oil is a renewable fuel, and it can be used as a feedstock for production of chemicals. Accordingly, developments of industrial-scale fast pyrolysis processes are underway. For example, the Fortum Otso bio-oil plant in Joensuu, Finland [96], is the first of its kind; it is an economical and energy-efficient industrial-scale fast pyrolysis plant integrated with a combined heat and power process.

Fast pyrolysis of various biomass types, including wood, agricultural by-products, energy crops, and solid wastes, has been intensively studied, and comprehensive review papers are available [90,92]. However, data on the fast pyrolysis of sugarcane vinasse are not available in the literature.

Aside from fast pyrolysis, another thermochemical conversion process that has been studied for the production of bio-oil from biomass is direct liquefaction, also known as hydrothermal liquefaction (HTL). This process is similar to SCWG in that water is used as a solvent or reaction medium, and wet biomasses do not require prior drying. However, unlike SCWG, whose goal is to obtain as much gaseous product as possible, the target of HTL is to maximize bio-oil throughput. Moreover, HTL processes are carried out at moderate temperatures, 280–370 °C, under subcritical water conditions [97,98]. Although several pilot-scale HTL tests, as listed in the review paper by Toor *et al.* [97], have been conducted for various biomass fuels, no large-scale HTL technologies exist at present.

For vinasse, the only HTL study available in the literature is the work by Serikawa and co-workers [10]. These investigators studied HTL of vinasse at 300 °C using a bomb-type batch reactor both with and without the addition of a catalyst: $Na_2CO_3$, $H_2SO_4$, zeolites, or fluid catalytic cracking (FCC). Their report shows that, compared to the HTL results without a catalyst, the bio-oil yield increased with the addition of $H_2SO_4$, while $Na_2CO_3$ decreased the yield. The maximum oil yield obtained under the HTL conditions was about 20 wt % on a dry vinasse basis when $H_2SO_4$ or FCC was used as a catalyst. They also reported that the concentrations of sulfur and nitrogen in the bio-oil were low with the FCC catalyst. However, here too, potassium recovery from HTL processes for fertilizer is challenging since most of the potassium is water-soluble.

## 3.5. Behavior of ash and ash-forming elements during biomass thermochemical conversion

Properties important for the design, development, and operation of biomass thermochemical conversion processes include the release of inorganics and ash-melting behavior [99]. The release of inorganics from biomass fuel is assumed to be related to the distribution of ash-forming elements in the fuel. It is suggested that the $H_2O$- and $NH_4Ac$-soluble portions of the ash-forming elements are effectively released during combustion or gasification [51]. Fuel fractionation of various biomass fuels and biomass-containing waste streams have been studied, and a database [100] of fuel fractionation is available at Åbo Akademi. From the database, the distribution of the $H_2O$- and $NH_4Ac$-soluble ash-forming elements over the HCl-soluble and rest fractions of the ash-forming elements can be retrieved for a number of biomass fuels. However, information in the literature on the levels of the $H_2O$- and $NH_4Ac$-soluble ash-forming elements released in practice during a thermochemical conversion process is very limited. Frandsen and co-workers [101] studied the release of inorganic elements from wood chips, bark, waste wood, and straw in lab-scale and pilot-scale reactors under combustion conditions. Their report shows the correlation between the fraction of the $H_2O$- and $NH_4Ac$-soluble ash-forming elements from fuel fractionation and the amounts of the ash-forming elements released during combustion is more complicated than proposed by Zevenhoven [51].

The characteristic ash-melting temperatures for ash deposits from recovery boilers are: the initial or first melting, sticky, flow, and complete melting temperatures represented by $T_0$, $T_{15}$, $T_{70}$, and $T_{100}$, respectively [11,102,103]. $T_0$ is the temperature at which the ash first begins to melt and below which there is no liquid phase, while $T_{100}$ is the temperature above which the ash is 100% molten. The sticky temperature, $T_{15}$, also known as the initial deformation temperature [102], is the temperature at which 15-20% of the ash is molten, and the ash sticks to a metal surface. However, at $T_{70}$, the flow temperature, also referred to as the radical deformation temperature [102,103], 70% of the ash is liquid, and the ash, instead of sticking, flows down a vertical metal surface. $T_{15}$ and $T_{70}$ determine the tendency of ash deposit formation and growth, bed agglomeration, slagging, and corrosion in boilers and gasifiers.

Ash-melting characteristics for black liquor, which shares some fuel properties with vinasse, are well-studied, and data are available in the literature [11,102,103]. However, vinasse ash-melting behavior has not been well-

investigated. Only Cortez and Pérez [7] mention 700 °C as the “ash fusion” temperature for vinasse.

# 4. MATERIALS AND METHODS

## 4.1. Materials

### 4.1.1. Vinasse sample collection and preparation

The vinasse sample used in this work was obtained from a sugar mill in Ethiopia. The mill distills ethanol from molasses. The sample was collected during the 2014/2015 production season, and for practical reasons, it was dried onsite at 105 °C for 24 h before shipping. The dried vinasse was ground to < 1 mm particle size in the laboratory. A further drying test of the dried and ground vinasse showed that it had a moisture content of 7.2 wt %. From this point forward in this thesis, the dried and ground vinasse is referred to as the dried vinasse, or the vinasse, for simplicity.

### 4.1.2. Vinasse char and ash

The vinasse char used for the TGA experiments described in section 4.2.3 was produced in the SPR described in section 4.2.1, whereas the ash sample used to investigate the vinasse ash melting characteristics, described in section 4.2.6, was produced at 500 °C in a muffle furnace. The char and ash production methods are described in sections 4.2.2 and 4.2.6, respectively.

### 4.1.3. Elemental compositions of the vinasse and its char and ash

The ash content of the vinasse, obtained after ashing a portion of the vinasse sample overnight at 540 °C in a muffle furnace, was 34.1 on a wt % dry vinasse basis. The ash content of the vinasse is within the 20–40 wt % [6,7,104] range available in the literature. The higher heating value (HHV) of the vinasse, which was determined by combusting samples of it in an oxygen combustion calorimeter, was 14 MJ/kg dry vinasse. The HHV value of the vinasse is similar to those of the vinasses used for combustion [6,7] and gasification [6] studies.

Table 2 lists the elemental compositions of the vinasse and its char and ash on a wt % original dry fuel basis. The procedures for the elemental analyses are outlined in section 4.3.1. As seen in the table, K and Ca are the dominant cationic inorganic elements in the vinasse and its char and ash, whereas Cl and S are the major anionics.

***Table 2.*** *Elemental compositions of the vinasse and its char and ash (wt % vinasse, dry basis). Data for the vinasse and its char are from* ***Paper III****. Data for the vinasse ashes are from* ***Paper V****.*

| Materials | Elemental composition | | | | | | | | | | | | | |
|---|---|---|---|---|---|---|---|---|---|---|---|---|---|---|
| | C | H | N | O | K | Na | Ca | Mg | Si | Fe | Al | P | S | Cl |
| Vinasse | 32.9 | 4.5 | 1.0 | 36.4 | 14.1 | 0.4 | 3.2 | 0.6 | 0.6 | 0.1 | 0.03 | 0.1 | 2.7 | 6.2[a] |
| Char | 10.1 | 0.4 | 0.4 | 17.1 | 13.5 | 0.3 | 3.1 | 0.6 | 0.6 | 0.1 | 0.03 | 0.1 | 1.6 | 4.6[a] |
| Ash[b] | 2.5[c] | n.a.[d] | n.a. | 13.5[c] | 9.5 | 0.4 | 3.2 | 0.5 | 0.6 | 0.1 | 0.1 | 0.1 | 1.7 | 4.9[a] |
| Ash[b, c] | 2.5 | n.a. | n.a. | 13.5 | 9.0 | 0.5 | 3.7 | 0.8 | 0.7 | 0.1 | 0.1 | 0.1 | 1.4 | 2.5 |

*[a]Results are from IC. [b]The ash was produced at 500 °C. [c]Results are from SEM-EDX. [d]n.a. = analysis was not done.*

### 4.1.4. Chemical compositions of the vinasse and its ash

The main water-soluble organic components of the dried vinasse, identified by the NMR described in section 4.3.2, were polyols (predominantly glycerols) and organic acids (mainly lactic acid, and to a lesser extent acetic acid). Some residual traces of carbohydrates, proteins, and aromatic groups are also present in the vinasse. Several studies, e.g., [105–108], also reported that glycerols, organic acids, sugars, proteins, and ethanol are the main water-soluble organic components of vinasse. However, no ethanol was present in the vinasse used in this work, possibly owing to the vinasse sample treatment, drying at 105 °C. The major inorganic compounds detected by the XRD, described in section 4.3.2, for the ash produced at 500 °C were KCl, $K_2(SO_4)$, $Na_2(CO_3)$, $Ca_3(PO_4)_2$, $K_2Ca(CO_3)_2$, MgO, and $SiO_2$.

### 4.1.5. Other agro-industrial biomass chars

The biomass chars used to investigate the influence of K/C ratio on the gasification reactivities of the chars were produced from Kiwi Branches (KB), Olive Branches (OB), Grape Pomace (GP), Torrefied Grape Pomace (TGP), and Sugarcane Bagasse (SCB). The first four biomass samples were supplied, dried and ground to < 1 mm particle size, by the Technical University of Lisbon, Portugal, whereas the SCB sample was obtained from the same sugar mill as the vinasse. However, unlike with the vinasse, the SCB sample was collected during the 2015/2016 production season together with other biomass samples, which were used to generate the data used to establish the background information of this thesis. Torrefaction may influence the gasification reactivities of biomass chars [109]. Torrefied grape pomace has not been investigated in this regard. Table 3 lists selected elemental compositions of the five biomass fuels and their chars from **Paper IV**. Elemental analyses of the original fuels and their chars were carried out according to the procedures

described in section 4.3.1. The ash contents of the fuels, which were obtained in the same manner as that of the vinasse, are also given in Table 3. The table shows that the ash contents of the biomass fuels are approximately one order of magnitude lower than that of the vinasse. Moreover, the concentrations of K in the chars shown in Table 3, after converting to a wt % dry fuel basis, are lower by about one order of magnitude than the vinasse char K content shown in Table 2. The K concentrations for the biomass chars given in Table 3 can be expressed on a wt % original fuel basis using the char yields given in section 4.2.2. Furthermore, for the chars given in Table 3, the SCB chars contain the highest level of Si, while the KB chars have the lowest. It is well-established that K in biomass fuels catalyzes $CO_2$ gasification reactions, whereas several reports, for example [110,111], show that high levels of Si in the fuels inhibit gasification reactivities. However, not all forms of K in biomass fuels are catalytically active; for example, KCl does not catalyze biomass gasification reactions. Hence, assuming that all the Cl in the vinasse chars given in Table 2 exists as KCl, only about 60% of the K in the chars is available for catalytic gasification reactions.

***Table 3.*** *Selected elemental compositions of KB, OB, GP, TGP, and SCB and their chars. Data from* ***Paper IV****.*

| Original fuels | Elemental composition (wt % fuel, db[a]) | | | | | Ash content |
|---|---|---|---|---|---|---|
| | C | H | N | K | Si[c] | (wt % fuel, db) |
| KB | 46.9 | 6.2 | 0.7 | n.a.[b] | n.a. | 2.6 |
| OB | 46.6 | 6.0 | 0.7 | n.a. | n.a. | 2.8 |
| GP | 49.1 | 6.4 | 1.8 | n.a. | n.a. | 4.0 |
| TGP | 62.1 | 6.1 | 2.1 | n.a. | n.a. | 5.2 |
| SCB | 48.3 | 6.8 | 0.1 | n.a. | n.a. | 3.4 |
| Chars | Elemental composition (wt % char) | | | | | |
| KB | 80.5 | 0.2 | 0.2 | 2.5 | 0.1 | n.a. |
| OB | 73.7 | 0.2 | 0.2 | 4.1 | 0.5 | n.a. |
| GP | 74.3 | 0.2 | 0.3 | 4.3 | 0.5 | n.a. |
| TGP | 73.2 | 0.3 | 0.6 | 4.5 | 0.7 | n.a. |
| SCB | 74.1 | 0.1 | 0.05 | 2.2 | 3.9 | n.a. |

*[a]db: dry basis. [b]n.a.: analysis was not done. [c]Results are from SEM-EDX.*

## 4.2. Experimental methods

### 4.2.1. Fast pyrolysis experiments

Fast pyrolysis of the dried vinasse was studied using two different reactors: a drop-tube-type reactor and a quartz-glass reactor, also referred to as a single-particle reactor (SPR). The former reactor was used to obtain product

distribution and yield (char, bio-oil, and gas) during fast pyrolysis of the vinasse at 400 and 500 °C. It was not possible to feed the vinasse into the drop-tube-type reactor at temperatures higher than 500 °C since most of the vinasse remained stuck to the sample feeding system described below. For this reason, and to obtain char yield trends with temperature in the temperature range of 400–600 °C, the SPR was used. Moreover, the SPR is a simpler setup than the drop-tube-type reactor. Nevertheless, in both reactors, the fast pyrolysis reaction was carried out in $N_2$ gas atmosphere and similar pyrolysis heating rates were attained. However, the residence time of pyrolysis vapors in the SPR was about 4 s, whereas the residence time was 5–6 times longer in the drop-tube-type reactor. The pyrolysis vapor residence time in the drop-tube-type reactor is longer than the typical 0.5–5 s [112] range for fast pyrolysis. Detailed descriptions of the two reactors and the fast pyrolysis experimental procedures are available in **Paper II**. General descriptions of the reactors and experimental procedures are given below.

*Fast pyrolysis experiments in the drop-tube-type reactor*

Figure 5 shows the schematic diagram of the fast pyrolysis experimental setup in the drop-tube-type reactor. The setup has three main parts: the drop-tube-type reactor, the bio-oil recovery system, and the pyrolysis gas analysis section. These three parts are indicated in the figure by the enclosed boxes A, B, and C, respectively. The drop-tube-type reactor (A) is the heart of the setup. It is made of steel; has an internal diameter of 0.08 m and an overall height of 1.12 m; and consists of a preheater, a char holder, and a pyrolyzer. Nitrogen ($N_2$) gas, which purges pyrolysis gases from the reactor, enters the reactor from the bottom at a flow rate of 3 $l_N$/min, and it was preheated before entering the char holder. The char holder was used to recover the pyrolysis chars for the purpose of mass balance and char analysis. To retain the chars in the char holder, a stainless steel wire mesh was placed on a perforated steel plate and inserted between the char holder and the preheater.

The reactor was inserted in an electrically heated furnace, and the temperature of the reactor was controlled automatically to the desired point by setting the furnace temperature. The temperature inside the reactor was measured at four different locations: in the preheater, in the char bed, above the char bed, and close to the top/upper lid of the reactor. These temperatures are indicated in the figure as TC-0, TC-1, TC-2, and TC-3, respectively. The temperatures were measured using K-type thermocouples, and the data were logged with a computer. The controlled reactor temperature was the

temperature in the char bed, TC-1. A plot of the temperature profiles of TC-0, TC-1, TC-2, and TC-3 as a function of time (in minutes) for typical experiments can be found in the Appendix of **Paper II**.

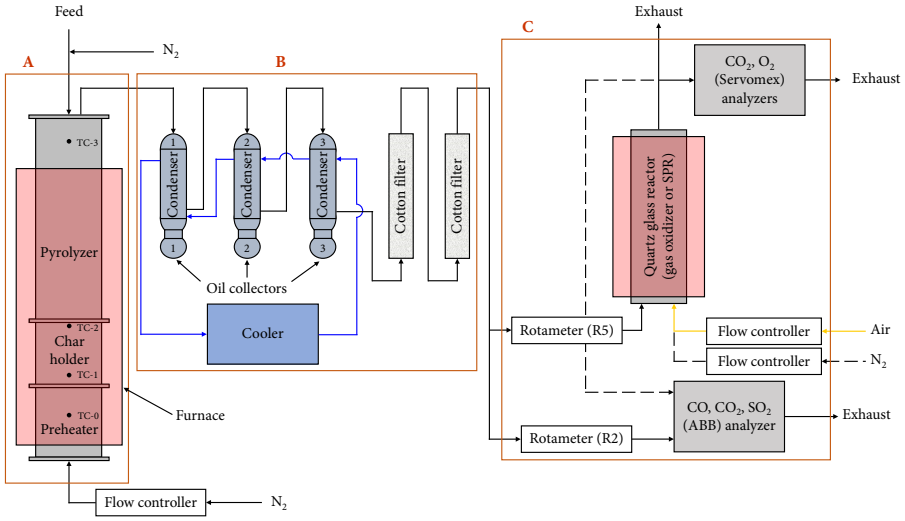


***Figure 5**. Schematic drawing of the fast pyrolysis experimental setup in the drop-tube-type reactor. Adapted with permission from **Paper II**. Copyright 2019 © American Chemical Society*

For sample feeding into the reactor from the top side, an airtight feeding system was used. It consists of a plastic bottle with a flexible hose connected to it. The flexible hose was then connected to a vertical steel pipe, which enters the reactor from the upper lid and extends a few centimeters into the reactor. The steel feed pipe was provided with an $N_2$ gas supply line for sample feeding in pulses. Short $N_2$ pulses were used for the sample feeding.

The bio-oil recovery system (B) consists of a series of three condensers, two cotton filters installed after the third condenser, and a cryostat cooler. Each condenser was fitted with an oil collector underneath. In addition, a stainless steel (SST) pipe connects the reactor with the first condenser, whereas silicon tubes were used to connect the condensers, cotton filters, and the last condenser with the first filter. The pyrolysis vapors were condensed in the condensers, which were cooled to -40 °C using the cryostat cooler, and the pyrolysis oils were partly recovered into the oil collectors. A part of the pyrolysis oils condensed in the condensers remained stuck to the condenser walls. Oils were also condensed in the SST pipe and silicon tube connections as well as on the upper lid of the pyrolyzer. Oil aerosols, tiny oil droplets that

were carried over from the condensers with non-condensable gases, were captured in the cotton filters.

The non-condensable gases leaving the last cotton filter were supplied to the gas analysis section, enclosed by box C in the figure, of the setup. This part of the setup consists of the SPR and two gas analyzers as the main units. The dashed lines shown in the gas analysis system show the connections used during the fast pyrolysis experiments in the SPR described below. The flow of the non-condensable gases exiting from the last cotton filter was split into two streams. One stream was mixed with air and oxidized at 900 °C in the SPR, which was enclosed in an electrically heated oven, and analyzed for $CO_2$ by using the Servomex gas analyzer. The other stream was routed through the ABB gas analyzer for CO, $CO_2$, and $SO_2$ analysis. The gas flow rates to the SPR and ABB gas analyzer were measured using rotameters, whereas the airflow rate to the reactor was maintained at 2.41 $l_N$/min.

After the desired temperature for pyrolysis in the drop-tube-type reactor was reached, about 40 g of the dried vinasse sample was weighed into the plastic sample feeding bottle described above. The sample was fed into the pyrolyzer in batches of about 8–10 g each. Injection of the sample batch with short and pressurized $N_2$ pulses disperses the finely ground sample, which is rapidly heated while falling onto the char bed. The experiment was stopped when the CO and $CO_2$ readings from the gas analyzers were close to 0.01%. The net sample weight fed to the pyrolyzer was determined by subtracting the weight of the sample left in the feeding system from the initial weight of the sample weighed into the plastic bottle. Part of the sample was stuck to the walls of the steel-pipe part of the feeding system, which was exposed to a temperature of 100–150 °C near the upper part of the pyrolyzer. The sample left in the feeding system was carefully recovered after each experiment, weighed, and found to be completely dry. The pyrolysis experiment was repeated three times at both 400 and 500 °C. The average dry solids fed to the pyrolyzer at 400 or 500 °C was about 30 grams. In addition, at each temperature, about 3 grams of moisture from the feed sample entered the reactor. This moisture was ultimately recovered with the bio-oils in the oil recovery system.

*Fast pyrolysis experiments in the SPR*

Fast pyrolysis of the dried vinasse in the SPR, illustrated in Figure 5, was carried out at 400, 450, 500, 550, and 600 °C. In this case, the gas connections indicated by the dashed lines in the figure were used. The non-condensable gas lines entering the SPR and ABB gas analyzer from the cotton filters shown in the

figure were plugged. The air supply line was replaced with $N_2$, and a part of the exhaust gas from the SPR was routed to the ABB gas analyzer. The SPR has a manual sample insertion probe (not shown in the figure), which allows a sample to be held in a cold environment and then inserted, within 1–2 s, into the hot reactor. Detailed descriptions of the SPR are available elsewhere [113,114]. About 100–120 mg of the dried vinasse was weighed into a sample holder made of quartz glass and mounted on the sample insertion probe. Then, the sample was inserted from the cold environment into the hot SPR and pyrolyzed until the CO and $CO_2$ readings from the ABB gas analyzer were 0.0%. After the pyrolysis was over, the probe was retracted to the cold environment, and the char was quenched in $N_2$. Finally, the sample holder with char in it was removed from the probe and weighed to 0.1 mg accuracy. The pyrolysis experiment was repeated three times at each temperature.

*Determination of the fast pyrolysis product yields*

*Char yields*: The char yields from both reactors were obtained gravimetrically. To determine the char yield from the drop-tube-type reactor, the pyrolysis chars were first carefully recovered from the char holder, pyrolyzer walls, and surfaces of the thermocouples. Then, the total recovered char was weighed to 0.1 mg accuracy, and the result was reported as char yield on a wt % dry vinasse basis. The reported results were average values of the experiments repeated three times at each temperature. For the char yield determination from the SPR, the char weight was obtained from the weight difference between the empty quartz-glass sample holder and the sample holder with char in it. Here too, the char weight obtained was expressed on a wt % dry vinasse basis, and at each temperature, the average value of the three experiments was reported as the char yield from the SPR.

*Bio-oil yields:* The bio-oil yields from the drop-tube-type reactor were also obtained gravimetrically. The bio-oil yields were determined as follows: First, after the pyrolysis was complete, the temperature of the condensers was adjusted from -40 °C to 5 °C using the cryostat cooler. Then, the cryostat cooler was stopped, and the different units in the bio-oil recovery system (B) were dismounted. Finally, the weights of bio-oils recovered in the different units were obtained from the weight difference between the units with the bio-oils in them and their corresponding weights without the bio-oils. Most of the oil recovered from the oil collectors was from the first stage. For recovery of the oil left sticking on the upper lid, the lid was thoroughly washed with acetone, which was then collected onto a glass tray. The acetone was allowed to

evaporate from the oil-acetone mixture over a period of approximately two weeks. The weight of the oil recovered from the lid was then determined by subtracting the weight of the empty glass tray from the glass tray with oil in it after evaporation of the acetone. The bio-oils recovered from different units were weighed to 0.01 g accuracy. The weights of the oils from the different units were totaled; moisture from the vinasse was deducted; and the results were reported as oil yield on a wt % dry vinasse basis. The reported results were the average values of the experiments repeated three times at each temperature.

*Gas yields:* The non-condensable gas yield for the vinasse fast pyrolysis in the drop-tube-type reactor was obtained as follows:

(a) The total mass of carbon released directly as CO and $CO_2$ during pyrolysis of the sample was determined from the ABB CO and $CO_2$ concentration results and the total gas flow from the pyrolyzer.

(b) The total mass of carbon in the non-condensable gases released as CO, $CO_2$, and hydrocarbons was calculated based on the $CO_2$ concentration of the oxidized gas. In other words, the total mass of carbon in the non-condensables was calculated based on the $CO_2$ concentration results obtained from the Servomex gas analyzer and the total gas flow from the pyrolyzer.

(c) The difference between the total mass of carbon obtained in (b) and (a) was assumed to be the total mass of carbon in the non-condensables released as hydrocarbons. Methane ($CH_4$) was assumed to be the main component of these hydrocarbons. The assumption was based on the report by Bhattacharya *et al.* [115]. Their report shows that the main hydrocarbon, on a mass basis, in the gaseous product during pyrolysis of black liquor solids is $CH_4$.

(d) The total mass of sulfur in the non-condensable gases was obtained by subtracting the amount of sulfur retained in the chars from the amount in the dried vinasse. The sulfur released during pyrolysis of the vinasse was assumed to be in the non-condensable gases as $SO_2$ and $H_2S$.

(e) The mass of sulfur released as $SO_2$ was determined from the ABB $SO_2$ analysis and the total gas flow from the pyrolyzer.

(f) The mass of sulfur present as $H_2S$ in the gases was obtained from the difference between the mass of sulfur obtained in (d) and (e).

Thus, the gas yield on a wt % dry vinasse basis was obtained from the sum of the amount of CO, $CO_2$, $CH_4$, $SO_2$, and $H_2S$ in the gas.

Moreover, the CO and $CO_2$ concentrations in the gases released from the pyrolysis of the dried vinasse in the SPR, at the five different temperatures,

were measured with the ABB gas analyzer. This enabled determination of the CO to CO + $CO_2$ mass ratio as a function of temperature and comparison of the results with those from the drop-tube-type reactor.

### 4.2.2. Char production in the SPR

The vinasse chars used for the experiments in the TGA were obtained by pyrolysis of vinasse droplets at 800 °C in 100 vol % $N_2$ in the SPR shown in Figure 5 and described in section 4.2.1. To prepare the droplets, the dried vinasse was first diluted to a dry solids content of 67.4 wt % with ultrapure water. Samples of the diluted vinasse were then mounted on thin platinum wire hooks so that each of the samples (or droplets) weighs about 10 mg. The diameter of each droplet can be assumed to be approximately 2–2.5 mm. The assumption is based on the diameter of black liquor droplets, with similar weights and dry solids content as those of the vinasse droplets, used in the study by Saw *et al.* [116]. The procedures used for the pyrolysis of the vinasse droplets are similar to those described in section 4.2.1 for the fast pyrolysis of the dried vinasse in the SPR except for the following: 1) Thin platinum wire hooks were used as sample holders instead of the quartz-glass sample holders. 2) The pyrolysis time in the SPR was 20 s. 3) After the droplets were pyrolyzed in the SPR, the chars were scraped off the wire hooks, ground and homogenized with a mortar and pestle, and stored in an airtight container. The ground and homogenized char was analyzed for its elemental composition according to the procedures outlined in section 4.3.1, and the analysis results are given in Table 2, section 4.1.3. The char yield, including ash, on a wt % dry vinasse basis, was 52.5±3.4. The char yield was obtained gravimetrically as per the procedures described in section 4.2.1. It was not possible to put the dried vinasse sample directly into the DSC-TGA setup because of its swelling properties. Moreover, it was desirable to get uniform sample particle size; hence, a separate char production stage was necessary.

The KB, OB, GP, TGP, and SCB chars used for the $CO_2$ gasification experiments in the TGA were produced in the SPR in the same manner described above for the vinasse chars. However, in this case, about 500 mg pellets of the dried biomass samples were used instead of droplets, and thin platinum wire mesh was used as a sample holder. Also, the pyrolysis time used for each pellet was 120 s. The char yields, including ash, on a wt % original dry fuel basis from the SPR for the KB, OB, GP, TGP, and SCB were 19.7±0.2, 20.3±0.0, 27.9±0.1, 37.8±0.1, and 17.1±0.2, respectively. Selected elemental analyses results of the five different chars are provided in Table 3, section 4.1.5.

### 4.2.3. TGA experiments in $N_2$ and $CO_2$

TGA experiments of the vinasse chars produced at 800 °C in the SPR were carried out in $N_2$ and $CO_2$ gas atmospheres using a DSC-TGA setup (NETZSCH, Germany). The setup is supplied with 99.99% pure $CO_2$ and 99.99% pure $N_2$ gases as well as synthetic air. For the experiments, three different gas atmospheres at three different isothermal temperatures were used. The gas atmospheres used were 100 vol % $N_2$, 20 vol % $CO_2$/80 vol % $N_2$, and 40 vol % $CO_2$/60 vol % $N_2$, whereas the isothermal temperatures were 600, 700, and 800 °C.

For the TGA experiments, about 5 mg of the char sample was put into an alumina pan and placed in the DSC-TGA furnace purged with 100 mL/min $N_2$. The system was first heated from room temperature to 40 °C at 20 °C/min. Then, the temperature of the system was raised from 40 °C to the gasification temperature at a heating rate of 40 °C/min. After an additional two minutes isothermal period at the reaction temperature, the flow rate of the $N_2$ gas was reduced, and $CO_2$ gas was supplied to obtain the desired gasification atmosphere. Finally, the system was run isothermally until the mass loss curve leveled off with only ash remaining. In the case of the experiments in the $N_2$ gas atmosphere, the 100 mL/min $N_2$ flow rate was maintained for an isothermal period of three hours. The 600 °C and some of the 700 °C experiments were run for extended isothermal periods; whereafter, the final residues were burned off with synthetic air after reducing the $N_2$ gas flow to 20 mL/min. Each experiment was repeated twice, and the average value was reported.

In the case of the $CO_2$ gasification experiments with the KB, OB, GP, TGP, and SCB chars in the TGA, about 9 mg char sample weights were used. The gasification experiments were conducted in the 40 vol % $CO_2$/60 vol % $N_2$ gas condition at 800 °C. According to Perander *et al.* [24] and Dupont *et al.* [117], mass transfer limitations are not expected to be significant for $CO_2$ gasification of biomass chars at 800 °C in TGA tests. Nonetheless, for very reactive biomass chars (e.g., reference [118]), mass transfer limitations may occur at temperatures lower than 800 °C. In addition to the experiments in $CO_2$, some TGA tests using samples of the KB, OB, GP, TGP, and SCB chars in the 100 vol % $N_2$ gas atmosphere were also performed.

### 4.2.4. Determination of $CO_2$ gasification rates and K/C ratios

The instantaneous $CO_2$ gasification rates for the KB, OB, GP, TGP, and SCB chars were determined based on the char mass loss versus time results obtained from the TGA experiments described in the previous section, section 4.2.3. For

these chars, the results from the TGA experiments are given in Figure 16, section 5.2.2. The gasification rates were calculated using Eq. (5). The degree of char conversion at time $t$, represented by $X$ in Eq. (5), was calculated using Eq. (6). In Eq. (5), $\Delta m$ is the char sample weight change between measurement intervals of 0.4 s; $\Delta t$ is the time interval of 0.4 s; and $\Delta X$ represents the change in the degree of char conversion between the measurement intervals. In Eqs. (5) and/or (6), $m_t$ is the char weight at time $t$, while $m_i$ and $m_f$ are the initial and final char sample weights from the TGA, respectively. For the calculations, the char sample weight loss during heating to the target temperature and the final residue/ash left in the TGA, given in Figure 16, section 5.2.2, were excluded. Figure 6 shows char conversion, on ash-free basis, as a function of time for the five biomass chars from **Paper IV**. For the TGA experiments carried out with the vinasse chars, it was not possible to determine the char conversion nor the gasification rate due to the reasons explained in section 5.3.

$$rate = \frac{1}{m_t}\left(\frac{\Delta m}{\Delta t}\right) = \frac{1}{1-X}\left(\frac{\Delta X}{\Delta t}\right) \quad (5)$$

$$X = \frac{m_t - m_i}{m_i - m_f} \quad (6)$$

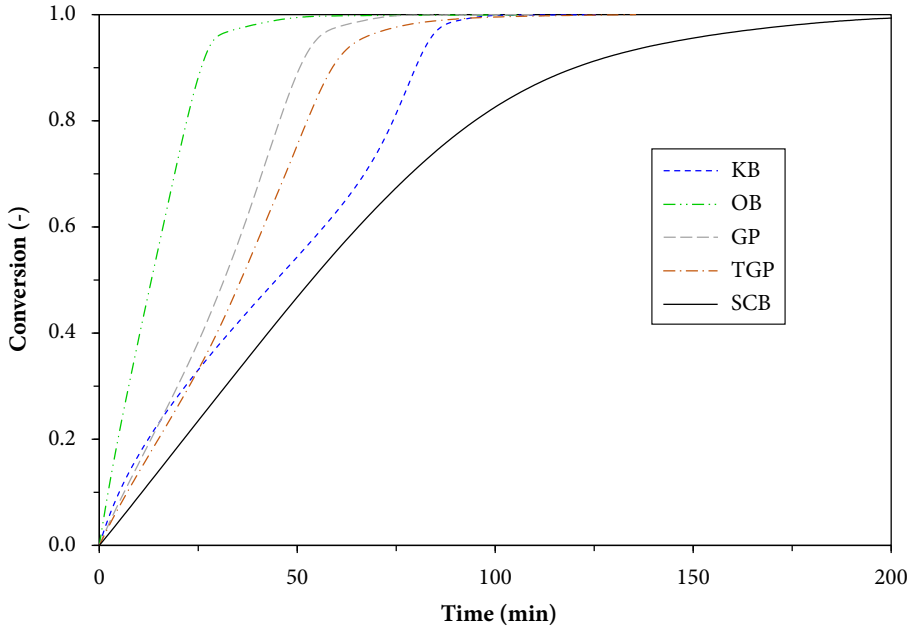


***Figure 6.*** *Char conversion, on ash-free basis, versus time under $CO_2$ gasification conditions at 800 °C for the five biomass chars. Adapted with permission from* ***Paper IV****. Copyright 2018 © American Chemical Society.*

The K/C ratios as a function of char conversion for the five biomass chars were determined as follows. First, the C contents throughout the conversion were determined from the char mass loss results (given in Figure 16, section 5.2.2) obtained from the TGA. A part of the char mass loss in the TGA can be attributed to loss of ash-forming matter, but on a relative basis, almost the entire char mass loss can be ascribed to loss of C. Then, the K contents during char conversion were determined as per the following procedures. (1) The initial chars and final residues/ashes from the TGA experiments described in section 4.2.3 were analyzed for their K contents according to the procedures described in section 4.3.1. (2) Interrupted TGA runs, i.e., TGA runs with shorter durations, were performed to obtain K contents of partially reacted chars at two intermediate points during the char conversion. The two durations chosen for the interrupted TGA runs corresponded to 30% and 70% char conversions. The K contents of the partially reacted chars from the interrupted TGA runs were also analyzed as per the procedures described in section 4.3.1. (3) On the basis of the K values obtained under (1) and (2), K contents for a given degree of conversion on a wt % char basis were determined. Figure 7 exemplifies K contents as a function of conversion for KB and SCB chars. The values for the other biomass chars can be found from the Appendix of **Paper IV**. The determined initial char-K contents may differ from the char-K contents when the char gasification started since some K might have been lost before $CO_2$ gas was supplied to the reactor. Based on the K contents of the partially reacted chars from the interrupted TGA runs, this effect is not expected to be significant.

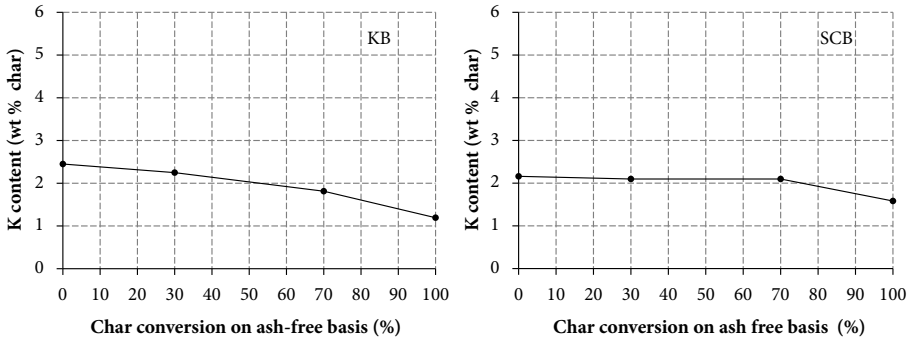


***Figure 7.*** *K content as a function of conversion, ash-free basis, for KB and SCB chars. Adapted with permission from* ***Paper IV****. Copyright 2018 © American Chemical Society.*

### 4.2.5. Release of vinasse ash-forming elements

The levels of vinasse ash-forming elements or inorganics released during combustion and gasification of the vinasse were determined using the SPR shown in Figure 5, section 4.2.1. In addition to $N_2$ gas and synthetic air, the SPR is supplied with $CO_2$ gas, which was used for the gasification experiments. Both the $N_2$ and $CO_2$ gases were 99.99% pure. The gas conditions used in the SPR were 10 vol % $O_2$/90 vol % $N_2$ for the combustion and 50 vol % $CO_2$/50 vol % $N_2$ for the gasification experiments. To determine the levels of the inorganics released, the dried vinasse was first combusted/gasified in the SPR at 900 °C. The amounts of the inorganics released were then calculated based on the elemental analyses and ash yield results from the combustion and gasification experiments. The experimental procedures with the SPR are similar to those described in sections 4.2.1 and 4.2.2. However, in this case, the vinasse samples used were about 200 mg each, and the experiments were repeated at least ten times in each gas atmosphere. The ashes from the combustion and gasification experiments were recovered separately, ground to a fine powder, and stored in airtight containers for further analyses. Complete combustion of the vinasse sample took approximately 3 min, whereas the time required for gasification to complete was about 10 min. The ash yields obtained from the SPR under combustion and gasification conditions were 28.3±1.0 and 26.5±1.0, respectively, on a wt % original dry vinasse basis.

Moreover, the levels of inorganics released from the vinasse chars during the TGA experiments in $N_2$ and $CO_2$ and those released during fast pyrolysis of the vinasse at 400 and 500 °C in the drop-tube-type reactor were determined. To determine the release levels, the final residues from the TGA experiments, or in the case of the fast pyrolysis experiments, the chars from the drop-tube-type reactor, were first analyzed for their inorganics. The levels of inorganics released were then determined based on the elemental analysis results, the char or residue yields, and the elemental composition of the parent fuel given in Table 2. Furthermore, to investigate the release of ash-forming matters from the vinasse chars as a function of time, interrupted TGA runs were conducted in 40 vol % $CO_2$/60 vol % $N_2$. The durations used for the interrupted TGA experiments were 30, 80, and 130 min.

Elemental analyses of the ashes from the SPR, the residues from the final and interrupted TGA runs, and the chars from the drop-tube-type reactor were carried out according to the procedures described in section 4.3.1.

### 4.2.6. Ash-melting behavior

The melting characteristics of vinasse ash with temperature were assessed as follows. First, the vinasse ash was produced by ashing the dried vinasse at 500 °C in a muffle furnace (Naber, Germany). Then, the melting behavior of the ash was calculated using FactSage software version 7.2 [119], and finally, the results were validated by measurements using a DSC-TGA (TA Instruments, USA).

*Vinasse ash production*

For the production of the vinasse ash, a low temperature, 500 °C, was used compared to the standard ashing temperature, 550±10 °C. The low temperature used was to minimize the loss of ash-forming elements from the vinasse. The ashing experiments were conducted according to CEN/TS 14775 standard except for the ashing temperature, 500 °C, and holding times. It took almost three days for the ashing to complete, i.e., to burn off the organic fraction of the vinasse completely. Complete removal of the organic fraction from the vinasse during the ashing was verified using a DSC-TGA test. For the test, about 8 mg of the ash sample was placed in the DSC-TGA and heated to 500 °C in synthetic air, 20 vol % $O_2$/80 vol % $N_2$. The system was then kept isothermal at 500 °C for about 50 min. No significant change in the weight of the ash sample was observed during the isothermal period, indicating that complete removal of the organic carbon was achieved in the muffle furnace. Further details of the procedures for the ashing experiments are available in **Paper I**. The vinasse cannot be put in the DSC-TGA directly for the same reason stated earlier in section 4.2.2. The ashing experiments were repeated three times, and the ashes from the three experiments were mixed and ground to a fine powder and stored in an airtight container. The ground ash was characterized for its elemental composition according to the procedures described in section 4.3.1, and the results are given on a wt % dry vinasse basis in Table 2, section 4.1.3. The ash yield at 500 °C on a wt % dry vinasse basis was 34.8, which is slightly higher than the 34.1 wt % dry vinasse value obtained under standard ashing conditions.

*Thermodynamic modeling of ash chemistry*

Thermodynamic modeling based on the Gibbs energy minimization technique is a useful tool for calculating the chemical equilibrium of a complex system. Accurate thermodynamic data for all relevant phases of the system are important to reliably predict the chemical equilibrium. In this thesis work, FactSage software version 7.2 [119] was used to calculate the melting

characteristics of vinasse ash as a function of temperature. The FactSage calculations were made using three different inputs: the original fuel composition, the ash composition determined by SEM-EDX, and the ash composition determined by ICP-OES and IC. In the latter case, the C and O analysis results of the ash from SEM-EDX were used. In the case of the original fuel composition as input, air was added to the system so that the flue gas contained 4 vol % $O_2$. For the FactSage calculations, the databases used were FTpulp for the alkali salt phases, FToxid for the molten slag phase and solid oxide/silicate phases, and the FactSage pure substance database for the gas components and other solid compounds. In addition, thermodynamic data not available in the commercial FactSage databases were used for the interaction of alkali salts with calcium and magnesium compounds in the molten salt phase. These data have been published by Lindberg and Chartrand [120] and described in the review paper by Lindberg *et al.* [121].

*DSC-TGA measurements*

For the DSC-TGA measurements with the ash produced at 500 °C, the gas conditions used in the DSC-TGA were 100 vol % $N_2$ and 90 vol % $CO_2$/10 vol % $N_2$. The $CO_2$ gas atmosphere was used to suppress ash weight loss as a result of carbonate decomposition. About 10 mg of the ash sample was weighed into an alumina pan and placed in the DSC-TGA furnace, which was being purged with either 100 mL/min $N_2$ or 90 mL/min $CO_2$ and 10 mL/min $N_2$. The temperature of the system was first raised from room temperature to 900 °C at 10 °C/min, and the system was then cooled down to 200 °C at the same rate. During heating, the formation of the first melt was seen as an endothermic peak in the DSC curve, while the solidification of the final melt during cooling resulted in an exothermic peak. Mass loss during heating was observed from the TGA curve. Universal Analysis software, version 4.5A, was used to evaluate the DSC-TGA data. The DSC-TGA experiments were repeated two times in each gas atmosphere, and the average values were reported.

## 4.3. Analytical methods

### 4.3.1. Elemental analyses

The C, H, and N contents of the vinasse and its chars, as well as those of the vinasse pyrolysis oils, were analyzed using a FLASH 2000 organic elemental analyzer (Thermo Scientific, UK). The oxygen contents of the vinasse and its chars from the vinasse fast pyrolysis in the drop-tube-type reactor and the sulfur contents of the vinasse pyrolysis oils were also determined by the organic

elemental analyzer. For the analyses, about 2 mg samples of the vinasse and its chars and oils were used. The analyzer was calibrated with sulphanilamide, cystine, methionine, and BBOT (2,5-Bis(5-tert-butyl-2-benzo-oxazol-2-yl) thiophene) organic analytical standards (Thermo Scientific, UK). Detailed descriptions of the analysis procedures are given in **Paper III**. Moreover, specific procedures followed for the analysis of the pyrolysis oils with the organic elemental analyzer are described in **Paper II**.

The ash-forming elements, except chloride, of the vinasse and its chars and ashes were analyzed with an Optima 5300 DV ICP-OES (PerkinElmer, USA). Prior to analysis with the ICP-OES, samples of the vinasse and its chars and ashes were digested with acid, $HNO_3$ or $HNO_3$ and HF, in an Anton Paar Multiwave 3000 microwave oven. The digested samples were then diluted with ultrapure water, and the diluted samples were analyzed with the ICP-OES. Commercial standards, i.e., IQC-026 for multi-elements, ICP-015 for phosphorus, and ICP-016 for sulfur, all from Ultra Scientific (RI, USA) were used for calibration of the ICP-OES. All the acids used were of Suprapur grade (Merck, Germany).

The Cl contents of the vinasse and its chars and ashes were analyzed using an 881 Compact IC Pro ion chromatograph (IC; Metrohm, Switzerland). The Na, K, S, and Cl contents of the final residues from the TGA experiments, as well as the residues from the interrupted TGA runs, were also analyzed with the IC. Prior to analysis with the IC, the char, ash, and residue samples were leached in ultrapure water and filtered with 45 μm syringe filters. The aqueous solutions were then analyzed for Cl or for Na, K, S, and Cl in the case of the aqueous solutions from the residues from the TGA experiments using the IC. The IC was calibrated with various concentrations of the cations and anions prepared from Suprapur grade commercial standards from Merck (Germany). For analyzing the Cl content of the vinasse, the vinasse sample was first combusted in a 1341 oxygen bomb calorimeter (Parr, USA). The residue from the calorimeter was then leached in ultrapure water, and the aqueous solution was analyzed for Cl using the IC. Details of the experimental procedures for the analysis of the cations and anions with the IC are available in **Paper III**. The procedures for the combustion of the vinasse sample in the oxygen bomb calorimeter and leaching of the residues from the calorimeter for Cl analysis are described in **Paper I**.

In addition to the analysis with the ICP-OES/IC, elemental analysis of the vinasse ash produced at 500 °C in the muffle furnace was done using SEM-EDX (LEO, Germany). This was to determine the C and O contents of the ash

and for comparison of the elemental analyses results from the SEM-EDX with those from the ICP-OES/IC. The C and O contents of the ash obtained from the SEM-EDX were used as input data for the FactSage calculations described in section 4.2.6. Prior to analysis with SEM-EDX, about 0.2 g of the ash sample was pressed into a 10 mm diameter pellet. Additional descriptions of the procedures for the elemental analysis of the ash with the SEM-EDX can be found in **Paper V**.

All the elemental analyses with the organic elemental analyzer, ICP-OES, IC, and SEM-EDX were carried out in triplicates, and average values were reported. The elemental analyses results, except for the bio-oils, were reported on a wt % original dry fuel basis. The char or ash yield values were used to convert the elemental analyses results from a wt % char or ash basis to a wt % original dry fuel basis. The elemental compositions of the vinasse and its char, as well as that of the vinasse ash produced at 500 °C, are given in Table 2, section 4.1.3. For the vinasse ashes produced in the SPR under combustion and gasification conditions, the elemental analyses results are provided in Table 5, section 5.4.

Selected elemental analyses of KB, OB, GP, TGP, and SCB and their chars were carried out in the same way described above for the elemental analyses of vinasse and its chars. However, in this case, the Si contents of the chars were analyzed using the SEM-EDX. The elemental analyses results, on a wt % char basis, of the fuels and their chars are given in Table 3, section 4.1.5. In addition, the final residues/ashes and partially reacted chars from the TGA runs were leached in ultrapure water, and the leachates were analyzed for their K contents using the ICP-OES. The results, on a wt % char basis, for the KB and SCB residues and partially reacted chars are given in Figure 7, section 4.2.4, and in the Appendix of **Paper IV** for the rest of the residues and partially reacted chars.

### 4.3.2. Chemical compositions of the vinasse and its ash

The water-soluble organic constituents of the vinasse sample used in this work were identified using solution-state NMR spectroscopy. The $^{1}H$ and $^{13}C$ NMR spectra were recorded using a Bruker Avance III HD 500 MHz spectrometer (Germany) equipped with Bruker CryoProbe (Germany). Topspin software, version 3.5, was used to process the spectra. Prior to analysis, 15–20 mg of the vinasse sample was dissolved in approximately 1 mL of 99.9% deuterium oxide ($D_2O$; Sigma-Aldrich). The experiment was repeated three times to establish repeatability.

The main inorganic compounds present in the vinasse ash produced at 500 °C in the muffle furnace were identified using an Empyrean XRD (Panalytical, Netherlands) equipped with a PIXcel$^{3D}$ detector (Panalytical, Netherlands). The XRD operating parameters used for the analysis are described in **Paper V**. The raw XRD data were analyzed using X'pert HighScore software (Panalytical, Netherlands), and the database used for the inorganic materials was PDF-4+ from the International Center for Diffraction Data (Newtown Square, PA, USA).

Both the water-soluble organic components of the vinasse obtained from the NMR and the inorganic compounds in the vinasse ash identified by the XRD are described in section 4.1.4.

### 4.3.3. Analyses of the pyrolysis oils

*Water contents and chemical compositions*

The water contents and chemical compositions of the vinasse pyrolysis oils from the fast pyrolysis experiments, described in section 4.2.1, were analyzed using a volumetric Karl Fischer titrator (Metrohm, Switzerland) and a GC-MS (Agilent Technologies, USA), respectively. The analyzed oils were only those recovered into the oil collector of the first-stage condenser. The amounts of bio-oils obtained from the second-stage and third-stage oil collectors were not sufficient to carry out the Karl Fischer titration and GC-MS analysis. The commercial reagent used for the titration was Apura CombiTitrant 5 (Merck, Germany), and HYDRANAL-Methanol dry (Sigma-Aldrich, Germany) was used as a solvent for the bio-oils. The procedures for the analysis of the oils with the GC-MS were adapted from Aho *et al.* [22]. Prior to analysis with the GC-MS, all the bio-oil samples were diluted with methanol in the oil to a methanol ratio of 2:3. Further details of the procedures for the analyses of the oils with the Karl Fischer titrator and the GC-MS are available in **Paper II**.

*Acidity*

The total acid number (TAN) of a bio-oil is a measurement of acidity for the bio-oil. It is defined as the amount of potassium hydroxide (KOH) in milligrams needed to neutralize all the acids in 1 gram of a bio-oil sample. The TAN values for the bio-oils obtained from the vinasse fast pyrolysis experiments, described in section 4.2.1, were determined using a potentiometric titrator (Metrohm, Switzerland). The titration was carried out according to ASTM D 664. The titrant used was 0.1 M KOH (KOH in isopropanol) (Merck, Germany). The solvent used for the bio-oils was

prepared by mixing toluene, isopropanol, and ultrapure water. Both the toluene and isopropanol were HPLC grades (Fisher Scientific, UK), whereas the reagent used for calibration of the titration setup was 99.5% pure potassium hydrogen phthalate (KPH) (Merck, Germany). The titration setup was first calibrated using the KPH as a titer, and then a blank titration was performed using 125 mL of the solvent for the bio-oils. Finally, 0.1–1.0 g of the bio-oil samples were titrated, and their TAN values were calculated using the experimental data generated from the titration and a correlation relating the experimental data with TAN. The experimental data generated from the titration and the correlation used to calculate the TAN values are described in the Appendix of **Paper II**.

# 5. RESULTS AND DISCUSSION

## 5.1. Fast pyrolysis results

### 5.1.1. Fast pyrolysis product yields

Figure 8 shows the pyrolysis product yields on a wt % dry vinasse basis at 400 and 500 °C from the drop-tube-type reactor. The results shown in the figure are average values of the experiments repeated three times at each temperature. The pyrolysis product yields were calculated based on the amounts of the pyrolysis products, i.e., chars, bio-oils, and gases, obtained from the experiments conducted in the drop-tube-type reactor. The amounts of the pyrolysis products in grams are available in **Paper II**. The char yields given in the figure include the ash (inorganics) contained in the chars, whereas the oil yields are presented on a water-free basis. The water-free oil yield was obtained by subtracting the water formed by pyrolysis, given as pyrolysis water in the figure, from the total pyrolysis oil yield, excluding moisture from the vinasse. The values for the pyrolysis water yields were calculated based on the analyzed and average water contents of the bio-oils and the amounts of pyrolysis liquids produced. The calculations are described in detail in section 5.1.3. The "balance" shown in the figure is probably due to soot and oil left sticking on the thermocouples and the internal surface of the reactor.

For the char yield at 400 or 500 °C, the maximum deviation of the experimental value from the average value was about ±5%. For the water-free oil, pyrolysis water, and gas yields, the deviations were about ±5, ±15, and ±10%, respectively, at 400 °C. The corresponding deviations at 500 °C were about ±5, ±20, and ±2%. These deviations indicate good repeatability of the pyrolysis experiments in the drop-tube-type reactor.

Figure 8 shows that the char yield decreased as the temperature was increased from 400 to 500 °C, while the gas yield increased. The char and gas yield trends with temperature are similar to those for woody biomasses [93,122–125] and agricultural biomass residues [126–129]. The decrease in char yield and increase in gas yield trends are due to the increased decomposition of the organic fraction of biomass at higher temperatures.

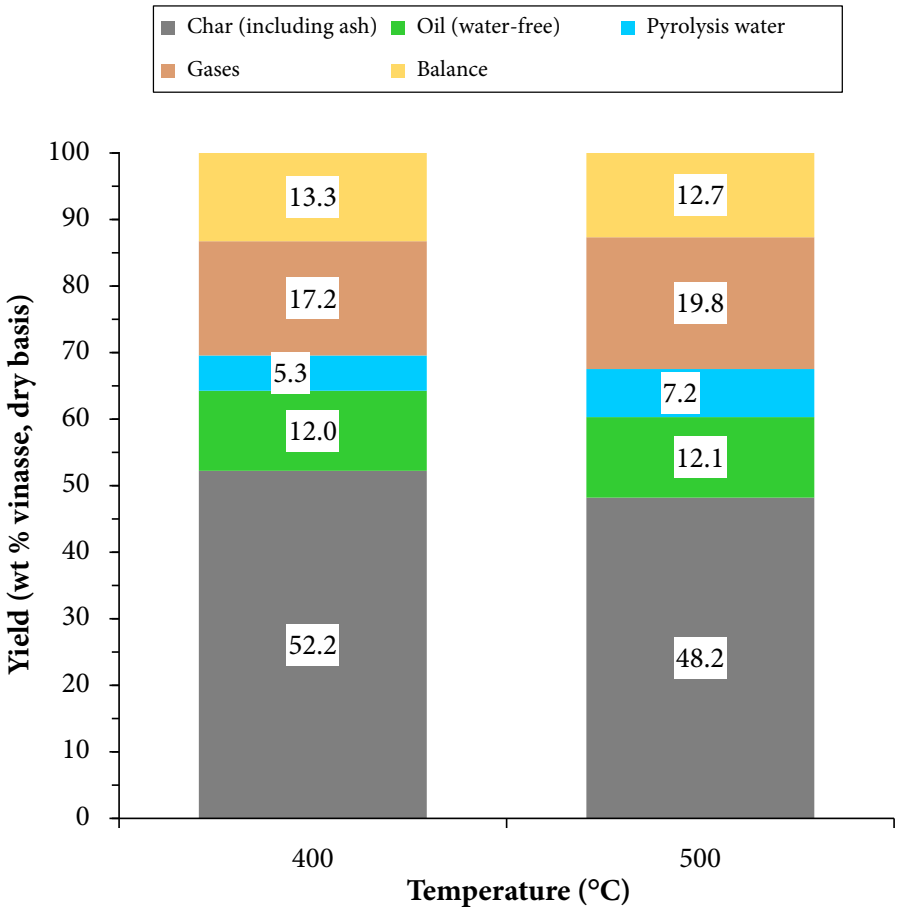


***Figure 8.*** *Vinasse fast pyrolysis product yields from the drop-tube-type reactor. Adapted with permission from* ***Paper II****. Copyright 2019 © American Chemical Society.*

The water-free bio-oil yield (liquid organics), given in Figure 8, is almost independent of temperature, while the pyrolysis water yield increased when the temperature was increased from 400 to 500 °C. The organic liquid yield results are rather low compared to the typical 30–70% [130] yields for biomass. Tests for black liquor solids using the same experimental setup, procedures, and conditions as for the vinasse revealed that the water-free bio-oil yield was also low, about 10 on a wt % dry black liquor basis [131]. The black liquor solids had, on a wt % dry black liquor basis, a sodium concentration of 19.5 and an ash content of 47.4. High levels of ash-forming elements, especially alkali metals, in these fuels may be the reason for the low oil yield results. According to the studies by Oasmaa *et al.* [132] and Fahmi *et al.* [133], biomass fast

pyrolysis product yields strongly correlate with the level of inorganics in the biomasses. These authors have reported organic liquid yields, on a wt % dry biomass basis, of 55–65 for biomasses yielding ≤1 wt % ash and 25–40 for agricultural biomass residues which produce about 5 wt % ash. In particular, Coulson [23] and Aho *et al.* [22] have reported a reduction in pyrolysis organic liquid yields of 15–20 on a wt % dry fuel basis with an increase of 0.5–1.0 on a wt % dry fuel basis in the concentration of alkali metals in biomass fuels. Alkali metals in biomass fuels are known to catalyze secondary reactions in the vapor phase of the pyrolysis product, thereby reducing the organic liquid yield and increasing the gas and water yields.

Figure 9 shows char yield results, on a wt % dry vinasse basis, from the fast pyrolysis experiments carried out in the SPR. The results given in the figure are average values of the experiments repeated three times at each temperature. The maximum difference between the experimental and average char yield values at each temperature was in the range of ±1–±5%, indicating good repeatability of the experiments. For comparison, the average char yield results from the drop-tube-type reactor are also shown in the figure. Here too, the results from the SPR show that the char yield decreases with temperature in the temperature range of 400–600 °C. Moreover, the strong agreement in the char yield results from the two reactors indicates that similar pyrolysis heating rates were attained in both reactors. It is well-established that char yield during biomass fast pyrolysis decreases with increasing heating rate, and vice versa.

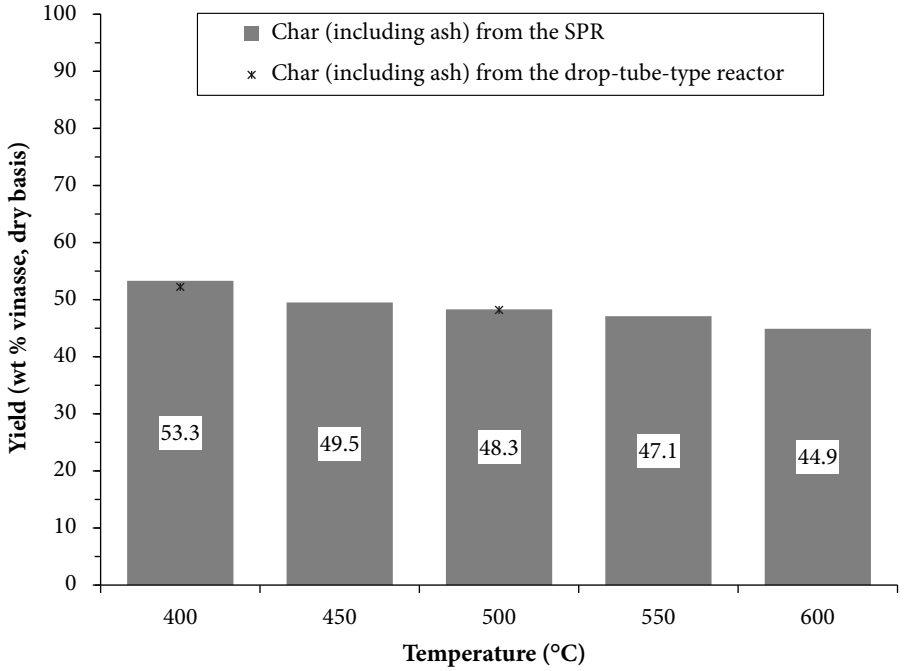


***Figure 9.*** *Char yields from the SPR and drop-tube-type reactor. Reprinted with permission from* ***Paper II****. Copyright 2019 © American Chemical Society.*

### 5.1.2. Analyses of the pyrolysis chars

Figure 10 shows elemental analysis results, on a wt % dry vinasse basis, of the vinasse chars produced at 400 and 500 °C in the drop-tube-type reactor. The results given in the figure are average values of the analyzed chars from the three repeated pyrolysis experiments in the drop-tube-type reactor. A comparison of the results given in the figure with the elemental composition of the parent fuel given in Table 2, section 4.1.3, reveals that 87–88% of the K and 45–55% of the carbon from the vinasse were retained in the chars produced at 400 and 500 °C. The retention of most of the K and half of the carbon from the vinasse in the chars has the following important practical implications:

a) Pyrolysis may be an interesting option for the recovery of K from vinasse for fertilizer.
b) Returning the chars to the soil would sequester approximately 50% of the carbon in the vinasse that would otherwise contribute to environmental pollution. It has been shown that application of biochars to the soil is a viable option for carbon sequestration [134]. Moreover, studies have suggested that application of biochars produced from

vinasse to soil reduces soil runoff and loss [135] and also reduces the concentration of toxic metals in plants grown on soils contaminated with the metals [136].

c) The pyrolysis oils and gases could be burned in a boiler with lower ash-related problems to produce steam, rather than burning the vinasse directly.

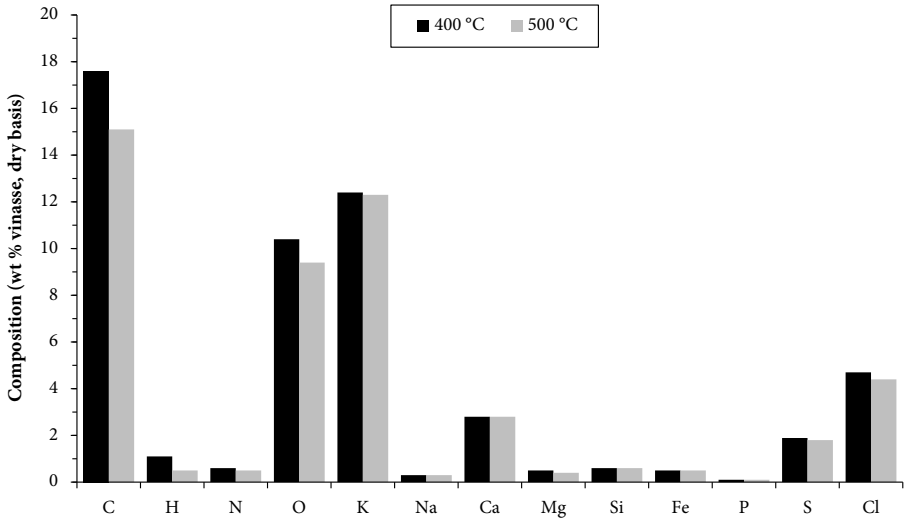


***Figure 10.*** *Elemental composition of the vinasse chars produced in the drop-tube-type reactor at 400 and 500 °C (wt % vinasse, dry basis). Data from* ***Paper II****.*

### 5.1.3. Analyses of the pyrolysis oils

Table 4 lists the water contents and pyrolysis water yields, elemental and chemical compositions, and TAN values of the bio-oils produced at 400 and 500 °C in the drop-tube-type reactor. The values given in the table are average values of the results from the experiments repeated three times at each temperature.

The water content of the bio-oils produced at both 400 and 500 °C and collected from the first-stage oil collector from the Karl Fischer titrator was 90±3 wt %. The analyzed water content includes moisture evaporated from the vinasse sample. For the oils produced at either 400 or 500 °C and collected from the second-stage and third-stage oil collectors, the amounts were sufficient neither for the Karl Fischer titration nor for the GC-MS analysis. The water contents, including moisture from the vinasse, given in the table are for the total amount of pyrolysis liquid produced at 400 or 500 °C. The water contents

were calculated based on the analyzed water content, total amounts of pyrolysis liquids produced, and the experimental observations given in **Paper II**. The total amount of pyrolysis liquid produced was obtained from the sum of the amounts of bio-oils collected from all units, i.e., oil collectors, condensers, upper lid, SST connection line, silicon tubes, and cotton filters. The amounts collected from the different units (in grams) are available in **Paper II**. The average water contents of the bio-oils given in the table are higher than the 15–30 wt % [137] range reported in the literature for bio-oils produced from different biomass feedstocks. The pyrolysis water yields, given in the table on a wt % dry vinasse basis, were calculated from the average water contents of the bio-oils by excluding moisture from the vinasse.

***Table 4.*** *Water contents and pyrolysis water yields, elemental and chemical compositions, and TAN values of the bio-oils produced at 400 and 500 °C in the drop-tube-type reactor. Data from P**aper II**.*

| Water contents and pyrolysis water yields | 400 °C | 500 °C |
|---|---|---|
| Water content (wt %) | 55.3 | 58.4 |
| Pyrolysis water yield (wt % vinasse, dry basis) | 5.3 | 7.2 |
| Elemental compositions of the oils from the condensers, top lid, and SST connection line (wt % water-free oil)[a] | | |
| C | 55–65 | 55–65 |
| H | 7.5–8 | 7.5–8 |
| N | 2.5–3 | 3–4.5 |
| S | 0.5–1 | 1.5–4 |
| TAN values (mg KOH/ g bio-oil) | | |
| Oils from the first-stage oil collector | 15–20 | 15–20 |
| Oils from the condensers, top lid, and SST connection line[a] | 85–125 | 85–125 |
| Chemical composition | | |
| Oils from the first-stage oil collector | butanediols, cyclopentenones, cyclopentanones, phenols, methylated pyridines | |

[a]*Values are for the bio-oils left after evaporation of the acetone used for the recovery of the oils.*

The C, H, N, and S results given in Table 4 are for the bio-oils collected from the condensers, top lid, and SST connection line and from the amount that remained after evaporation of the acetone used for the recovery of the oils. The C and H contents of the bio-oils at both temperatures and collected from the different units are in the same range, indicating that only high-molecular-weight organics remained after evaporation of the acetone. The C and H results

of the bio-oils are within the range available in the literature for woody biomasses [92,94,122] and agricultural biomass residues [126]. However, it can be seen from the table that the N and S contents of the bio-oils increased when the temperature was raised from 400 to 500 °C: the N content increased by about 1 wt %, whereas the S content increased three- to four-fold. The presence of N in the vinasse oils is consistent with the GC-MS analysis results given in the table. The C, H, N, and S analysis results for the oils collected from the first-stage oil collector were not reported because the results were unreliable due to the high water content of the oils. During analysis of these oils, condensation of water vapors on the gas transfer line between the combustion chamber and the detector of the analyzer was observed, indicating that only a fraction of the gas was able to reach the detector.

Based on the elemental analysis results given in the table and the correlation available in Channiwala and Parikh [138], the HHVs of the bio-oils left in the condensers, top lid, and SST line after acetone evaporation were estimated. For the calculation, the ash contents of the bio-oils were considered negligible. The calculation yields HHVs of 25–30 MJ/kg for the oils from these units. In practice, however, the average HHVs of the vinasse oils will be lower than this range due to their water contents. Nevertheless, the calculated HHVs provide the information that the bio-oils can be burned in a boiler to generate heat and power.

Table 4 lists results from the GC-MS for the major chemical composition of the bio-oils collected from the first-stage oil collector. The list reveals that the organic molecules present in the bio-oils are thermal degradation products of the organic constituents of the vinasse. The butanediols, cyclopentenones, cyclopentanones, and phenols identified by the GC-MS are probably from the sugars in the vinasse, whereas the N-containing compounds, such as methylated pyridine, are probably from the proteins.

The TAN results given in the table for the bio-oils are of two categories: the oils collected from the first-stage oil collector and those recovered from the condensers, top lid, and SST connection line. As can be seen from the table, the acidity of the bio-oils produced at both 400 and 500 °C and recovered from the first-stage oil collector is significantly lower than the typical 50–100 [139] values for bio-oils from other biomasses. This is mainly because the vinasse oils from the oil collectors were predominantly water. Nevertheless, for the bio-oils recovered from the condensers and SST transfer line and left after evaporation of the acetone used for the recovery of the oils, the acidity is close to the typical range found in the literature for bio-oils from other biomass fuels.

### 5.1.4. Analyses of the pyrolysis gases

Figure 11 shows CO/(CO + $CO_2$) mass ratio as a function of temperature for the pyrolysis experiments performed in the SPR. For comparison, CO/(CO + $CO_2$) ratio results from the experiments carried out in the drop-tube-type reactor are also included in the figure. The results from the two reactors show that the predominant component in the gaseous vinasse fast pyrolysis product is $CO_2$. The high level of $CO_2$ in the gaseous product is probably due to the decomposition of low molecular weight organic compounds present in the vinasse. The low molecular weight organic compounds (discussed in section 4.1.4) in the vinasse contain weak functional groups, including carboxyl groups. These functional groups are easily cleaved, releasing $CO_2$ as the main gas component. A similar case was reported by Bhattacharya *et al.* [115] for pyrolysis of black liquor solids. In addition to the decomposition of organic compounds with weak functional groups, the catalytic effect of the inorganics in the vinasse, discussed in section 5.1.1, might have also enhanced the conversion of pyrolysis vapors to $CO_2$. Moreover, the results given in the figure show that the CO level in the gaseous product increased with temperature.

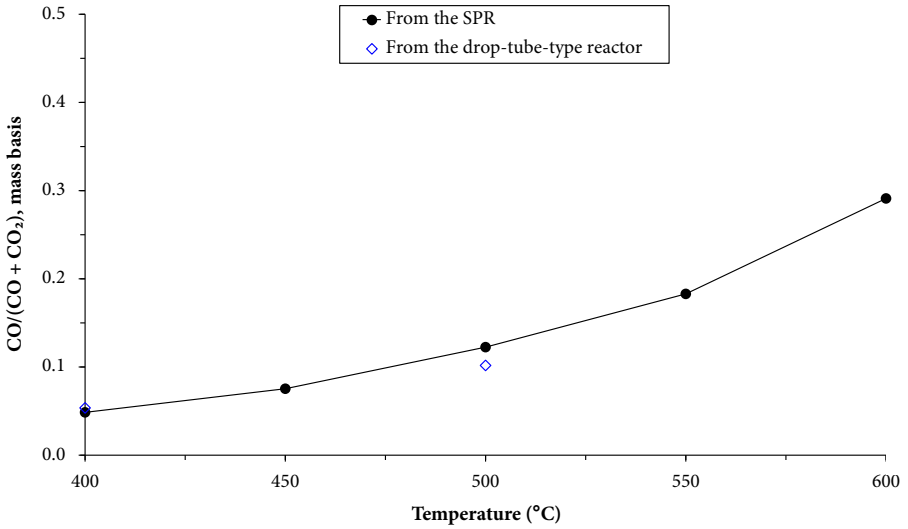


***Figure 11**. CO/(CO + $CO_2$) mass ratio as a function of temperature for vinasse fast pyrolysis in the SPR and drop-tube-type reactor. Adapted with permission from **Paper II**. Copyright 2019 © American Chemical Society.*

The strong agreement of the CO/(CO + $CO_2$) results from the two reactors reveals an important point about the influence of residence time of the pyrolysis vapors on the fast pyrolysis product distribution. The residence time

of pyrolysis vapors was longer in the drop-tube-type reactor than in the SPR. This could have yielded less CO in the drop-tube-type reactor than in the SPR as a result of the higher chance of secondary reactions in the vapor phase in the former reactor. It is well-established that secondary reactions in the vapor phase product of biomass pyrolysis convert CO to $CO_2$. However, similar levels of CO concentration in the pyrolysis gases were obtained from both reactors at 400 or 500 °C. A similar observation can be made from Figure 9 in which the longer residence time of pyrolysis vapors in the drop-tube-type reactor could have produced higher char yields than those obtained from the SPR. However, the char yield results from the two reactors at 400 or 500 °C were approximately the same. The similar levels of CO concentrations and char yields obtained from the two reactors indicate that differences in the residence time of pyrolysis vapors in the reactors had little or no effect on the pyrolysis product distribution. This further reinforces the suggestion that the alkali content of the vinasse may be the controlling factor for the vinasse fast pyrolysis product distribution.

### 5.1.5. Optimum pyrolysis temperature

Figure 12 shows the char yield and CO/(CO + $CO_2$) ratio results, given in Figures 9 and 11, from the SPR. As seen from the figure, the CO to CO + $CO_2$ ratio increased as the pyrolysis temperature was raised, while the char yield decreased. The increase in CO concentration in the pyrolysis gases improves the energy content of the gases for co-combustion in a boiler with other solid fuels, such as bagasse, in the integrated sugar-ethanol process to generate more heat and power. However, increasing the pyrolysis temperature is disadvantageous from a potassium recovery perspective since higher temperatures favor the release of potassium from the vinasse into the vapor-phase product. (More discussion on the influence of temperature on potassium release is given in section 5.4). Furthermore, alkali and alkali chlorides in the liquid and gaseous pyrolysis products will have adverse effects on the downstream equipment that utilizes the pyrolysis liquids and gases. Therefore, the choice of the optimum temperature for vinasse fast pyrolysis requires trade-offs between potassium recovery vis-à-vis energy content of the pyrolysis gases.

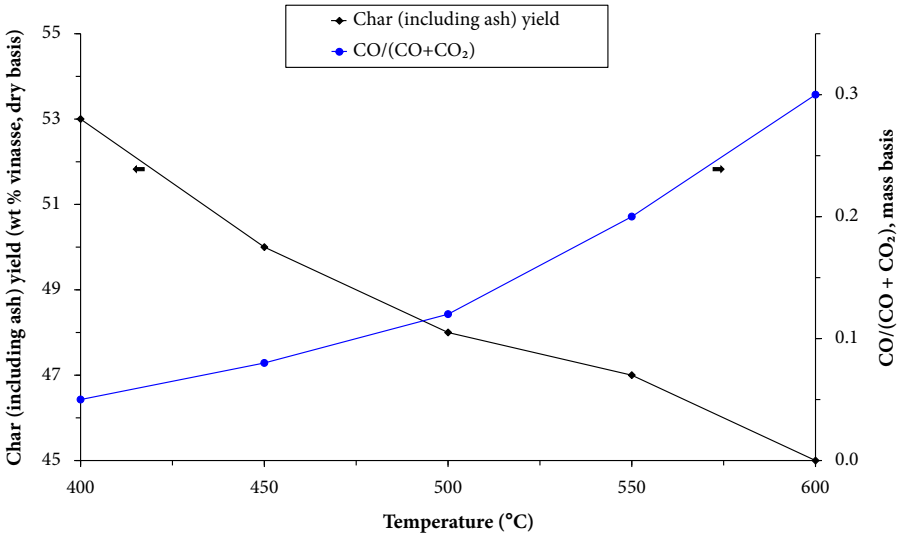


***Figure 12.*** *Char (including ash) yield and CO/(CO + $CO_2$) ratio as a function of temperature from the SPR. Data from* ***Paper II****.*

## 5.2. TGA results in $N_2$ and $CO_2$

### 5.2.1. TGA results in $N_2$

Figure 13 shows results, on a wt % dry vinasse basis, of the TGA experiments for the vinasse chars carried out in 100% $N_2$ at 600, 700, and 800 °C. The vinasse char yield value given in section 4.2.2 was used to convert the char weight loss results from the TGA to a wt % dry vinasse basis. As seen from the figure, about 3 wt %, on a dry vinasse basis, of sample weight was lost below 160 °C. This sample weight loss was mainly due to drying. The drying stage was followed by a stage of secondary pyrolysis which showed up as the sample weight loss during heating to the target temperature. The secondary pyrolysis indicates that 20 s at 800 °C was not enough for pyrolysis to complete.

The sample weight dropped below the vinasse ash content for the experiments at 700 and 800 °C, revealing significant loss of ash-forming matter from the char sample. The drop in the sample weight is higher for the 800 °C run than for the 700 °C run. After decreasing the isothermal temperature to 540 °C, the temperature used for vinasse ashing, the final residues of the 600 and 700 °C runs were burned off with synthetic air after 260 and 200 min, respectively, to determine the level of combustible matter left in the residues. It can be seen from the figure that only a small amount of the combustible matter was left in the residue after 200 min for the run at 700 °C. This shows that most of the carbon in the sample was consumed before 200 min. However,

for the 600 °C experiment, about 3 wt %, on a dry vinasse basis, of organic carbon was burned off after 260 min before the weight leveled off with 37.5 wt %, on a dry vinasse basis, of ash content.

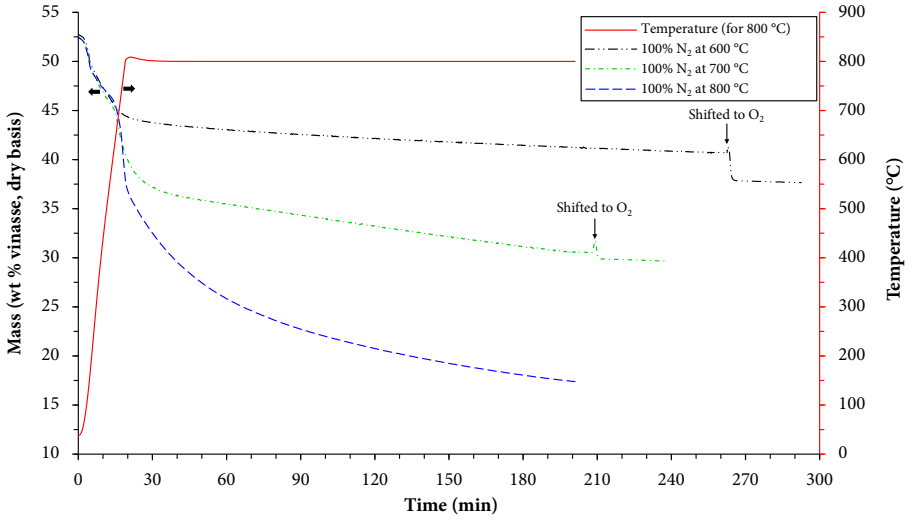


***Figure 13**. Mass (wt % vinasse, dry basis) and temperature (°C) in 100% $N_2$ at 600, 700, and 800 °C for the vinasse chars. Adapted with permission from **Paper III**. Copyright © 2016 Elsevier.*

The vinasse char sample weight losses at 600, 700, and 800 °C given in Figure 13 can be explained by the various mechanisms described below.

*a) Reduction of alkali carbonates and vaporization of alkali metals*

In a 100 vol % $N_2$ gas atmosphere, several investigators reported significant sample weight loss through reduction of alkali carbonates by carbon, according to Eqs. (1), (2), and (7), and ultimately vaporization of alkali metals as per Eq. (8). As already described in section 3.3, these mechanisms were observed for studies with graphitized carbon, ash-free coal chars doped with $K_2CO_3$, and black liquor chars. According to Kopyscinski *et al.* [84], these mechanisms play a significant role at temperatures of 700 °C and above. Stoichiometrically, complete reduction of 1 mole of alkali carbonate, according to Eq. (9), yields 2 moles of the alkali metal in its vapor form and 3 moles of CO gas. A similar mechanism might have occurred for the 700 and 800 °C vinasse char results shown in Figure 13.

$$M_2CO_3 + C \leftrightarrow (\text{-}CO_2M) + (\text{-}COM) \quad (1)$$

$$(\text{-}CO_2M) + C \leftrightarrow (\text{-}COM) + CO(g) \quad (2)$$

$$(\text{-}COM) + C \leftrightarrow (\text{-}CM) + CO(g) \quad (7)$$

$$(\text{-CM}) \leftrightarrow (\text{-C}) + \text{M(g)} \quad (8)$$

$$M_2CO_3 + 2C \leftrightarrow 2M(g) + 3CO(g) \quad (9)$$

The residue from the 800 °C experiment was inspected by an optical microscope. The appearance of the residue indicated that organic carbon was left in the residue after 200 min. The presence of a small amount of organic carbon in the residue is probably the cause of vaporization of the alkali metals according to the reaction in Eq. (8). This was verified by removing the organic carbon by $CO_2$ gasification in the TGA at 800 °C and then shifting the gas atmosphere to 100% $N_2$. After shifting the gas to 100% $N_2$, the sample weight remained almost constant with a negligible rate of weight loss (about 0.004%/min). However, for the residue from the 800 °C experiment shown in Figure 13, which still contains organic carbon, the rate of weight loss after 150 min is one order of magnitude higher, and the weight continued to decrease.

The reduction of carbonates on carbon forming the reduced species, (–COM) and/or (–CM), was verified using FTIR tests. The tests were performed for the vinasse char and its residue from the TGA experiment carried out at 800 °C in 100% $N_2$. Description of the FTIR and the procedures for the associated tests are available in **Paper III**. The FTIR spectra for the vinasse char indicated strong and medium absorbance intensities in the ranges of 1700–1300 and 900–850 $cm^{-1}$, respectively, which are characteristics of absorption bands for carbonates. However, these peaks were either absent or weak in the spectra for the vinasse residue, most likely due to changes in the structures of the carbonates as a result of reduction on carbon. Moreover, a new absorption band in the spectra for the vinasse residue appeared in the range from 550 to 450 $cm^{-1}$, which was probably related to the reduced forms of alkali carbonates.

*b) Evaporation of alkali chlorides*

According to Jensen *et al.* [140], KCl evaporates completely from wheat straw in the temperature range of 700–830 °C during pyrolysis of the straw in a laboratory-scale batch reactor. A similar observation was reported by Knudsen *et al.* [141] for barley and rice straw. The report from Knudsen *et al.* indicates that a high Cl/K mole ratio is a governing factor for the loss of K from the biomass fuels via evaporation of KCl at temperatures between 700 and 800 °C. In their report, the Cl/K mole ratios for the barley and rice straw were about 0.4 and 0.5, respectively. Similarly, the significant char weight loss shown in Figure 13 for the 700 and 800 °C experiments may be due to evaporation of KCl. The Cl/K mole ratio for the vinasse char given in Table 2, section 4.1.3, is

similar to that of the barley straw reported by Knudsen and co-workers. The presence of KCl in vinasse ash was verified by the XRD analysis described in section 4.3.2.

Furthermore, the melting characteristics of the vinasse char ash were calculated using the FactSage software described in section 4.2.6. The elemental composition of the vinasse char given in Table 2, section 4.1.3, and the FactSage databases described in section 4.2.6 were used as inputs for the FactSage calculations. Results of the calculations show that the alkali salts in the char ash start to melt at about 620 °C, and all alkali salts are fully molten at about 660 °C. These temperatures are close to the thermal events observed at about 620 and 740 °C in the DSC signals during the TGA experiments in 100% $N_2$ at 700 and 800 °C. During the heating-up period in 100% $N_2$, the onset of the endothermic peaks were observed in the DSC signals at about 620 and 740 °C in all the 100% $N_2$ experiments at 700 and 800 °C. After each endothermic peak, a sharp drop in the char sample weight was observed (as illustrated in Figure 13) for the 700 and 800 °C experiments, probably due to evaporation, mainly of KCl, from the sample.

*c) Sulfate reduction*

In addition to char weight losses due to reduction of alkali carbonates and evaporation of alkali chlorides, the char sample weight losses shown in Figure 13 may be due to reduction of alkali sulfates. According to Li and van Heiningen in their study of black liquor char gasification [81,142], $Na_2SO_4$ reduction was the main cause for black liquor char weight loss at temperatures above 600 °C. Moreover, according to Cameron and Grace [143], a molten mixture of alkali carbonates, $(Na,K)_2CO_3$, catalyzes a $Na_2SO_4$ reduction on Kraft black liquor char with $CO_2$ as the major product. Likewise, catalytic reduction of $(Na,K)_2SO_4$ appears to result in the vinasse char sample weight losses shown in Figure 13, mainly due to $CO_2$ release. As shown in the figure, reduction of the alkali sulfates is faster for the 700 and 800 °C experiments than for the 600 °C experiment. Stoichiometrically, complete reduction of $K_2SO_4$ in the vinasse char drops the char sample weight by about 6 wt % on a dry vinasse basis.

The presence of $K_2SO_4$ in vinasse char was verified from the FTIR tests described under (a) above. The FTIR spectra for the vinasse char showed strong and medium absorbance intensities in the ranges of 1200–1050 $cm^{-1}$ and 650–590 $cm^{-1}$, respectively, which are specific ranges for sulfate ions. However, neither absorption band was detected by the FTIR for the residue from the

TGA experiment carried out at 800 °C in 100% $N_2$, indicating that the alkali sulfates might have been completely reduced to alkali sulfides.

*d) Autogasification*

Although reductions of alkali carbonates (a) and sulfates (c) result in significant char sample weight loss in the TGA, these processes may not consume all of the organic carbon in the vinasse char. Complete reductions of the alkali carbonates and sulfates in the char would require only about 30% of the organic carbon, which is about 3 wt % on a dry vinasse basis. Other mechanisms, such as autogasification, might have contributed to the consumption of carbon from the sample in 100% $N_2$. Järvinen *et al.* [144] suggested in their study that autogasification of a biofuel could occur beyond the drying and devolatilization stages when the gasifying agent, $CO_2$, is released due to processes such as sulfate reduction.

However, for the 600 °C experiments shown in Figure 13, the rates for the above (a) to (d) mechanisms are slow. Consequently, the char sample weight loss at 600 °C is small compared to the weight losses at 700 and 800 °C as shown in the figure.

Results of the TGA tests conducted at 800 °C in 100 vol % $N_2$ with the KB, OB, GP, TGP, and SCB chars revealed that the char weight losses after a holding time of about 200 min in the TGA were ≤ 5%. This suggests that, unlike with the vinasse chars, mass loss from these chars in pure $N_2$ gas atmosphere via the mechanisms mentioned above is negligible.

### 5.2.2. TGA results in $CO_2$

Figure 14 shows results, on a wt % dry vinasse basis, from the TGA experiments for the vinasse chars carried out in 20% $CO_2$/80% $N_2$ and 40% $CO_2$/60% $N_2$ at 600, 700, and 800 °C. As seen from the figure, the 600 °C experiments were run for longer periods, and the residues were finally burned off with synthetic air after 260 min. Prior to burning of the residue, the isothermal temperature, 600 °C, was dropped to 540 °C, the temperature used for vinasse ashing.

When $CO_2$ gas was added to the system after the $N_2$ gas flow was decreased to 80% or 60% for the experiments at 700 and 800 °C, a weight gain was first observed, as shown in the figure. This might be due to buoyancy or possibly from $CO_2$ reacting with the reduced forms of carbonate-carbon complexes. Similar weight gains were reported for black liquor chars [142,145] and graphitized carbon [82] when $CO_2$ was supplied to the system. For the experiments at 600 °C, $CO_2$ was used from the beginning, i.e., also during the heating-up period. After this initial oxidation phase, the weight of the sample

continued to decrease. For the 800 °C experiments, the sample weight levels off with only ash remaining after about 150 min. For the experiments at 700 °C, the sample weight continued to decrease even after 200 min, probably due to a lower rate of evaporation of alkali metal salts compared to the rate at 800 °C. Inspection of the final residues from the 700 and 800 °C experiments in $CO_2$ by the optical microscope showed that the organic carbon was completely consumed. The amount of carbon burned off from the residues of the experiments in $CO_2$ at 600 °C after 260 min, as shown in the figure, is about 1.5 wt % dry vinasse. This amount is half of the amount burned off from the residue of the experiment at the same temperature in 100% $N_2$ (shown in Figure 13) after the same holding time. This indicates that $CO_2$ gasification was probably contributing to the loss of carbon from the sample at 600 °C.

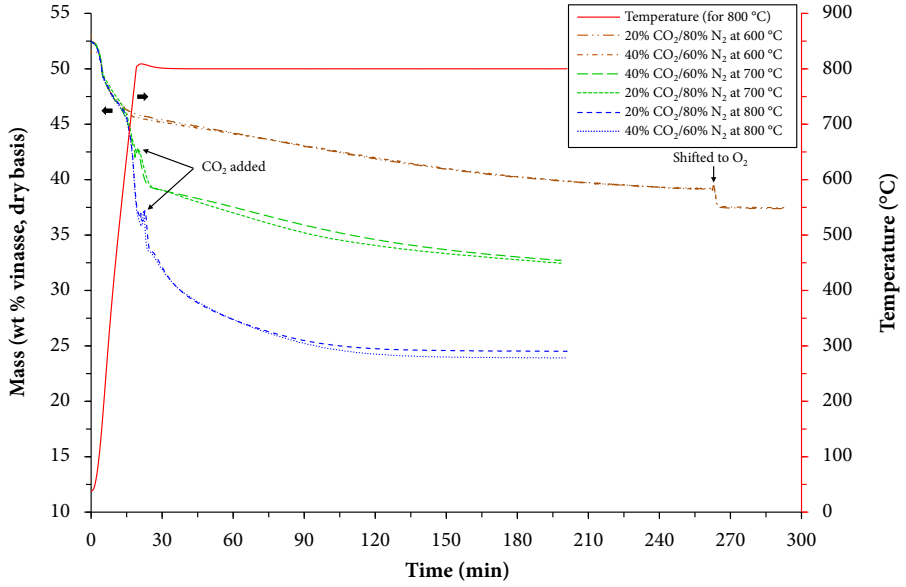


***Figure 14**. Mass (wt % vinasse, dry basis) and temperature (°C) in 20% $CO_2$/80% $N_2$ and 40% $CO_2$/60% $N_2$ at 600, 700, and 800 °C for the vinasse chars. Adapted with permission from **Paper III**. Copyright © 2016 Elsevier.*

The vinasse char $CO_2$ gasification may be described by the $CO_2$ gasification mechanism, described in section 3.3, for graphitized carbon as per the reactions given in Eqs. (2) and (3).

$$(\text{-}CO_2M) + C \leftrightarrow (\text{-}COM) + CO(g) \quad (2)$$

$$(\text{-}COM) + CO_2(g) \leftrightarrow (\text{-}CO_2M) + CO(g) \quad (3)$$

As seen in Figure 14, the sample weight loss curves for the two different concentrations of $CO_2$, 20% $CO_2$ and 40% $CO_2$, at a given temperature are almost the same. This may be due to saturation of the vinasse char surfaces with $CO_2$ at these concentrations. Consequently, under these conditions, the gasification reaction appears to be zero order in $CO_2$.

Figure 15 shows mass (wt % vinasse, dry basis) and temperature (°C) in the 40% $CO_2$/60% $N_2$ and 100% $N_2$ at 800 °C with the total amount of ash-forming matters released from the chars added to the corresponding residues on the TGA curves. The total amounts of the ash-forming matters released on a wt % dry vinasse basis were obtained from the sum of Na, K, S, Cl, and $CO_3$ released. The release levels for these ash-forming matters were determined based on their concentrations in the residues from the TGA and in the vinasse char. The Na, K, S, and Cl contents of the char and residues, on a wt % dry vinasse basis, are given in Table 2, section 4.1.3, and Table 6, section 5.4, respectively. The concentrations of $CO_3$ in the char and residues were estimated from charge balances based on the inorganic elemental compositions of the chars and residues. Details of the charge balance are available in **Paper III**.

As can be seen from Figure 15, after the releases are added back, the levels of the ash-forming matters for the experiments in $N_2$ and $CO_2$ are approximately the same. This indicates that the release of ash-forming matters can account for most of the difference between the runs in $N_2$ and $CO_2$.

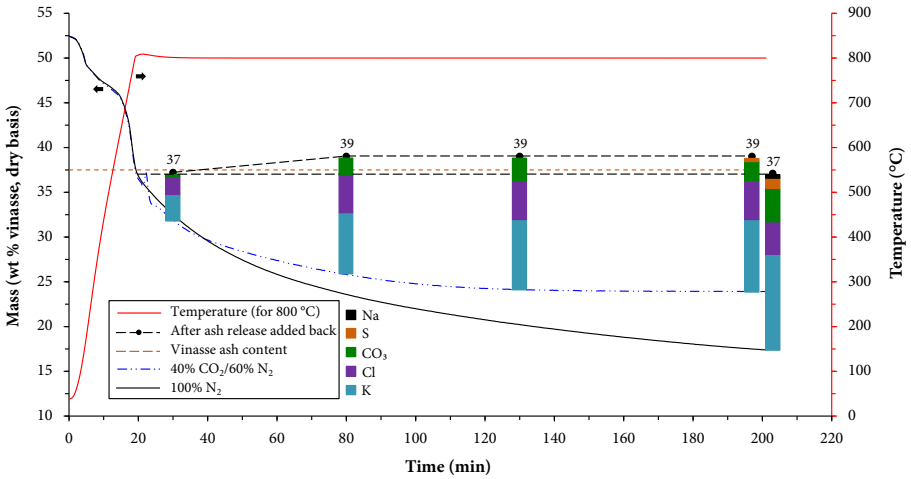


***Figure 15**. Mass (wt % vinasse, dry basis) and temperature (°C) in 40% $CO_2$/60% $N_2$ and 100% $N_2$ at 800 °C with total release of ash-forming matter added. Adapted with permission from **Paper III**. Copyright © 2016 Elsevier.*

Figure 16 shows results, on a wt % original dry fuel basis, from the TGA experiments in the 40% $CO_2$/60% $N_2$ gas atmosphere at 800 °C for the KB, OB, GP, TGP, and SCB chars. The char yields, given in section 4.2.2 for these fuels, were used to convert the char weight loss results obtained from the TGA to a wt % original dry biomass basis. The results shown in the figure were not published in any of the papers used in this thesis work. However, the char conversions, gasification rates, and K/C ratios described in sections 4.2.4 and 5.3 and published in **Paper IV** were determined based on the results given in the figure.

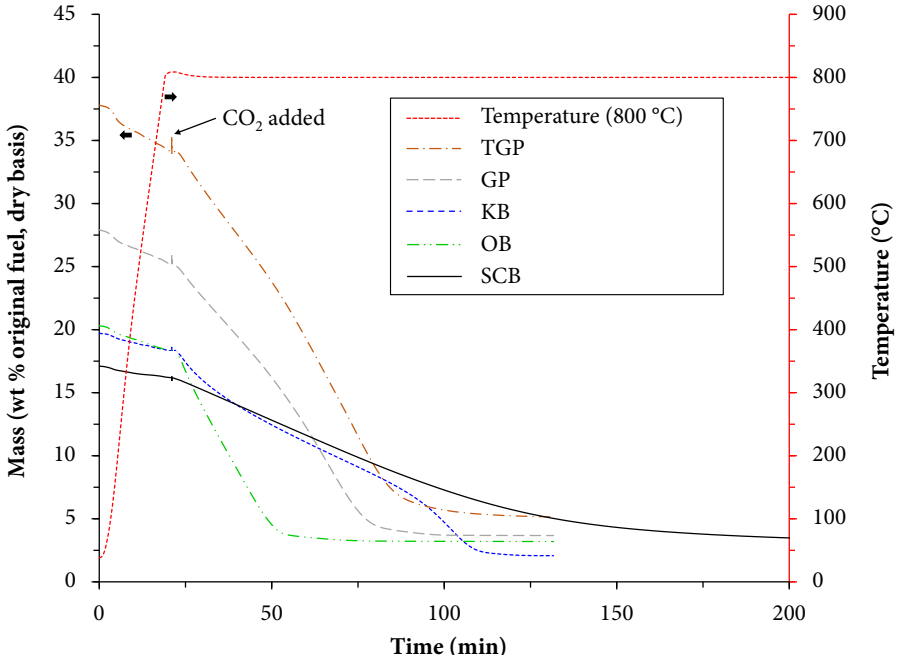


***Figure 16**. Mass (wt % original fuel, dry basis) and temperature (°C) in 40% $CO_2$/60% $N_2$ at 800 °C for the KB, OB, GP, TGP, and SCB chars. Data not published previously.*

As seen from Figure 16, the sample weight loss during heating to the gasification temperature, for all the chars, was ≤ 3 on a wt % original dry fuel basis. As previously explained for the vinasse chars, in section 5.2.1, this char weight loss is most likely due to drying followed by secondary pyrolysis. After $CO_2$ gas was added to the system, the mass loss curves for the chars flattened after 50-200 min with only ash remaining, as shown in the figure. The levels of ash obtained from the TGA for all the chars are approximately the same as the ash contents of the corresponding fuels given in Table 3, section 4.1.5. This

indicates that, in contrast to the results for the vinasse chars discussed earlier, the effect of loss of ash-forming matter on the overall char weight loss was insignificant for these chars. Moreover, Figure 16 shows that it took approximately 50, 80, 90, and 110 min for the mass loss to level off for the OB, GP, TGP, and KB chars, respectively. However, the time required for the mass loss to stabilize for the SCB chars was exceptionally long, more than 200 min. Given that the same gasification conditions, i.e., the same temperature, $CO_2$ concentration, sample amount, and reactor type, were used for all the chars, the variability in the reaction time indicates that the chars had different reactivities. According to Di Blasi [146], such variations in the char reactivities can be explained by differences in the chemical structure, porosity, and inorganic constituents of the chars. The following section further discusses the influence of the latter factor, mainly the K/C ratio, on char reactivity. However, the role of char chemical structure and porosity on char reactivity is beyond the scope of this work.

## 5.3. Influence of K/C ratio on $CO_2$ gasification rates

Figure 17 shows the instantaneous gasification rate ($s^{-1}$) versus K/C ratio for the five biomass chars. The results are for 0% to 97% char conversion. The top-right-corner figure in Figure 17 provides a magnified version of the rate vs. K/C ratio for char conversion between 0% and 80%.

As seen from the figure, for all the chars except for the SCB, the rate first increased, then reached a maximum, and finally decreased with K/C ratio. For the SCB chars, the rate initially increased with K/C ratio, and then remained almost constant after attaining a maximum. The increase in the rates with K/C ratio is almost linear in the range of 0% to 80% conversion for all the chars. The increase is steeper for the KB chars than for the others, suggesting that the KB chars are more reactive than the rest of the chars. However, the increase in the rate for the SCB chars is the least steep, indicating that these chars are the least reactive. Moreover, as seen from the figure, the rates for OB, GP, and TGP increased with K/C ratio in similar fashions in the range of 0% to 80% char conversion. The similar increases in the gasification rates for the GP and TGP, in the range of 0% to 80% char conversion, indicate that the influence of torrefaction on the catalytic gasification reactivity of GP is not significant. In addition, it has been suggested that the char gasification rate under initial and moderate degrees of char conversion is non-catalyzed for biomass fuels [147]. However, the results of the present study do not support that hypothesis. Instead, the instantaneous gasification rate increased linearly with the K/C

ratio from 0% to 80% of char conversion, indicating that the gasification reactions are catalytic.

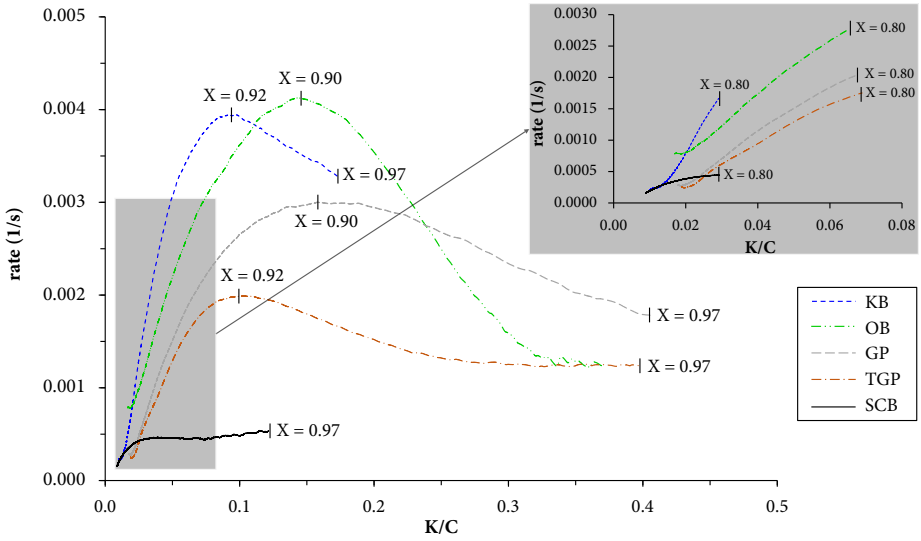


***Figure 17.*** *Instantaneous gasification rate at 800 °C as a function of K/C mole ratio for the five biomass chars for 0% to 97% char conversion. The top-right-corner figure shows the results for 0% to 80% char conversion. X refers to the degree of char conversion on ash-free basis. Adapted with permission from* ***Paper IV****. Copyright 2018 © American Chemical Society.*

As can be seen from Figure 17, the degree of conversion at which the maximum rates are observed for the KB, OB, GP, and TGP chars is in the range of 90% to 92%. For the SCB chars, the maximum rate was achieved at about 97% char conversion. It is interesting to see that the maximum rates for all the chars are attained when the K/C ratios are approximately 0.1, whereafter the rates, except that of the SCB chars, started to decrease. The decrease in the rates for the four chars after reaching a maximum may be due to accumulation of impurities or products in the pores [24] and/or to a decrease in the specific internal surface area [148]. While several studies, e.g., [111,148], have suggested that the maximum gasification rate for biomass chars occurs at a given degree of conversion, the results of the present study do not agree with that hypothesis. Instead, the results of the present work imply that the maximum rate occurs when the K/C ratio is close to 0.1. This K/C ratio value may be the point at which the gasification rate is saturated with respect to the catalyst. Nevertheless, a similar catalyst/carbon saturation ratio was reported by Mims and Pabst [149] for pure carbon and coal chars.

The low reactivity of the SCB char is most likely attributed to its high Si content. This is because Si inhibits char gasification reactivity by forming non-catalytic silicates [150]. Analysis of the SCB char with the SEM-EDX described in section 4.3.1 revealed that the carbon-rich zones of the chars, where most of the gasification reactions take place, had K/Si ratios, on a weight basis, of 3.3±1.5, while the ratio for the entire char was about 0.5. This indicates that most of the K found in the carbon-rich zones of the char was not bound to silicates. Thus, the formation of potassium silicates during gasification, which makes the K unavailable for catalytic reactions, may be the cause for the low gasification reactivity observed for the SCB char in Figure 17.

For the results from the TGA experiments at 800 °C in $CO_2$ (as shown in Figure 14, section 5.2.2, for the vinasse chars), it is difficult to assess the influence of K/C ratio on the gasification reactivity. This is because, as described in section 5.2.2, the char-sample weight loss in the TGA was dominated by loss of ash-forming matter. Consequently, determination of the amount of char carbon gasified by $CO_2$ (or the amount left in the residue) as a function of time, and hence the char conversion and gasification rate, was not possible with the present experimental methods. Nevertheless, the K/C ratio in the initial vinasse char can be estimated based on its elemental composition given in Table 2, section 4.1.3, by excluding the K existing in the char as KCl. The calculation yields a K/C ratio of about 0.3, which is three times higher than the value at which the maximum gasification rates were observed for the biomass chars given in Figure 17. At such a high K/C ratio, the oversaturation of the vinasse char surface by the catalyst might lead to a low char reactivity. However, further work is required to validate this claim.

## 5.4. Release of vinasse ash-forming elements

Tables 5 and 6 list results for the analyses of inorganics in the vinasse ashes (produced in the SPR at 900 °C) and in the residues from the TGA experiments (conducted at 700 and 800 °C), respectively. The results given in the tables are on a wt % dry vinasse basis. As with the original fuel, K, Ca, S, and Cl are the dominant ash-forming elements in the vinasse ashes and residues given in the tables. Furthermore, analysis of the ashes produced at 900 °C in the SPR in $O_2$ and $CO_2$ gas conditions with the XRD, described in section 4.3.2, revealed that KCl, CaO, $K_2SO_4$, $K_2CO_3$, MgO, $Ca_3(PO_4)_2$, $Ca_2SiO_4$, and $Ca_2SiO_4{\cdot}0.05Ca_3(PO_4)_2$ were the major components of the ashes. However, the reduced forms of ash-forming compounds, such as CaS and $K_2S_3$, were detected only in the ash produced at 900 °C in $CO_2$.

***Table 5**. Results for analysis of inorganics in the vinasse ashes produced in the SPR at 900 °C under combustion and gasification conditions (wt % vinasse, dry basis). Data from **Paper V**.*

| Gas Conditions | Elemental composition | | | | | | | | | |
|---|---|---|---|---|---|---|---|---|---|---|
| | Na | K | Ca | Mg | Si | Fe | Al | P | S | Cl |
| Combustion (10% $O_2$/90% $N_2$) | 0.3 | 12.8 | 3.1 | 0.5 | 0.7 | 0.1 | 0.03 | 0.1 | 2.0 | 3.5 |
| Gasification (50% $CO_2$/50% $N_2$) | 0.2 | 8.6 | 2.7 | 0.4 | 1.1 | 0.1 | 0.03 | 0.1 | 1.4 | 3.0 |

***Table 6**. Results for analysis of inorganics in the residues from the TGA experiments conducted at 700 and 800 °C (wt % vinasse, dry basis). Data from **Paper III**.*

| Inorganics | 40% $CO_2$/60% $N_2$ interrupted runs | | | 40% $CO_2$/60% $N_2$ | 100% $N_2$ |
|---|---|---|---|---|---|
| | 30 min | 80 min | 130 min | 200 min | 200 min |
| | | | 700 °C | | |
| Na | 0.5 | 0.4 | 0.4 | 0.5 | 0.5 |
| K | 12.6 | 9.3 | 6.9 | 6.8 | 6.7 |
| S | 1.5 | 0.9 | 0.8 | 1.0 | 0.9 |
| Cl | 4.3 | 3.8 | 1.8 | 1.5 | 2.7 |
| | | | 800 °C | | |
| Na | 0.6 | 0.5 | 0.4 | 0.4 | 0.2 |
| K | 10.6 | 6.5 | 5.3 | 5.3 | 2.3 |
| S | 2.4 | 2.3 | 2.2 | 1.3 | 0.6 |
| Cl | 2.4 | 0.6 | 0.2 | 0.2 | 1.0 |

Figure 18 shows the levels of vinasse ash-forming elements released during combustion and gasification of the vinasse at 900 °C in the SPR. The total $H_2O$- and $NH_4Ac$-soluble fractions of the ash-forming elements in the dried vinasse are also included in the figure. Values for the total $H_2O$- and $NH_4Ac$-soluble fractions of the ash-forming elements were obtained by adding the $H_2O$- and $NH_4Ac$-soluble portions from the fuel fractionation given in Figure 4, section 2.5. The values for total $H_2O$- and $NH_4Ac$-soluble fractions are represented by asterisks in Figure 18. The release levels in the figure are given as percentages of the ash-forming elements in the original dry fuel. The values for the release levels were obtained by subtracting the concentrations of the ash-forming elements in the ash given in Table 5 from their corresponding amounts in the parent fuel given in Table 2, section 4.1.3.

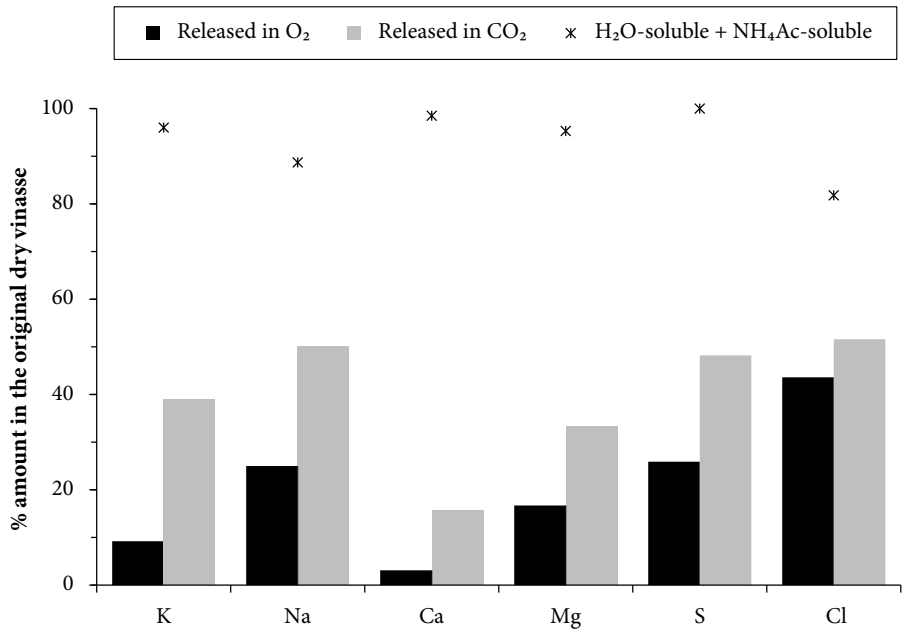


***Figure 18**. Total $H_2O$- and $NH_4Ac$-soluble fractions of vinasse ash-forming elements and the inorganics released during combustion and gasification at 900 °C in the SPR. Adapted with permission from **Paper V**. Copyright 2019 © American Chemical Society. Further permissions related to the material excerpted should be directed to the American Chemical Society.*

The results given in Figure 18 can be summarized as follows: (a) Although 50%, 72%, 55%, and 85% respectively of the Si, Fe, Al, and P in the vinasse are $H_2O$- and $NH_4Ac$-soluble (see section 2.5), none of these ash-forming elements was released at 900 °C under combustion and gasification conditions. For this reason, these ash-forming elements were not included in the figure. (b) The K, Na, Ca, Mg, S, and Cl released from the vinasse at 900 °C in the SPR under combustion conditions were 9%, 25%, 3%, 17%, 26%, and 44% of the amounts in the vinasse, respectively. The corresponding release numbers in $CO_2$ for the inorganics were 39%, 50%, 16%, 33%, 48%, and 52%. The levels of each of these ash-forming elements released in $CO_2$ are higher than the amounts released in $O_2$. The higher levels of inorganics released under gasification conditions than under combustion may be due to differences in the holding times and gas atmospheres used in the SPR. The influences of these two factors, as well as of temperature, on the release of K and Cl in the vinasse are discussed below. As already stated in the Background section, K and Cl were selected for the

discussion as these ash-forming elements are the main causes of the ash-related problems in thermochemical conversion processes.

*Influence of holding time*

Figures 19 (A) and (B) show the effects of holding time on the release of K and Cl, respectively, during the vinasse char $CO_2$ gasification experiments in the TGA at 700 and 800 °C. The values given in the figures were calculated based on the results given in Tables 2 and 6 in a fashion similar to those given in Figure 18. The amounts of K and Cl released from the vinasse during the char production stage, i.e., about 5% and 25% respectively of the amounts in the vinasse, were not considered in the calculation. This is because the char production was carried out in a 100% $N_2$ gas atmosphere. As seen from the figures, the levels of K and Cl released increased considerably with the holding time up to 130 min and then remained almost constant afterward at both temperatures. As discussed in sections 5.2.1 and 5.2.2, the increases in the release of the K and Cl with holding time may be due to evaporation of KCl from the vinasse char. Therefore, the longer holding time used in the SPR during gasification than during combustion might have also resulted in the higher release of inorganics in the $CO_2$ gas atmosphere than in the $O_2$ shown in Figure 18. For pulverized biomass fuels [151], it has been shown that holding time strongly influences the release of ash-forming elements during thermochemical conversion of biomass fuels.

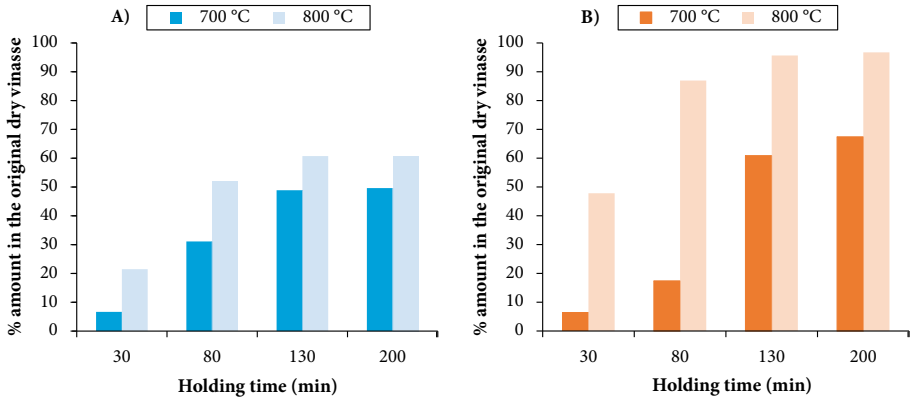


***Figure 19**. Release of A) K and B) Cl in $CO_2$ at 700 and 800 °C as a function of holding time. Data from **Paper III**.*

*Influence of gas atmosphere*

In addition to holding time, the relatively reducing $CO_2$ gas atmosphere compared to the $O_2$ might have enhanced the release of inorganics during the

vinasse $CO_2$ gasification in the SPR shown in Figure 18. For example, Figures 20 (A) and (B) show the respective levels of K and Cl released from the vinasse char during the TGA experiments in $N_2$ and $CO_2$ gas atmospheres after the same holding time, 200 min, in the TGA. The values given in the figures were obtained based on the results in Tables 2 and 6 in the same manner as those given in Figure 18. As seen from Figure 20 (A), more K was released from the vinasse char in $N_2$ than in $CO_2$ owing to successive reductions of alkali carbonates on carbon and ultimately vaporization of the alkali metals. This mechanism was discussed previously in sections 5.2.1 and 5.2.2. Similarly, the detection of the reduced forms of ash-forming compounds only in the ash produced at 900 °C in $CO_2$ indicates that release of alkali metals through reduction of alkali carbonates also occurs in $CO_2$. However, as seen from Figure 20 (B), the release levels for Cl are more pronounced in $CO_2$ gas atmosphere than in $N_2$. At temperatures above 700 °C, higher levels of Cl release in $CO_2$ than in $N_2$ were also observed by Björkman and Strömberg [152] for sugarcane trash. Yet, as shown in Figure 18, less Cl was released in $O_2$ than in $CO_2$ at 900 °C.

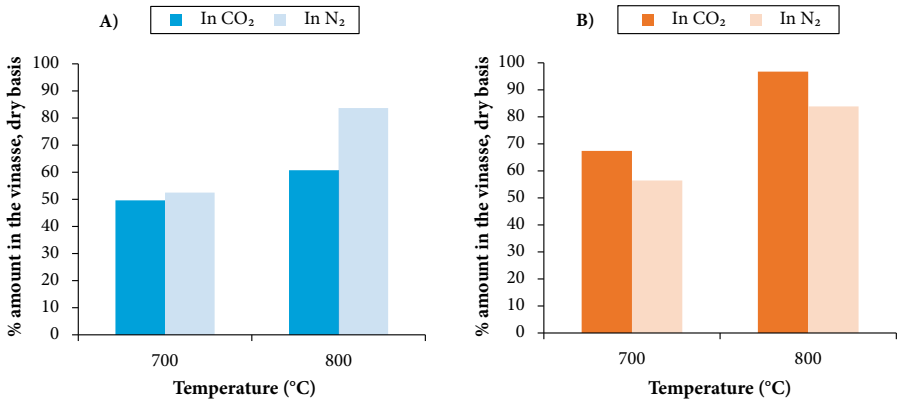


***Figure 20**. Release of A) K and B) Cl at 700 and 800 °C under pyrolysis ($N_2$) and gasification ($CO_2$) conditions. Data from **Paper III**.*

*Influence of temperature*

The influence of temperature on the release of K and Cl from the vinasse can be observed in Figures 19 and 20. As those figures show, for a given holding time, the levels of K and Cl released increased considerably as the temperature was raised from 700 to 800 °C irrespective of the gas atmosphere. For example, when the temperature was raised from 700 to 800 °C in $N_2$, K and Cl release from the vinasse char increased from about 50–55% to about 80–85% after a

holding time of 200 min. The various mechanisms responsible for the increased levels of K and Cl release with temperature are discussed in section 5.2.

In general, not all of the $H_2O$- and $NH_4Ac$-soluble fractions of the vinasse ash-forming elements were released during pyrolysis, gasification, combustion under the present experimental conditions. For other biomasses, Frandsen *et al.* [101] reported that there is no direct correlation between the release levels of ash-forming elements during combustion and the $H_2O$- and $NH_4Ac$-soluble fractions of the ash-forming elements from the chemical fractionation. One possible reason mentioned by Frandsen *et al.* for the deviations is the interaction between the released inorganic elements and those remaining in the ash, where the two fractions may react, forming a non-released species. For example, according to Johansen *et al.* [153], Si in biomass fuels plays a significant role in the retention of alkalis in the ash as silicates during pyrolysis and combustion of the biomass. Si in the vinasse might have played a similar role. The presence of silicates in the vinasse ashes was confirmed from the XRD analysis, as discussed above. Nevertheless, the release of significant levels of K and Cl in the vinasse at temperatures of 700 °C and above indicates that vinasse is a problematic fuel for combustion and gasification in conventional boilers and gasifiers.

From the perspective of minimizing the release of K and Cl from the vinasse, a low-temperature thermochemical conversion process with a short residence time of the product char in the process is recommended. To this end, fast pyrolysis of the vinasse in the temperature range of 400–500 °C could be an option. As previously discussed in section 5.1.2, the K and Cl released during fast pyrolysis of the dried vinasse at 400 and 500 °C in the drop-tube-type reactor were 12–13% and 25%, respectively, of the amounts in the vinasse. These release levels can be lowered even further if a system for continuous withdrawal of the chars from the drop-tube-type reactor is devised.

## 5.5. Ash-melting behavior

Figure 21 shows melt fraction as a function of temperature based on the FactSage calculations for the vinasse and for the vinasse ash produced at 500 °C. The results are based on the elemental compositions of the vinasse and its ash given in Table 2, section 4.1.3, as inputs for the FactSage thermodynamic calculations. Figure 22 shows the DSC measurement results as a function of temperature for the vinasse ash produced at 500 °C from the TGA experiments.

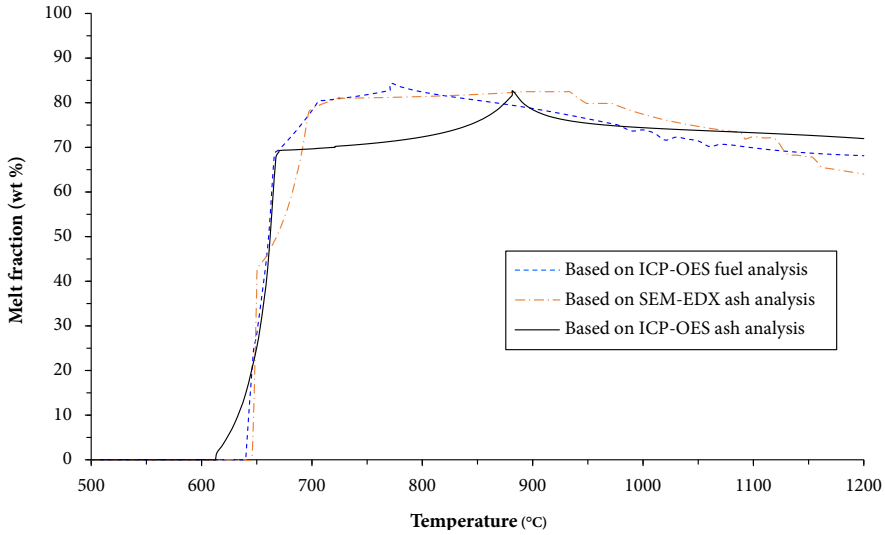


***Figure 21***. *Melt fraction (wt %) versus temperature (°C) based on the FactSage calculations for vinasse and for vinasse ash produced at 500 °C. Adapted with permission from* ***Paper V***. *Copyright 2019 © American Chemical Society. Further permissions related to the material excerpted should be directed to the American Chemical Society.*

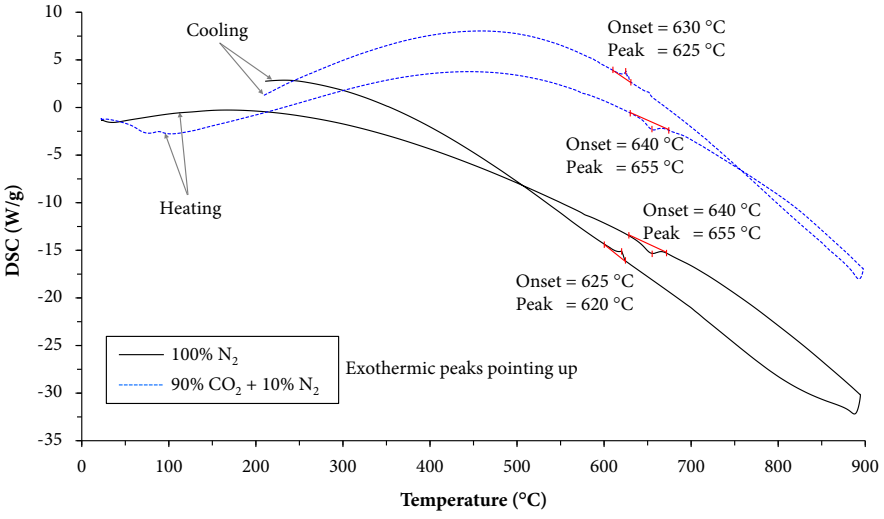


***Figure 22***. *Results of DSC (W/g) measurements in 100% $N_2$ and 90% $CO_2$/10% $N_2$ versus temperature (°C) for vinasse ash produced at 500 °C. Adapted with permission from* ***Paper V***. *Copyright 2019 © American Chemical Society. Further permissions related to the material excerpted should be directed to the American Chemical Society.*

As can be seen from Figure 21, the vinasse ash-melting curves are generally very similar whether the fuel or ash elemental composition was used as input data for the FactSage thermodynamic calculations. The calculations show that the vinasse characteristic ash-melting temperatures, i.e., $T_0$, $T_{15}$, and $T_{70}$, are 640–645, 650, and 670–690 °C, respectively. However, a lower $T_0$ value, about 612 °C, was obtained from the FactSage calculations when the ash elemental analysis results from ICP-OES were used as input data for the FactSage software. This may be due to the higher Cl value obtained from the IC for the ash. Moreover, it can be observed from the figure that the melt fraction does not reach 100% due to the presence of high-temperature melting oxide phases in the ash. The high-temperature melting oxide phases obtained from the FactSage thermodynamic calculations were CaO(s), MgO(s), $Ca_3Al_2O_6$(s), $Ca_2SiO_4$(s), and $Ca_2Fe_2O_5$(s). Furthermore, as seen from the figure, the melt fraction starts declining at temperatures above 850 °C as a consequence of evaporation of alkali chlorides, which are the main components in the melt phase.

The $T_0$ result obtained from the FactSage calculations agrees with the DSC measured value, 640 °C in both the $N_2$ and $CO_2$ gas atmospheres, during heating up the ash sample as shown in Figure 22. However, it can be seen from the figure that the $T_0$ value shifted from 640 °C to 625 °C in $N_2$ and to 630 °C in $CO_2$ upon crystallization of the molten ash. These shifts in the $T_0$ value are most likely due to changes in the composition of the molten ash as a result of ash sample weight losses in the DSC-TGA. Ash sample weight losses of about 30% and 27% in the $N_2$ and $CO_2$ gas atmospheres, respectively, were observed in the DSC-TGA. These losses were mainly due to evaporation of alkali chlorides and decomposition of carbonates present in the vinasse ash (see section 4.1.4).

The melting of most of the vinasse ash, 70%, in a narrow temperature range, 640–690 °C, indicates that KCl is probably the dominant ash-forming matter in the ash. The presence of KCl in the vinasse ash was verified by the XRD analysis, as discussed in section 4.1.4. Here too, the low-temperature melting of the ash suggests that vinasse is a difficult fuel for conventional thermochemical conversion processes.

# 6. CONCLUSIONS AND RECOMMENDATIONS FOR FUTURE WORK

In this thesis work, characteristics of vinasse thermochemical conversion were studied. Fast pyrolysis, $CO_2$ gasification, release of ash-forming elements during pyrolysis, gasification, and combustion, and ash-melting behavior were the thermochemical conversion properties of vinasse studied. These properties are important for modeling, design, and development of industrial-scale thermochemical conversion processes for vinasse. In addition, the influence of K/C ratio on the gasification reactivities of chars from agro-industrial biomasses was studied. The conclusions drawn from this study and some suggestions for future work are presented below.

## 6.1. Conclusions

Results of the vinasse fast pyrolysis in the drop-tube-type reactor at 400 and 500 °C revealed that the water-free pyrolysis-oil yield was low compared to the yields from other biomass fuels. Moreover, the organic liquid yield was independent of temperature in the temperature range considered. However, the char yield decreased, and the gas yield increased with temperature. The low bio-oil yield and high gas and water yields were probably due to the high K content of the vinasse. For other biomass fuels, it is well-established that alkali metals catalyze secondary reactions in the vapor phase of the pyrolysis product, thereby decreasing the organic liquid yield and increasing the gas and water yields. Moreover, about 45–55% of the carbon and more than 85% of the K from the vinasse were recovered with the chars.

Results from the DSC-TGA experiments at 600–800 °C in $CO_2$ and $N_2$ gas atmospheres showed that the vinasse char sample weight losses were dominated by release of inorganics. Reduction of alkali carbonates and sulfates by carbon, evaporation of alkali chlorides, and autogasification are the main mechanisms by which the char sample weight losses occurred. These mechanisms, except for evaporation of the alkali chlorides, were in part responsible for the consumption of the organic carbon from the vinasse chars. However, complete removal of the organic carbon from the chars was achieved only in the $CO_2$ gas atmosphere at temperatures of 700 °C and above. Furthermore, in the $CO_2$ gas concentration range considered, the gasification reaction for the vinasse chars appears to be zero order in $CO_2$.

For other agro-industrial biomasses with ash contents of approximately one order of magnitude lower than that of the vinasse, the char sample weight

losses in the TGA at 800 °C in $CO_2$ were mainly due to gasification of carbon by $CO_2$. For these fuels, the char gasification rates increased almost linearly with the K/C ratio from 0% to 80% char conversion. After the gasification rates reached a maximum at a K/C ratio of around 0.1, the rates started to decrease, suggesting that the catalytic char gasification rates might have been saturated with respect to K. Chars from one of the biomass fuels, sugarcane bagasse, had a high Si content and a lower reactivity. The formation of potassium silicates during gasification, deactivating the catalytic effect of the K, was probably the cause of the low reactivity of chars from this fuel. For the vinasse chars, however, it was not possible to assess the influence of K/C ratio on the gasification rate with the present experimental methods. This was because the significant levels of inorganics released from the vinasse chars during gasification hampered determination of the amount of char carbon gasified as a function of time, and consequently, determination of char conversion and gasification rates.

Results of analyses of the ashes/residues from the SPR/DSC-TGA showed that significant levels of the K, Na, Ca, Mg, S, and Cl in the vinasse and its chars were released under combustion, gasification, and inert gas conditions. However, none of the Si, Al, Fe, and P in the vinasse was released under the present experimental conditions although 50–70% of the Si, Al, and Fe and almost all of the P in the vinasse were $H_2O$- and $NH_4Ac$-soluble. Holding times, temperature, and gas atmosphere are the main factors that influenced the release of K and Cl from the vinasse. In general, temperatures of above 700 °C and longer holding times increased the release of K and Cl considerably, and the release levels were more severe in reducing gas atmospheres than in oxidizing conditions. However, Cl release was found to be higher in $CO_2$ than in $N_2$.

The FactSage calculation and DSC measurement results showed that the vinasse ash initial melting temperature is in the range of 640–645 °C. Results of the FactSage calculations also indicated that 15% and 70% of the ash is molten at about 650 °C and 670–690 °C, respectively. However, the ash melt fraction does not reach 100% below 1200 °C due to the presence of high temperature melting oxide phases in the ash.

The significant amounts of alkali and alkali chlorides released from the vinasse and the low temperature melting of the vinasse ash indicate that vinasse is a difficult fuel for conventional combustion and gasification processes. In particular, the use of a bubbling/circulating fluidized bed technology, state-of-the-art technology for combustion/gasification of solid fuels, for heat and

power production from vinasse appears impossible due to the high risk of bed agglomeration. Nevertheless, there are some potential alternative options that may enable the recovery of energy and inorganic chemicals from vinasse while minimizing some of the limitations of applying wet vinasse to the soil. Table 7 summarizes the pros and cons of these options based on the findings in this work and the information available in the literature.

One option is the low-temperature fast pyrolysis process. This process has the advantage of producing biochar with a high K content for fertilizer, which at the same time sequesters approximately half of the carbon from the vinasse. In addition, the pyrolysis oils and gases can be burned in a boiler with lower ash-related problems than burning the original fuel directly. However, the low bio-oil yield and the high water content of the bio-oil makes the fast pyrolysis process unattractive for bio-oil production from vinasse. Another option is combustion of vinasse in a black liquor recovery boiler type in which the fuel is spray-fed into the boiler in coarse droplets. Such a system could minimize the formation of ash fumes during combustion, and the subsequent ash-related problems, while allowing most of the inorganics to be recovered as bottom ash for use as fertilizer. However, low electrical power efficiency due to low steam parameters is the inevitable drawback of this system. A third alternative is the high-temperature entrained flow gasifier of the type demonstrated for black liquor. Still, this option requires installation of syngas cleaning device(s) and a separate process for the recovery of inorganic chemicals from the aqueous-phase bottom product.

***Table 7.*** *Summary of the pros and cons of potential alternative options for vinasse thermochemical conversion.*

| Option/Process | Pros | Cons |
|---|---|---|
| Low-temperature fast pyrolysis for bio-oil production | + environmental pollution reduction<br>+ production of K-rich bio-char for fertilizer<br>+ combustion of pyrolysis oils and gases for heat and power production<br>+ less ash-related problems from combustion of the pyrolysis oils and gases | – low bio-oil yield<br>– high water content of the bio-oil<br>– low calorific value of the pyrolysis gases |
| Combustion in black liquor recovery boiler type | + complete removal of COD and BOD<br>+ recovery of energy, power, and inorganic chemicals<br>+ well-established technology for black liquor<br>+ simpler furnace than that of a black liquor recovery boiler | – low power efficiency<br>– corrosion |
| High-temperature entrained flow gasification | + complete removal of COD and BOD<br>+ syngas production and recovery of inorganic chemicals<br>+ proved to be viable for black liquor on pilot-scale level | – syngas cleaning<br>– aqueous-phase bottom ash processing<br>– corrosion<br>– has not been scaled up to commercial-scale |
| Fluidized bed combustion or gasification | + well-established technology for thermal conversion of solid fuels<br>+ potential for electric power production | – bed agglomeration<br>– corrosion |

## 6.2. Recommendations for future work

From the perspective of minimizing the release of K and Cl from vinasse, a low-temperature thermochemical conversion process with a short residence time of the product char in the process is recommended. To this end, fast pyrolysis of the vinasse in the temperature range of 400–500 °C presents an interesting option. The release levels of K and Cl during fast pyrolysis of the vinasse at 400 and 500 °C in the present drop-tube-type reactor are low, and can be minimized further if a system for continuous removal of the chars from the reactor is devised.

The vinasse gasification and combustion experiments in the DSC-TGA and SPR at temperatures between 700 and 900 °C resulted in the release of inorganics from the vinasse to a high degree. In particular, the high levels of alkali chlorides released at the gasification/combustion temperatures coupled with the low-temperature melting property of the vinasse ash are bottlenecks for the implementation of a gasification/combustion process for vinasse on an industrial scale. Nevertheless, two processes worth investigating for vinasse are the high-temperature entrained flow gasification and combustion in a black liquor recovery boiler type. A pilot-scale plant of the entrained flow gasification process has been demonstrated to be successful for black liquor. The latter process allows a simpler furnace design, i.e., no need to have a reducing gas atmosphere in the lower furnace, than that of the black liquor recovery boiler.

Finally, it is important to demonstrate how the fuel characterization data generated in this work can be utilized in practice. For this purpose, conducting process modeling for vinasse thermochemical conversion using, for example, computational fluid dynamics enables understanding of properties of the fuel in detail on industrial-scale thermochemical conversion systems.

# REFERENCES


[1] Srirangan K, Akawi L, Moo-Young M, Chou CP. Towards sustainable production of clean energy carriers from biomass resources. Applied Energy 2012;100:172–86.

[2] Polack JA, Day DF, Cho YK. Gasohol from sugarcane-stillage disposition. Louisiana: 1981.

[3] Sarangi BK, Mudliar SN, Bhatt P, Kalve S, Chakrabarti T, Pandey RA. Compost from sugarmill pressmud and distillery spentwash for sustainable agriculture: A review. Dynamic Soil, Dynamic Plant 2008;2:35–49.

[4] Pant D, Adholeya A. Biological approaches for treatment of distillery wastewater: A review. Bioresource Technology 2007;98:2321–34.

[5] Christofoletti CA, Escher JP, Correia JE, Marinho JFU, Fontanetti CS. Sugarcane vinasse: Environmental implications of its use. Waste Management 2013;33:2752–61.

[6] Patel N. Studies on the combustion and gasification of concentrated distillery effluent (Ph.D. thesis). Indian Institute of Science, 2000.

[7] Cortez LAB, Pérez LEB. Experiences on vinasse disposal. Part III: Combustion of vinasse-#6 fuel oil emulsions. Brazilian Journal of Chemical Engineering 1997;14:9–18.

[8] Nandy T, Shastry S, Kaul SN. Wastewater management in a cane molasses distillery involving bioresource recovery. Journal of Environmental Management 2002;65:25–38.

[9] Sydney EB, Larroche C, Novak AC, Nouaille R, Sarma SJ, Brar SK, Letti LAJ, Soccol VT, Soccol CR. Economic process to produce biohydrogen and volatile fatty acids by a mixed culture using vinasse from sugarcane ethanol industry as nutrient source. Bioresource Technology 2014;159:380–6.

[10] Serikawa RM, Funazukuri T, Wakao N. Effects of acid and alkali added in high-pressure oil conversion of sugar-cane vinasse. Kagaku Kogaku Ronbunshu 1993;19:544–548.

[11] Adams TN, Frederick WJ, Grace TM, Hupa M, Iisa K, Jones AK, Tran H. Kraft recovery boilers. Atlanta: Tappi Press; 1997.

[12] de Resende AS, Xavier RP, de Oliveira OC, Urquiaga S, Alves BJR, Boddey RM. Long-term effects of pre-harvest burning and nitrogen and vinasse applications on yield of sugar cane and soil carbon and nitrogen

stocks on a plantation in Pernambuco, N.E. Brazil. Plant and Soil 2006;281:339–51.

[13] Jiang Z-P, Li Y-R, Wei G-P, Liao Q, Su T-M, Meng Y-C, Zhang H-Y, Lu C-Y. Effect of long-term vinasse application on physico-chemical properties of sugarcane field soils. Sugar Tech 2012;14:412–7.

[14] Prado RM, Caione G, Campos CNS. Filter cake and vinasse as fertilizers contributing to conservation agriculture. Applied and Environmental Soil Science 2013:1–8.

[15] Yang S-D, Liu J-X, Wu J, Tan H-W, Li Y-R. Effects of vinasse and press mud application on the biological properties of soils and productivity of sugarcane. Sugar Tech 2013;15:152–8.

[16] de Oliveira BG, Carvalho JLN, Cerri CEP, Cerri CC, Feigl BJ. Soil greenhouse gas fluxes from vinasse application in Brazilian sugarcane areas. Geoderma 2013;200–201:77–84.

[17] Bergeron C, Carrier DJ, Ramaswamy S. Biorefinery co-products: Phytochemicals, primary metabolites and value-added biomass processing. 1st ed. Chichester: John Wiley & Sons, Ltd; 2012.

[18] Brown RC. Thermochemical porocessing of biomass: Conversion into fuels, chemicals and power. 1st ed. Chichester: John Wiley & Sons, Ltd; 2011.

[19] Crocker M. Thermochemical conversion of biomass to liquid fuels and chemicals. 1st ed. Cambridge: Royal Society of Chemistry; 2010.

[20] Baxter LL, Miles TR, Miles Jr. TR, Jenkins BM, Milne T, Dayton D, Bryers RW, Oden LL. The behavior of inorganic material in biomass-fired power boilers: Field and laboratory experiences. Fuel Processing Technology 1998;54:47–78.

[21] Wang L, Weller CL, Jones DD, Hanna MA. Contemporary issues in thermal gasification of biomass and its application to electricity and fuel production. Biomass and Bioenergy 2008;32:573–81.

[22] Aho A, DeMartini N, Pranovich A, Krogell J, Kumar N, Eränen K, Holmbom B, Salmi T, Hupa M, Murzin DY. Pyrolysis of pine and gasification of pine chars — Influence of organically bound metals. Bioresource Technology 2013;128:22–9.

[23] Coulson M. Pyrolysis of perennial grasses from Southern Europe. Thermalnet Newsletter 2006:6–7.

[24] Perander M, DeMartini N, Brink A, Kramb J, Karlström O, Hemming J, Moilanen A, Konttinen J, Hupa M. Catalytic effect of Ca and K on $CO_2$ gasification of spruce wood char. Fuel 2015;150:464–72.

[25] Nazari L, Yuan Z, Souzanchi S, Ray MB, Xu C (Charles). Hydrothermal liquefaction of woody biomass in hot-compressed water: Catalyst screening and comprehensive characterization of bio-crude oils. Fuel 2015;162:74–83.

[26] Cortes-Rodríguez EF, Fukushima NA, Palacios-Bereche R, Ensinas AV, Nebra SA. Vinasse concentration and juice evaporation system integrated to the conventional ethanol production process from sugarcane — Heat integration and impacts in cogeneration system. Renewable Energy 2018;115:474–88.

[27] Fukushima NA, Palacios-Bereche MC, Palacios-Bereche R, Nebra SA. Energy analysis of the ethanol industry considering vinasse concentration and incineration. Renewable Energy 2019;142:96–109.

[28] Pina EA, Palacios-Bereche R, Chavez-Rodriguez MF, Ensinas AV, Modesto M, Nebra SA. Reduction of process steam demand and water-usage through heat integration in sugar and ethanol production from sugarcane — Evaluation of different plant configurations. Energy 2017;138:1263–80.

[29] Pellegrini LF, de Oliveira Jr. S. Combined production of sugar, ethanol and electricity: Thermoeconomic and environmental analysis and optimization. Energy 2011;36:3704–15.

[30] Canilha L, Chandel AK, Milessi TSS, Antunes FAF, Freitas WLC, Felipe MGA, da Silva SS. Bioconversion of sugarcane biomass into ethanol: An overview about composition, pretreatment methods, detoxification of hydrolysates, enzymatic saccharification, and ethanol fermentation. Journal of Biomedicine and Biotechnology 2012:1–15.

[31] Gurría A, da Silva JG. OECD-FAO agricultural outlook 2018-2027: Sugar. Rome: 2018.

[32] Rein P. Cane sugar engineering. 1st ed. Berlin: Verlag Dr. Albert Bartens KG; 2007.

[33] Dias MOS, Junqueira TL, Rossell CEV, Filho RM, Bonomi A. Evaluation of process configurations for second generation integrated with first generation bioethanol production from sugarcane. Fuel Processing Technology 2013;109:84–9.

[34] Treedet W, Suntivarakorn R. Sugar cane trash pyrolysis for bio-oil production in a fluidized bed reactor. In: The Proceedings of the World Renewable Energy Congress, Linköping: Linköping University Electronic Press; Linköpings universitet; 2011, p. 140–147.

[35] Al Arni S, Bosio B, Arato E. Syngas from sugarcane pyrolysis: An experimental study for fuel cell applications. Renewable Energy 2010;35:29–35.

[36] Treedet W, Suntivarakorn R. Design and operation of a low cost bio-oil fast pyrolysis from sugarcane bagasse on circulating fluidized bed reactor in a pilot plant. Fuel Processing Technology 2018;179:17–31.

[37] Al Arni S. Comparison of slow and fast pyrolysis for converting biomass into fuel. Renewable Energy 2018;124:197–201.

[38] Treedet W, Suntivarakorn R. Fast pyrolysis of sugarcane bagasse in circulating fluidized bed reactor — Part A: Effect of hydrodynamics performance to bio-oil production. Energy Procedia 2017;138:801–5.

[39] Treedet W, Taechajedcadarungsri S, Suntivarakorn R. Fast pyrolysis of sugarcane bagasse in circulating fluidized bed reactor — Part B: Modelling of bio-oil production. Energy Procedia 2017;138:806–10.

[40] Varma AK, Mondal P. Pyrolysis of sugarcane bagasse in semi batch reactor: Effects of process parameters on product yields and characterization of products. Industrial Crops and Products 2017;95:704–17.

[41] Gabra M, Pettersson E, Backman R, Kjellström B. Evaluation of cyclone gasifier performance for gasification of sugar cane residue — Part 1: Gasification of bagasse. Biomass and Bioenergy 2001;21:351–69.

[42] Gabra M, Pettersson E, Backman R, Kjellström B. Evaluation of cyclone gasifier performance for gasification of sugar cane residue — Part 2: Gasification of cane trash. Biomass and Bioenergy 2001;21:371–80.

[43] Hassuani SJ, Leal MRLV, Macedo IC. Biomass power generation: Sugar cane bagasse and trash. 1st ed. Piracicaba: PNUD - Programa das Nações Unidas para o Desenvolvimento CTC - Centro de Tecnologia Canavieira; 2005.

[44] Jorapur R, Rajvanshi AK. Sugarcane leaf-bagasse gasifiers for industrial heating applications. Biomass and Bioenergy 1997;13:141–6.

[45] Hugot E. Handbook of cane sugar engineering. 3rd ed. Amsterdam: Elsevier Science Publishers BV; 1986.

[46] Leal MRLV, Galdos MV, Scarpare FV, Seabra JEA, Walter A, Oliveira COF. Sugarcane straw availability, quality, recovery and energy use: A literature review. Biomass and Bioenergy 2013;53:11–9.

[47] Ayres A. Variation of mineral content of sugar cane with age and season. Hawaiian Planters' Record 1933;37:197–206.

[48] Coates CE, Fieger EA, Salazar LG. The ratio of ash constituents in different cane varieties, a preliminary study. The Planter and Sugar Manufacturer 1928;80:421–2.

[49] Zevenhoven M, Yrjas P, Hupa M. Ash-forming matter and ash-related problems. In: Lackner M, Winter F, Agarwal AK, editors. Handbook of combustion: Part 4. Solid fuels, Weinheim: WILEY-VCH Verlag GmbH & Co. KGaA; 2010, p. 493–531.

[50] Benson SA, Holm PL. Comparison of inorganic constituents in three low-rank coals. Industrial and Engineering Chemistry Product Research and Development 1985;24:145–9.

[51] Zevenhoven M. Ash-forming matter in biomass fuels (Ph.D. thesis). Åbo Akademi University, 2001.

[52] Zevenhoven M, Yrjas P, Skrifvars B-J, Hupa M. Characterization of ash-forming matter in various solid fuels by selective leaching and its implications for fluidized-bed combustion. Energy & Fuels 2012;26:6366–86.

[53] Zevenhoven M, Blomquist J-P, Skrifvars B-J, Backman R, Hupa M. The prediction of behaviour of ashes from five different solid fuels in fluidised bed combustion. Fuel 2000;79:1353–61.

[54] Jordan AC, Akay G. Speciation and distribution of alkali, alkali earth metals and major ash forming elements during gasification of fuel cane bagasse. Fuel 2012;91:253–63.

[55] Werkelin J, Skrifvars B-J, Zevenhoven M, Holmbom B, Hupa M. Chemical forms of ash-forming elements in woody biomass fuels. Fuel 2010;89:481–93.

[56] van Loo S, Koppejan J. Handbook of biomass combustion and co-firing. 1st ed. Enschede: Twente University Press; 2002.

[57] Kujala P, Hull R, Engstrom F, Jackman E. Alcohol from molasses as a possible fuel and economics of distillery effluent treatment. Sugar y Azucar 1976;71:28–39.

[58] Cortez LAB, Rossell CEV, Jordan RA, Leal MRLV, Lora EES. R & D needs in the industrial production of vinasse. In: Cortez LAB, editor. Sugarcane bioethanol — Research and development for productivity and sustainability. 1st ed., São Paulo: Editora Edgard Blücher; 2014, p. 619–636.

[59] Akram M, Tan CK, Garwood R, Thai SM. Vinasse — A potential biofuel — Cofiring with coal in a fluidised bed combustor. Fuel 2015;158:1006–15.

[60] Reich GT. Production of carbon and potash from molasses distillers' stillage. Transactions of the American Institute of Chemical Engineers 1945;41:233–51.

[61] Chakrabarty R. Potash recovery — A method of disposal of distillery wastes and saving foreign exchange. In: The Proceedings of the Symposium on Ethyl Alcohol Production Techniques, New Delhi: Noyes Development Corporation; 1964, p. 93–97.

[62] Dymond GC. A review of fuel alcohol production and dunder disposal. In: The Proceedings of the 16th Annual Congress of the South African Sugar Technologists' Association, Durban: South African Sugar Technologists' Association; 1942, p. 43–44.

[63] Gupta SC, Shukla JP, Shukla NP. Recovery of crude potassium salts from spent wash of molasses distilleries by fluidized incineration. In: The Proceedings of the 36th Annual Convention of the Sugar Technologists' Association of India, 1968, p. 1–7.

[64] Dubey RS. Distillery effluents — Treatment and disposal. Sugar News Annual 1974:9–26.

[65] Monteiro CE. Brazilian experience with the disposal of waste water from the cane sugar and alcohol industry. Process Biochemistry 1975;10:33–41.

[66] Yamauchi T. Wastewater treatment in fermentation. Japan Kokai 1977;77:365–72.

[67] Sheehan GJ, Greenfield PF. Utilisation, treatment and disposal of distillery wastewater. Water Research 1980;14:257–77.

[68] Spruytenburg GP. Vinasse pollution elimination and energy recovery, from Hollandse Constructie Groep BV. International Sugar Journal 1982;84:73–4.

[69] Nilsson M. Energy recovery from distillery wastes, from Alfa-Laval AB. International Sugar Journal 1981;83:259–261.

[70] Larsson E, Tengberg T. Evaporation of vinasse — Pilot plant investigation and preliminary process design (M.Sc. thesis). Chalmers University of Technology, 2014.

[71] Moral MR. Process to obtain potassium sulfate from vinasse. US 2013/0089478 A1, 2013.

[72] Knoef HAM. Handbook on biomass gasification. 1st ed. Enschede: BTG biomass technology group BV; 2005.

[73] Sadhwani N, Adhikari S, Eden MR. Biomass gasification using carbon dioxide: Effect of temperature, $CO_2$/C ratio, and the study of reactions influencing the process. Industrial and Engineering Chemistry Research 2016;55:2883–91.

[74] Yakaboylu O, Harinck J, Smit KG, de Jong W. Supercritical water gasification of biomass: A literature and technology overview. Energies 2015;8:859–94.

[75] Basu P, Mettanant V. Biomass gasification in supercritical water — A review. International Journal of Chemical Reactor Engineering 2009;7:1–61.

[76] Reddy SN, Nanda S, Dalai AK, Kozinski JA. Supercritical water gasification of biomass for hydrogen production. International Journal of Hydrogen Energy 2014;39:6912–26.

[77] Kruse A. Supercritical water gasification. Biofuels, Bioproducts & Biorefining 2008;2:415–37.

[78] Loppinet-Serani A, Reverte C, Cansell F, Aymonier C. Supercritical water biomass gasification process as a successful solution to valorize wine distillery wastewaters. ACS Sustainable Chemistry and Engineering 2013;1:110–7.

[79] Richard T, Poirier J, Reverte C, Aymonier C, Loppinet-Serani A, Iskender G, Pablo EB, Marias F. Corrosion of ceramics for vinasse gasification in supercritical water. Journal of the European Ceramic Society 2012;32:2219–33.

[80] Costa M. Hydrothermal treatment of Vinasse (M.Sc. thesis). Aalto University, 2017.

[81] Li J, Van Heiningen ARP. Reaction kinetics of gasification of black liquor char. The Canadian Journal of Chemical Engineering 1989;67:693–7.

[82] Sams DA, Shadman F. Mechanism of potassium-catalyzed carbon/$CO_2$ reaction. AlChE Journal 1986;32:1132–7.

[83] Kapteijn F, Moulijn JA. Kinetics of the potassium carbonate-catalysed $CO_2$ gasification of activated carbon. Fuel 1983;62:221–5.

[84] Kopyscinski J, Rahman M, Gupta R, Mims CA, Hill JM. $K_2CO_3$ catalyzed $CO_2$ gasification of ash-free coal. Interactions of the catalyst with carbon in $N_2$ and $CO_2$ atmosphere. Fuel 2014;117:1181–9.

[85] Suzuki T, Nakajima H, Ikenaga N, Oda H, Miyake T. Effect of mineral matters in biomass on the gasification rate of their chars. Biomass Conversion and Biorefinery 2011;1:17–28.

[86] Mims CA, Pabst JK. Alkali-catalyzed carbon gasification kinetics: Unification of $H_2O$, $D_2O$, and $CO_2$ reactivities. Journal of Catalysis 1987;107:209–20.

[87] Moulijn JA, Cerfontain MB, Kapteijn F. Mechanism of the potassium catalysed gasification of carbon in $CO_2$. Fuel 1984;63:1043–7.

[88] Kapteijn F, Peer O, Moulijn JA. Kinetics of the alkali carbonate catalysed gasification of carbon: 1. $CO_2$ gasification. Fuel 1986;65:1371–6.

[89] Bridgwater AV. Renewable fuels and chemicals by thermal processing of biomass. Chemical Engineering Journal 2003;91:87–102.

[90] Mohan D, Pittman Jr. CU, Steele PH. Pyrolysis of wood/biomass for bio-oil: A critical review. Energy & Fuels 2006;20:848–89.

[91] Maschio G, Koufopanos C, Lucchesi A. Pyrolysis, a promising route for biomass utilization. Bioresource Technology 1992;42:219–31.

[92] Bridgwater AV. Review of fast pyrolysis of biomass and product upgrading. Biomass and Bioenergy 2012;38:68–94.

[93] Bridgwater AV, Meier D, Radlein D. An overview of fast pyrolysis of biomass. Organic Geochemistry 1999;30:1479–93.

[94] Czernik S, Bridgwater AV. Overview of applications of biomass fast pyrolysis oil. Energy & Fuels 2004;18:590–8.

[95] Jahirul MI, Rasul MG, Chowdhury AA, Ashwath N. Biofuels production through biomass pyrolysis — A technological review. Energies 2012;5:4952–5001.

[96] Enestam S, Björklund P, Engblom N, Hamaguchi M, Rautanen M, Wallmo H. Energy trends — Recent and future fuel related challenges. In: The Proceedings of the 20th International Conference on Impacts of Fuel Quality on Power Production and the Environment, Snowbird: 2014.

[97] Toor SS, Rosendahl L, Rudolf A. Hydrothermal liquefaction of biomass: A review of subcritical water technologies. Energy 2011;36:2328–42.

[98] Behrendt F, Neubauer Y, Oevermann M, Wilmes B, Zobel N. Direct liquefaction of biomass: Review. Chemical Engineering and Technology 2008;31:667–77.

[99] Enestam S. Prediction of ash behavior and deposit formation in fluidized bed combustion of biofuel mixtures. In: The Proceedings of the 18th International Conference on Fluidized Bed Combustion, Toronto: The American Society of Mechanical Engineers (ASME); 2005, p. 563–572.

[100] Zevenhoven M, Yrjas P, Backman R, Skrifvars B-J, Hupa M. The Åbo Akademi database: Fuel characterization. In: The Proceedings of the 18th International Conference on Fluidized Bed Combustion, Toronto: The American Society of Mechanical Engineers (ASME); 2005, p. 667–78.

[101] Frandsen FJ, van Lith SC, Korbee R, Yrjas P, Backman R, Obernberger I, Brunner T, Jöller M. Quantification of the release of inorganic elements from biofuels. Fuel Processing Technology 2007;88:1118–28.

[102] Backman R, Skrifvars B-J, Hupa M, Siiskonen P, Mäntyniemi J. Flue gas and dust chemistry in recovery boilers with high levels of chlorine and potassium. Journal of Pulp and Paper Science 1996;22:J119–26.

[103] Tran HN, Reeve DW, Barham D. Formation of kraft recovery boiler superheater fireside deposits. Pulp and Paper Canada 1983;84:T7–12.

[104] Robertiello A. Upgrading of agricultural and agro-industrial wastes: The treatment of distillery effluents (vinasses) in Italy. Agricultural Wastes 1982;4:387–95.

[105] Decloux M, Bories A. Stillage treatment in the French alcohol fermentation industry. International Sugar Journal 2002;104:509–17.

[106] Dowd MK, Johansen SL, Cantarella L, Reilly PJ. Low molecular weight organic composition of ethanol stillage from sugarcane molasses, citrus waste, and sweet whey. Journal of Agricultural and Food Chemistry 1994;42:283–8.

[107] España-Gamboa E, Mijangos-Cortes J, Barahona-Perez L, Dominguez-Maldonado J, Hernández-Zarate G, Alzate-Gaviria L. Vinasses: Characterization and treatments. Waste Management and Research 2011;29:1235–50.

[108] Parnaudeau V, Condom N, Oliver R, Cazevieille P, Recous S. Vinasse organic matter quality and mineralization potential, as influenced by raw material, fermentation and concentration processes. Bioresource Technology 2008;99:1553–62.

[109] Karlström O, Costa M, Brink A, Hupa M. $CO_2$ gasification rates of char particles from torrefied pine shell, olive stones and straw. Fuel 2015;158:753–63.

[110] Kannan MP, Richards GN. Potassium catalysis in air gasification of cellulosic chars. Fuel 1990;69:999–1006.

[111] Zhang Y, Ashizawa M, Kajitani S, Miura K. Proposal of a semi-empirical kinetic model to reconcile with gasification reactivity profiles of biomass chars. Fuel 2008;87:475–81.

[112] Demirbas A. Pyrolysis of ground beech wood in irregular heating rate conditions. Journal of Analytical and Applied Pyrolysis 2005;73:39–43.

[113] Karlström O, Brink A, Hupa M. Time dependent production of NO from combustion of large biomass char particles. Fuel 2013;103:524–32.

[114] Giuntoli J, de Jong W, Verkooijen AHM, Piotrowska P, Zevenhoven M, Hupa M. Combustion characteristics of biomass residues and biowastes: Fate of fuel nitrogen. Energy & Fuels 2010;24:5309–19.

[115] Bhattacharya PK, Parthiban V, Kunzru D. Pyrolysis of black liquor solids. Industrial & Engineering Chemistry Process Design and Development 1986;25:420–6.

[116] Saw WL, Nathan GJ, Ashman PJ, Hupa M. Influence of droplet size on the release of atomic sodium from a burning black liquor droplet in a flat flame. Fuel 2010;89:1840–1848.

[117] Dupont C, Jacob S, Marrakchy KO, Hognon C, Grateau M, Labalette F, Perez DDS. How inorganic elements of biomass influence char steam gasification kinetics. Energy 2016;109:430–5.

[118] Prestipino M, Galvagno A, Karlström O, Brink A. Energy conversion of agricultural biomass char: Steam gasification kinetics. Energy 2018;161:1055–63.

[119] Bale CW, Bélisle E, Chartrand P, Decterov SA, Eriksson G, Hack K, Jung I-H, Kang Y-B, Melançon J, Pelton AD, Robelin C, Petersen S. FactSage thermochemical software and databases — Recent developments. Calphad 2009;33:295–311.

[120] Lindberg D, Chartrand P. Thermodynamic evaluation and optimization of the (Ca + C + O + S) system. Journal of Chemical Thermodynamics 2009;41:1111–24.

[121] Lindberg D, Backman R, Chartrand P, Hupa M. Towards a comprehensive thermodynamic database for ash-forming elements in biomass and waste combustion — Current situation and future developments. Fuel Processing Technology 2013;105:129–41.

[122] Garcia-Perez M, Wang XS, Shen J, Rhodes MJ, Tian F, Lee W-J, Wu H, Li C-Z. Fast pyrolysis of oil mallee woody biomass: Effect of temperature on the yield and quality of pyrolysis products. Industrial and Engineering Chemistry Research 2008;47:1846–54.

[123] Guizani C, Valin S, Billaud J, Peyrot M, Salvador S. Biomass fast pyrolysis in a drop tube reactor for bio oil production: Experiments and modeling. Fuel 2017;207:71–84.

[124] Horne PA, Williams PT. Influence of temperature on the products from the flash pyrolysis of biomass. Fuel 1996;75:1051–9.

[125] Westerhof RJM, Brilman DWF, Van Swaaij WPM, Kersten SRA. Effect of temperature in fluidized bed fast pyrolysis of biomass: Oil quality assessment in test units. Industrial and Engineering Chemistry Research 2010;49:1160–8.

[126] Pattiya A, Sukkasi S, Goodwin V. Fast pyrolysis of sugarcane and cassava residues in a free-fall reactor. Energy 2012;44:1067–77.

[127] Pattiya A, Suttibak S. Fast pyrolysis of sugarcane residues in a fluidised bed reactor with a hot vapour filter. Journal of the Energy Institute 2017;90:110–9.

[128] Tsai WT, Lee MK, Chang YM. Fast pyrolysis of rice straw, sugarcane bagasse and coconut shell in an induction-heating reactor. Journal of Analytical and Applied Pyrolysis 2006;76:230–7.

[129] Yang SI, Wu MS, Wu CY. Application of biomass fast pyrolysis part I: Pyrolysis characteristics and products. Energy 2014;66:162–71.

[130] Toft AJ. A Comparison of integrated biomass to electricity systems (Ph.D. thesis). Aston University, 1996.

[131] Dirbeba MJ, Aho A, Demartini N, Brink A, Hupa M. Pyrolysis of sugarcane vinasse and black liquor at 400 and 500 °C. In: The Proceedings of the 13th International Conference on Energy for a Clean Environment, Ponta Delgada: Technical University of Lisbon; 2017.

[132] Oasmaa A, Solantausta Y, Arpiainen V, Kuoppala E, Sipilä K. Fast pyrolysis bio-oils from wood and agricultural residues. Energy & Fuels 2010;24:1380–8.

[133] Fahmi R, Bridgwater AV, Donnison I, Yates N, Jones JM. The effect of lignin and inorganic species in biomass on pyrolysis oil yields, quality and stability. Fuel 2008;87:1230–40.

[134] Matovic D. Biochar as a viable carbon sequestration option: Global and Canadian perspective. Energy 2011;36:2011–6.

[135] Sadeghi SH, Hazbavi Z, Harchegani MK. Controllability of runoff and soil loss from small plots treated by vinasse-produced biochar. Science of the Total Environment 2016;541:483–90.

[136] Houben D, Evrard L, Sonnet P. Beneficial effects of biochar application to contaminated soils on the bioavailability of Cd, Pb and Zn and the biomass production of rapeseed (Brassica napus L). Biomass and Bioenergy 2013;57:196–204.

[137] Oasmaa A, Meier D. Analysis, characterization and test methods of fast pyrolysis liquids. In: Bridgwater AV, editor. Fast pyrolysis of biomass: A handbook, Chippenham: CPL Press; 2002, p. 23–35.

[138] Channiwala SA, Parikh PP. A unified correlation for estimating HHV of solid, liquid and gaseous fuels. Fuel 2002;81:1051–63.

[139] Oasmaa A, Czernik S. Fuel oil quality of biomass pyrolysis oils — State of the art for the end users. Energy & Fuels 1999;13:914–21.

[140] Jensen PA, Frandsen FJ, Dam-Johansen K, Sander B. Experimental investigation of the transformation and release to gas phase of potassium and chlorine during straw pyrolysis. Energy & Fuels 2000;14:1280–5.

[141] Knudsen JN, Jensen PA, Dam-Johansen K. Transformation and release to the gas phase of Cl, K, and S during combustion of annual biomass. Energy & Fuels 2004;18:1385–99.

[142] Li J, van Heiningen ARP. Kinetics of $CO_2$ gasification of fast pyrolysis black liquor char. Industrial and Engineering Chemistry Research 1990;29:1776–85.

[143] Cameron JH, Grace TM. Kinetic study of sulfate reduction with kraft black liquor char. Industrial & Engineering Chemistry Fundamentals 1985;24:443–9.

[144] Järvinen MP, Zevenhoven R, Vakkilainen EK. Auto-gasification of a biofuel. Combustion and Flame 2002;131:357–70.

[145] Frederick WJ, Wåg KJ, Hupa M. Rate and mechanism of black liquor char gasification with $CO_2$ at elevated pressures. Industrial and Engineering Chemistry Research 1993;32:1747–53.

[146] Di Blasi C. Combustion and gasification rates of lignocellulosic chars. Progress in Energy and Combustion Science 2009;35:121–40.

[147] Umeki K, Moilanen A, Gómez-Barea A, Konttinen J. A model of biomass char gasification describing the change in catalytic activity of ash. Chemical Engineering Journal 2012;207–208:616–24.

[148] Bhatia SK, Perlmutter DD. A random pore model for fluid-solid reactions: I. Isothermal, kinetic control. AIChE Journal 1980;26:379–86.

[149] Mims CA, Pabst JK. Alkali-catalyzed carbon gasification. II. Kinetics and mechanism. Preprints of Papers, American Chemical Society, Division of Fuel Chemistry 1980;25:258–262.

[150] Bouraoui Z, Dupont C, Jeguirim M, Limousy L, Gadiou R. $CO_2$ gasification of woody biomass chars: The influence of K and Si on char reactivity. Comptes Rendus Chimie 2016;19:457–65.

[151] Okuno T, Sonoyama N, Hayashi J, Li C-Z, Sathe C, Chiba T. Primary release of alkali and alkaline earth metallic species during the pyrolysis of pulverized biomass. Energy & Fuels 2005;19:2164–71.

[152] Björkman E, Strömberg B. Release of chlorine from biomass at pyrolysis and gasification conditions. Energy & Fuels 1997;11:1026–32.

[153] Johansen JM, Jakobsen JG, Frandsen FJ, Glarborg P. Release of K, Cl, and S during pyrolysis and combustion of high-chlorine biomass. Energy & Fuels 2011;25:4961–71.

**RECENT REPORTS FROM THE COMBUSTION AND MATERIALS RESEARCH GROUP OF THE JOHAN GADOLIN PROCESS CHEMISTRY CENTRE:**

| | | |
|---|---|---|
| 15-01 | Petteri Kangas | Modelling the Super-Equilibria in Thermal Biomass Conversion: Applications and Limitations of the Constrained Free Energy Method |
| 15-02 | David Agar | The Feasibility of Torrefaction for the Co-Firing of Wood in Pulverised-Fuel Boilers |
| 16-01 | Tooran Khazraie Shoulaifar | Chemical Changes in Biomass during Torrefaction |
| 16-02 | Hao Wu | Chemistry of Potassium Halides and Their Role in Corrosion in Biomass and Waste Firing |
| 19-01 | Jingxin Sui | Initial Stages of Alkali Salt Induced High Temperature Corrosion Mechanisms: Experimental studies using a combination of chronoamperometry, scanning electron microscopy, X-ray photoelectron spectroscopy and time-of-flight secondary ion mass spectrometry |
| 19-02 | Hanna Kinnunen | The Role and Corrosivity of Lead in Recycled Wood Combustion |
| 19-03 | Jonne Niemi | Effects of Temperature Gradient on Ash Deposit Aging and Heat Exchanger Corrosion |

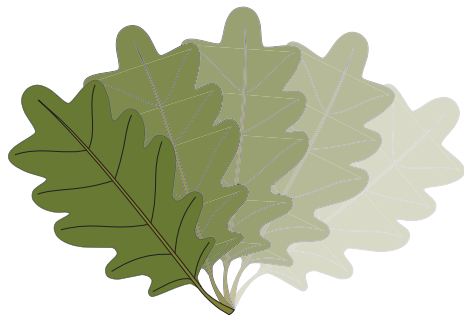

ISBN 978-952-12-3939-7 (printed)
ISBN 978-952-12-3940-3 (digital)
Åbo/Turku, Finland, 2020

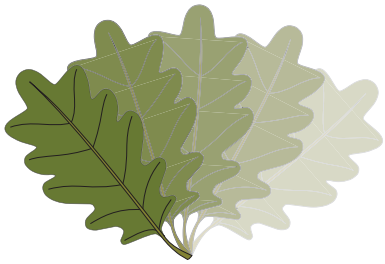

Johan Gadolin
Process Chemistry Centre

ISBN 978-952-12-3940-3